

THE REACTIVITY OF FLUORINATED RADICALS IN LIQUID PHASE

By

XIAO XIN RONG

A DISSERTATION PRESENTED TO THE GRADUATE SCHOOL  
OF THE UNIVERSITY OF FLORIDA IN PARTIAL FULFILLMENT  
OF THE REQUIREMENTS FOR THE DEGREE OF  
DOCTOR OF PHILOSOPHY

UNIVERSITY OF FLORIDA

1995

TO MOM, DAD AND XIAO JUN.

## ACKNOWLEDGMENTS

I wish to express my gratitude for the excellent guidance and friendship of my research advisor, Dr. William R. Dolbier, Jr. It is he who has made the fulfillment of this dream come true. His enthusiasm for chemistry and his understanding nature have been an inspiration to me throughout the course of my graduate studies. With Professor Dolbier, the chemistry is always surmountable and one comes away with a positive feeling towards oneself and the tasks ahead, which has led to an enjoyable and rewarding experience.

I would like to give my special thanks to my committee members, especially, Dr. David H. Powell for giving me a chance to work in the mass-spectrum lab. in the early years of my graduate studies, which made me learn mass spectrometry systematically. Such knowledge has given me a lot of benefits in my research work.

It is a pleasure to thank the many friends and colleagues I have met and worked with at the University of Florida. Due to my extended stay in the Dolbier group, thanks are required to a number of lab-mates; Conrad Burkholder for stimulating discussions, Michael Bartberger for his help in lab-management, Michelle Fletcher for her help in English to write this dissertation, Lu Lian, Rogelio Ocampo, Melvin Wagner, Luz Amalia, and more recently Xu Yuelian, Hao Jian, all for providing valuable friendships. Last and certainly not least, special thanks goes to Dr. Jing Yang. A true friend, Jing is greatly appreciated.

The love and support of my family was and will always be essential. No matter where I live, it is always "home" when I have been in times of stress. Thousands of dollars on telephone bills have always been an inspiration to me since I moved to the United States. Home is always the home wherever you are and whoever you are.

## TABLE OF CONTENTS

ACKNOWLEDGMENTS .....	iii
ABSTRACT .....	vii
CHAPTER	
1 AN OVERVIEW OF REDUCTION AND ADDITION IN RADICAL REACTIONS .....	1
Introduction .....	1
H-atom Transfer Reaction .....	3
Free Radical Addition and Cyclization .....	8
Methods for Determination of Rate Constants of Cyclization of 5-Hexenyl Radicals .....	16
Conclusion .....	20
2 FLUORINE AS SUBSTITUENTS IN THE RADICAL ADDITION AND CYCLIZATION REACTIONS .....	22
Introduction .....	22
The General Effect of the Fluorine Substituent in Organic Chemistry .....	23
The Effects of Fluorine Substitution on H-atom Transfer Reactions .....	31
The Effects of Fluorine Substituents on Radical Addition Reactions .....	32
Conclusion .....	36
3 THE REACTIVITY OF PERFLUOROALKYL RADICALS WITH SOME H-ATOM DONORS IN LIQUID SOLUTION .....	38
Introduction .....	38
Absolute Rate Determination of Hydrogen Abstraction for Perfluoro-n-alkyl Radicals .....	39
The Effects of Fluorine Substituents on H-atom Abstraction Reactions .....	49
Conclusion .....	54
4 THE REACTIVITY OF FLUORINATED 5-HEXENYL RADICALS .....	56
Introduction .....	56
Discussion on Determination of Absolute Rates of Cyclization Reactions for Fluorinated 5-Hexenyl Radicals .....	60
The Fluorine Substituent Effects on the Cyclization Reaction of 5-Hexenyl Radicals .....	66
Synthesis of Radical Precursors .....	72

Conclusion.....	74
5 EXPERIMENTAL.....	76
General Methods.....	76
Experimental Procedures for Those in Chapter 3.....	77
Tables of Data for the Reactions of Perfluoro-n-heptyl Radicals with Reducing Agents .....	79
Experimental Procedures for Those in Chapter 4.....	83
Tables of Data for the Reactions of Fluorinated 5-Hexenyl Radicals with Reducing Agents.....	100
APPENDIX: SELECTED $^{19}\text{F}$ NMR SPECTRA.....	104
REFERENCES .....	151
BIOGRAPHICAL SKETCH.....	157

Abstract of Dissertation Presented to the Graduate School  
of the University of Florida in Partial Fulfillment of the  
Requirements for the Degree of Doctor of Philosophy

THE REACTIVITY OF FLUORINATED RADICALS IN LIQUID PHASE

By

Xiao Xin Rong

August, 1995

Chairman: William R. Dolbier, Jr.  
Major Department: Chemistry

Based on kinetic studies, reactivities of fluorinated radicals in hydrogen atom abstraction reactions and intramolecular cyclizations were investigated in solution at room temperature. Effects of fluorine substituents on the rates of these reactions are discussed.

Using competitive methods, rate constants of hydrogen atom abstraction by the perfluoro-*n*-alkyl radical,  $n\text{-C}_7\text{F}_{15}\cdot$ , have been determined for a series of metal hydrides ( $\text{R}_3\text{MH}$ ,  $\text{M} = \text{Si}, \text{Ge}$ ), that is,  $\text{Et}_3\text{SiH}$  ( $7.5 \times 10^5 \text{ M}^{-1} \text{ s}^{-1}$ ),  $(\text{Me}_3\text{Si})_2\text{SiMeH}$  ( $1.6 \times 10^7 \text{ M}^{-1} \text{ s}^{-1}$ ),  $\text{Bu}_3\text{GeH}$  ( $1.5 \times 10^7 \text{ M}^{-1} \text{ s}^{-1}$ ),  $(\text{TMS})_3\text{SiH}$  ( $5.1 \times 10^7 \text{ M}^{-1} \text{ s}^{-1}$ ). All of these hydrides exhibited substantial rate enhancements relative to the analogous reductions of hydrocarbon radicals. The reduction by  $\text{PhSH}$  ( $3.3 \times 10^5 \text{ M}^{-1} \text{ s}^{-1}$ ) is, in contrast,  $\sim 400$  times slower than for hydrocarbon radicals. Transition state polar effects are invoked to rationalize the relative reactivity of perfluoro- versus hydrocarbon radicals in these hydrogen-transfer reactions. A Hammett study for H-atom transfer from arene thiols ( $\rho^* = -0.56$ ) provided further substantiation for this conclusion. A discussion of the relative reactivity of *t*-butoxyl and perfluoro-*n*-alkyl radicals is presented.

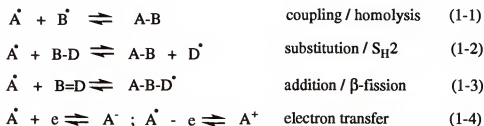
Based on the rate constants of reduction of hydrocarbon alkyl and perfluoro-n-alkyl radicals by metal hydrides ( $R_3MH$ , Table 1-1 and 3-3), the rate constants of intramolecular cyclization of the series of fluorinated 5-hexenyl radicals **35** to **44** were measured using competition methods. The regioselectivity of cyclization indicates that 5-exo ring closure is most favored for the fluorinated 5-hexenyl radicals which were studied. The effects of fluorine on the reactivity of cyclization are varied with differing degrees of fluorination of the radicals. If radicals have a fluorine-substituted olefinic component and an alkyl radical center (like **36**, **37** and **38**), the fluorine-substitution has negligible effect on the rate of cyclization of the 5-hexenyl radical. However, if radicals have a perfluoro-radical center and a hydrocarbon olefinic component (like **40** and **41**), the rates of 5-exo and 6-endo cyclization increase dramatically (up to 170 times as fast as that of unsubstituted 5-hexenyl radicals). These are the first examples of cyclizations where a substantial increase in rate is caused by lowering the SOMO of radicals without increasing the reversibility of 5-exo ring closure in 5-hexenyl radical systems. The vinyl fluorinated radical **35** is the only one for which the fluorine substituent makes the rate of 5-exo ring closure slower (about 10 times) without affecting the 6-endo ring closure relative to unsubstituted 5-hexenyl radical. Although they have different radical centers (alkyl or perfluoro-alkyl), those radicals having a perfluoro-olefinic component (like **39**, **42** and **43**) give rise to similar rates. The perfluorinated 5-hexenyl radical **43** is a mysterious system which has a rate constant which is unexpected in view of the above conclusions. Further study will be required for complete understanding.

# CHAPTER 1

## AN OVERVIEW OF REDUCTION AND ADDITION IN RADICAL REACTIONS

### Introduction

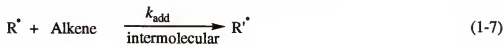
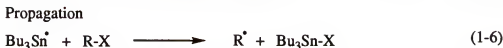
Radical reactions have been extensively studied and widely used in organic synthesis<sup>1,2</sup> since 1900 when Moses Gomberg<sup>3</sup> discovered the first free radical, triphenylmethyl radical. Kharasch by 1935 had defined and explored virtually all of the elementary mechanistic steps available to free radicals,<sup>4</sup> which are shown in Scheme 1-1.



Scheme 1-1. The elementary mechanistic pathways for free radicals<sup>4</sup>

Most free radical reactions take place within chain processes, and they can be rationalized in terms of these elementary steps. The *Tin Hydride Method*,<sup>2,5,6</sup> for example, is a radical chain process which involves those elementary steps which are shown Scheme 1-2. The initiation steps involve homolysis of radical initiators (such as AIBN) in followed by H-atom transfer of hydrides to generate tributyl tin radicals (eq.1-5). In the first propagation step, the tributyl tin radical abstracts a halogen atom from an organic substrate R-X (X= Cl,Br,I) generating the radical (eq.1-6). This radical R' can then undergo addition to a multiple bond to form radical R'' (eq.1-7), unimolecular rearrangement by either cleavage or an intramolecular addition reaction to form radical R''' (eq.1-8). The





Scheme 1-2. A radical chain process, Tin Hydride Method <sup>2,5,6,7</sup>

final propagation step is equation (1-9) in which the radicals  $\text{R}^\bullet$ ,  $\text{R}'^\bullet$  or  $\text{R}''^\bullet$  react with  $\text{Bu}_3\text{SnH}$  to form the  $\text{Bu}_3\text{Sn}^\bullet$  radical which will then continue the chain process.

The distribution of the reduced products  $\text{R-H}$  and  $\text{R'-H}$  or  $\text{R''-H}$  will depend on the reactivity of the radical  $\text{R}^\bullet$  in each elementary step represented by the rate constants  $k_H$  and  $k_{\text{add}}$  (or  $k_c$ ). For example, if the bimolecular or rearrangement processes are much faster than hydrogen abstraction, that is  $k_{\text{add}}$  (or  $k_c$ )  $\gg k_H$ , then the initial radical  $\text{R}^\bullet$  is converted to  $\text{R'-H}$  or  $\text{R''-H}$ . On the other hand, if  $k_{\text{add}}$  (or  $k_c$ ) and  $k_H$  are comparable, reactions (7 or 8) are competitive and mixtures of  $\text{R-H}$  and  $\text{R'-H}$  or  $\text{R''-H}$  result. Therefore, it is important to understand the reactivities of a partitioning radical with regard to each of the competing process in planning any new radical reaction.

Reactivities of radical reactions depend on "the complex interplay of polar, steric and bond strength terms."<sup>8</sup> The information about the factors influencing the reactivity of radical reactions comes from thermochemical and kinetic studies. The thermochemical approach was expressed in such generalizations<sup>9,10</sup> as 'radical reactions follow the most exothermic available pathway', and it leads to the conclusion that the relative rates of related reactions can be estimated from thermochemical information.<sup>11,12,13</sup> However, thermochemistry proves to not be the only factor, or even the predominant factor, which affects the outcome of free radical processes.<sup>4,9,10</sup> For homolytic substitution and addition

reactions those other effects which influence reactivities are polar effects which reflect the way in which the electronegativities of the substituent atoms affect the energy of the transition state structure<sup>14,15</sup> and the steric effect reflecting the contribution of non-bonded interactions to the energy of the transition state.<sup>9</sup> Numerous papers dealing with the study of the reactivity of radical reactions have been published. In this chapter, the review will focus on the H-atom transfer reaction and the radical addition reactions including intramolecular cyclization reactions.

### H-atom Transfer Reaction

In chemical synthesis, the majority of free radical applications deal with organo-metallic hydrides such as  $R_3M-H$  ( $M = Sn, Ge, Si$ ),<sup>6, 7,11,12</sup> which are hydrogen donors used to conduct free radical chain reactions. The properties of those hydrides as reducing agents have been extensively studied by Chatgililoglu and Ingold. Table 1-1 gives the kinetic parameters for the reactions of carbon-centered radicals (hydrocarbon alkyl radicals) with the hydrides  $R_3MH$  ( $M = Si, Ge, Sn$ )<sup>6,11,12</sup>. The related bond dissociation energies (BDE) are also shown.

Table 1-1. Kinetic parameters for the Reaction of Alkyl Radicals with  $R_3MH$  and Bond Dissociation Energies, BDE(M-H).

$R_3M-H$	BDE kcal mol <sup>-1</sup>	logA M <sup>-1</sup> s <sup>-1</sup>	$E_a$ kcal mol <sup>-1</sup>	$k_H^{298}$ 10 <sup>-5</sup> M <sup>-1</sup> s <sup>-1</sup>
Bu <sub>3</sub> SnH <sup>a</sup>	73.7 <sup>b</sup>	9.07	3.69	23
(TMS) <sub>3</sub> SiH <sup>c</sup>	79.0 <sup>b</sup>	8.86	4.47	3.8
Bu <sub>3</sub> GeH <sup>d</sup>	82.4 <sup>b</sup>	8.44	4.70	0.93
(TMS) <sub>2</sub> Si(Me)H <sup>c</sup>	83.0 <sup>c</sup>	8.89	5.98	0.32
Et <sub>3</sub> SiH <sup>c</sup>	90.1 <sup>b</sup>	8.66	7.98	0.0064

Ref. <sup>a</sup> 6, <sup>b</sup> 16, <sup>c</sup> 11, <sup>d</sup> 12.

Table 1-1 shows that the pre-exponential term (or 'A'-factor) varies very little for alkyl radicals abstracting H-atom from those hydrides. The variation of the rate by a factor

of 3600 is almost completely attributable to the difference in activation energy. Therefore, in H-atom transfer reactions any factor influencing the activation energy in the transition state will affect the reactivity of the reactions.

Benzenethiol (PhS-H) has a rate constant of  $1.1 \times 10^8 \text{ M}^{-1} \text{ s}^{-1}$  at RT, which is faster radical trapping agent in relative to the tin hydride. Such a property of benzenethiol has been used in the trapping of a radical with a half life of less than picosecond.

### The Strength of the Bond Broken and the Evans-Polanyi Equation

The first factor considered in the H-atom transfer reaction is the strength of bonds being broken BDE(M-H). The fact that the activation energies decrease with the decrease of the BDE(M-H) in the series of  $\text{R}_3\text{M-H}$  hydrides indicates that there is a direct relationship between the BDE and the activation energy of the hydrogen abstraction.



$$E_{\text{act}} = \alpha[\text{D(R-H)}] + \beta \quad (1-11)$$

$$\ln k_{\text{r}} = -(\alpha/RT)[\text{D(R-H)}] + (\ln A - \beta/RT) \quad (1-12)$$

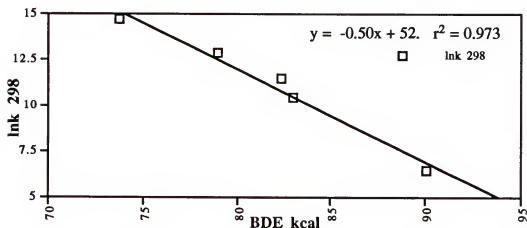


Figure 1-1. The Plot of  $\ln k$  vs BDE(M-H) for the Data in Table 1-1

The Evans-Polanyi equation<sup>17</sup> shows the relationship between the BDE (M-H) and the activation energy (eq. 1-11). It holds when there is no polarity effect or the polarity effect is constant in the transition states.<sup>10,17</sup> The equation (1-12) is deduced from the combination of equation (1-11) with the Arrhenius equation  $k = A e^{-E/RT}$ , which can be the replacement of equation (1-11) when the  $A$  factors are constant in a series of reactions. The meaning of the constant  $\alpha$  (or  $\alpha/RT$  in equation (1-12) at a certain temperature) is not very clear,<sup>10</sup> but the difference of the values between systems will indicate influencing levels for  $E_{act}$  by the BDE as well as other factors (see the following discussion). Figure 1-1 shows the plot of  $\ln k$  vs BDE for the data in Table 1-1. This relationship emphasizes the importance of the strength of the bond being broken. It is obvious that with BDEs<sup>12</sup> (S-H) of 82.0 kcal mol<sup>-1</sup>, benzenethiol can not fit in the line of the Figure 1-1, which can be the result of polar effects in the transition state (see the discussion in Chapter 3).

### The Polar Effect in H-atom Transfer Reactions

The kinetic behavior of *t*-butoxyl radical has been investigated extensively in H-atom abstraction reactions.<sup>18,19,20</sup> Table 1-2 shows some absolute rate constants for the reactions of *t*-butoxyl radicals with R<sub>3</sub>MH hydrides at 300K.<sup>19,20</sup> That the rates of *t*-butoxyl radicals with hydrides (R<sub>3</sub>MH) are at least 100 times faster than those of alkyl radicals indicates that there are factors other than the BDE(M-H) which influence the reactions dramatically. Although the BDE of the bond being formed for *t*-butoxyl radicals with hydrides, a *t*-BuO-H bond,<sup>18</sup> is 105 kcal mol<sup>-1</sup> while the BDE of the bond formed for alkyl radicals with hydrides, a C-H bond,<sup>18</sup> is about 100 kcal mol<sup>-1</sup>, the difference of 5 kcal mol<sup>-1</sup> from the bonds being formed can not totally account for the increase of the rates from alkyl radicals to *t*-butoxyl radicals since H-atom abstraction by *t*-butoxyl radicals have a rather 'early' transition state<sup>19a</sup>. It has been pointed out that the enhanced reactivity of *t*-butoxyl radical with metal hydrides was attributed to the polar effect<sup>19b,19c</sup> in the transition state as shown in Figure 1-3. The charge separation in transition states<sup>21</sup> can explain the

polar effect in the hydrogen abstraction reaction by *t*-butoxyl radicals. Since the SOMO-HOMO interaction is the more important one<sup>21,22</sup> in the abstraction reaction, the charge separation in the transition state will be those<sup>23</sup> in Figure 1-3. Because of the relative electronegativities of an oxygen atom versus an alkyl group, the transition state (b) should be lower in energy in comparison with the transition state (a). Actually, any charge separation would make it higher in the energy for TS (a) since the transition state with any negative charge on the alkyl group of the radical would not be stabilized by the polar effect.

Table 1-2. Absolute Rate Data for the Reactions of *t*-Butoxyl Radicals with R<sub>3</sub>MH at 300K

R <sub>3</sub> M-H	$k_H^{300} \times 10^{-5} \text{ M}^{-1} \text{ s}^{-1}$	lnk
Bu <sub>3</sub> SnH <sup>a</sup>	2200	19.21
(TMS) <sub>3</sub> SiH <sup>b</sup>	1100	18.52
Bu <sub>3</sub> GeH <sup>a</sup>	800	18.20
Et <sub>3</sub> SiH <sup>a</sup>	57	15.55

Ref. <sup>a</sup> 19, <sup>b</sup> 20.

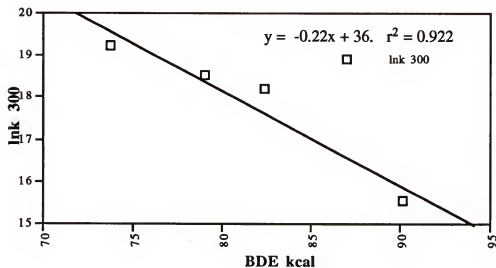


Figure 1-2. The Plot of lnk vs BDE for the Data in Table 1-2.



a) TS. of an alkyl radical with  $\text{R}_3\text{MH}$       b) TS. of a  $\text{O}^t\text{Bu}$  radical with  $\text{R}_3\text{MH}$

Figure 1-3. The charge separation in TS for hydrogen abstraction reactions.

A plot of  $\ln k$  vs  $\text{BDE}(\text{M-H})$  for the reactions of *t*-butoxyl radicals with the hydrides is shown in Figure 1-2. In a comparison of Figure 1-1 with Figure 1-2, it can be found that the slopes of the plots are different (0.50 for alkyl radicals and 0.22 for *t*-butoxyl radicals), meaning that the values of  $\alpha/\text{RT}$  are different. Because the steric effect in the system of alkyl or *t*-butoxyl radicals are not a dominant factor, the difference between the two radicals in the  $\alpha/\text{RT}$  must be from the polar effect.

Based on the frontier molecular orbital (FMO) theory,<sup>15,22</sup> the frontier orbital of the radical is the singly occupied orbital (SOMO) which will interact with both the highest occupied molecular orbital (HOMO) and the lowest unoccupied molecular orbital (LUMO) of the molecule it is reacting with. The "polar effect" is essentially the effect that electronegativities of the constituent atoms influence have on the energies of the orbitals so as to affect the interaction of SOMO-LUMO or SOMO-HOMO in reactions. Figure 1-4 shows

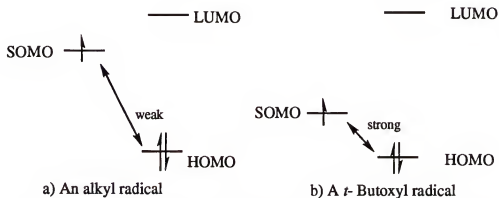


Figure 1-4. Frontier Orbital Interactions for (a) Alkyl Radicals, and (b) *t*-Butoxyl Radicals with SOMO-HOMOs.

the FMO explanation for the polar effect in hydrogen abstraction by alkyl and *tert*-Butoxyl radicals. The SOMO energies<sup>22</sup> of alkyl radicals and *tert*-Butoxyl radicals are -8.7 eV and -12 eV, respectively. Such a difference leads to a stronger interaction of the SOMO-HOMO for *tert*-Butoxyl radical as shown in Figure 1-4 (b). Thus, it is much more reactive than the alkyl radical toward the hydrides.

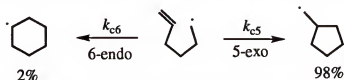
The knowledge of bond dissociation energies has always been regarded as fundamental to the understanding of chemical bonding and reactivity. However, the kinetic data shows that the polar effect is also important and sometimes can even be the dominant factor in determining the reactivity of radical reactions.<sup>10,15</sup>

### Free Radical Addition and Cyclization

Inter- and intra-molecular C-C bond formation (Scheme 1-3) by the addition of carbon-centered radicals to unsaturated bonds represents one of the most useful applications of free radical chemistry. Since a  $\sigma$ -bond is formed and a  $\pi$ -bond is broken, the addition reaction is strongly exothermic and has a low activation energy. Based on the Hammond postulate,<sup>24</sup> the transition states should lie very early (reactant like) on the reaction coordinate. This has been supported by experimental results<sup>25,26</sup> and theoretical calculations.<sup>26,27,28</sup>



a) Inter-molecular addition: methyl radicals addition to alkenes.



b) Intra-molecular addition: 5-hexenyl radical cyclization.

Scheme 1-3. Inter- and intra- molecular addition.

### The Transition Structures of Inter-molecular Addition and Cyclization Reactions.

Calculations<sup>26</sup> for addition of the methyl radical to ethylene (Scheme 1-3,a) have shown that the radicals attack the double bond unsymmetrically (attacking angle  $\theta = 109^\circ$ ) reflecting the stereoelectronic demands<sup>4</sup> of the transition structure incorporating the three atoms ( $C_1$ ,  $C_2$  and  $C_3$ ) in the interaction of the SOMO of radicals and the LUMO of ethylene as shown in Figure 1-5, a.<sup>26c</sup> The transition structure shows that the forming bond length ( $C_1-C_2$ ) is 2.27Å and the double bond is only partially broken ( $C_2-C_3$ , 1.38Å), which indicates a loose transition state. The nonplanar structure of the attacking radical and the bonding angle of  $\theta_2$  ( $<180^\circ$ ) represent the non-bonded interaction which determines the regiochemistry of intermolecular addition reactions. The variations are barely significant in attack angle  $\theta_1$  with variations both in the electronic character of the radical<sup>28b</sup> and substitution on the double bond.<sup>26c</sup>

Based on the transition structure of inter-molecular addition reactions, the transition structure of the 5-hexenyl radical cyclization was calculated by Beckwith and Schiesser<sup>27</sup> and Houk and Spellmeyer.<sup>28a</sup> Such calculations show that the exo-chair transition state (Figure 1-5,b) is favored by about 3 kcal mol<sup>-1</sup> relative to the endo-chair one (Figure 1-5,c). This has been supported by the fact<sup>29,30</sup> that the major cyclization of the 5-hexenyl radical is through the exo mode to form a cyclopentylcarbinyl radical even though it is not the thermochemically favored product.<sup>31</sup> In comparison with the transition structure of methyl radical addition to ethylene, the endo-chair model in Figure 1-5.c has an attacking angle  $\theta_4$  of  $94^\circ$ , very much reduced from the angle  $\theta_1$  ( $107^\circ$ ) in Figure 1-5, a. On the other hand, the exo-chair model has an attacking angle  $\theta_3 = 107^\circ$  which is the same as  $\theta_1$ . Again, such a geometry fits the requirement for overlap of the frontier orbitals (SOMO-LUMO interaction), and thus the exo-chair is the favored transition structure for cyclization of the 5-hexenyl radicals.



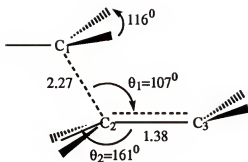
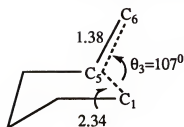
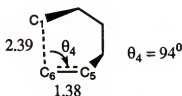
a) Transition structure for methyl radical to ethylene<sup>26c</sup>b) Exo-chair transition structure for cyclization of the 5-hexenyl radical<sup>28a</sup>c) Endo-chair transition structure for cyclization of the 5-hexenyl radical<sup>28a</sup>

Figure 1-5. The transition structures for radical addition and cyclization reactions


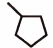

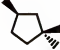
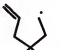
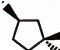





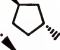
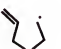
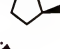

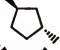

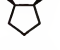
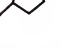
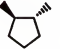
### Substituent Effects on the Cyclization of the 5-Hexenyl Radicals

The typical 5-hexenyl radical (Scheme 1-3,b) cyclizes predominantly to cyclopentylmethyl radical with a rate constant ( $k_{cx}$ ) of  $2.5 \times 10^5 \text{ s}^{-1}$  at  $25^\circ\text{C}$ ;<sup>6,32a</sup> the regioselectivity results primarily from stereoelectronic effects as shown in the exo-chair transition structure which leads to 5-membered ring. A variety of substituted analogues of the 5-hexenyl radical have been studied,<sup>32-37</sup> and the results show that the steric and polar effects of substituents are important in the reactions.

Substitutions on the olefin moiety and the radical center in the 5-hexenyl radical system might exert steric as well as electronic effects in the transition states for reactions. Basically, the alkyl substituents (like methyl, ethyl, iso-propyl and *t*-Butyl groups) are

considered as steric groups<sup>32,33,34</sup> because of their large 'size' and weak electronic effects. However, those that are small have strong electronic effects (like CN and OMe groups) and can introduce polar effects<sup>35,36</sup> in the transition state of reactions.

Table 1-3. Absolute rate constants<sup>a</sup> for cyclization of methyl-substituted 5-hexenyl radicals at 318K<sup>0</sup>.

Cyclization reactions			$k_{c5} \text{ s}^{-1} (\times 10^{-5})$
1			4.9 <sup>b</sup>
2			36
3			52
4			32
5	cis 		24
	trans 		45
6	cis 		70
	trans 		24
7	cis 		0.75
	trans 		36

Ref. <sup>a</sup> 32a, <sup>b</sup> 6.







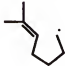

### Steric Effects

Table 1-3 shows the effect of the methyl substituents which are in the alkyl fragment of the 5-hexenyl radicals on the rate constants ( $k_{C5}$ ) of the cyclization. All rates increase when compared to the rate of the unsubstituted radical **1**. This effect has been interpreted by Beckwith et al.<sup>32a</sup> as the gem-dimethyl effect.<sup>37</sup> Canadell's calculation<sup>38</sup> also showed that the change of the activation entropy is favorable for the methyl-substituted radicals.

The other interesting result in Table 1-3 is the stereochemistry of the reactions. The ring closures of mono-substituted radicals are not constantly favored for trans or cis isomers but change depending on the positions of the methyl group in the radicals. For example, the ring closure of the radical **5** is favored for the trans-isomer, while the radical **6** is favored for the cis one. The rationalization<sup>4</sup> of the stereochemistry derives from the exo-chair like transition state in which a substituent in the pseudo-equatorial position is of lower energy than one in the pseudo-axial position.

If the alkyl groups are at the  $C_3$  of the 5-hexenyl radicals as in Table 1-4 (radicals **8** and **9**), the rates ( $k_{C5}$ ) of forming 5-membered ring decrease dramatically while the rates ( $k_{C6}$ ) increase. An alkyl groups at  $C_3$  is the only case which exhibits retardation of the 5-exo cyclization reaction, but enhances the 6-endo ring closure. It is also noteworthy that the methyl and the isopropyl groups have the same effects on the  $k_{C5}$ , but the  $k_{C6}$  increases twice by changing the methyl to the isopropyl groups. Beckwith has pointed out a purely steric reason to explain the results.<sup>4,32b</sup> Since the retardation of the methyl and the isopropyl groups is the same on the  $k_{C5}$ , the major reason for this is due to B strain engendered at the  $C_3$  atom by its change from  $sp^2$  to  $sp^3$  hybridization. The enhancement of  $k_{C6}$  by the steric effects is due to the non-bonded interaction between the  $C_3$  and the radical center, which leads the  $C_6$  to be closer to the radical center. Thus, the larger the alkyl group is, the stronger the interaction and the larger the  $k_{C6}$  is (see **8** and **9**).

Table 1-4. Absolute rate constants<sup>a</sup> for cyclization of Alkyl-substituted 5-hexenyl radicals at 338K<sup>0</sup>.

Radicals	$k_{c5} \text{ s}^{-1} (\times 10^{-5})$	$k_{c6} \text{ s}^{-1} (\times 10^{-5})$
1 	9.2 <sup>b</sup>	-
8 	0.25	0.41
9 	0.25	0.82
10 	13	0.17
11 	15	0.07
12 	21	0.31
13 	27	-
14 	12	0.20

<sup>a</sup> ref. 32 b).


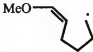
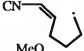
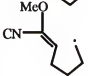
<sup>b</sup> Calculated from the Arrhenius parameters given in ref. 6.

If one puts another methyl group at the terminal position of the radical **8**, the rate constant  $k_{c5}$  increases about 50 times and  $k_{c6}$  decreases twice (radical **14**) in comparison with the radical **8**. There was no direct discussion on this result. However, since two methyl groups at the terminal position ( radical **13**) only increase the  $k_{c5}$  about 3 times as

fast as the unsubstituted radical (radical **1**), the methyl group at the terminal position (radical **14**) must release the B strain at C<sub>5</sub> in the transition state to assist the ring closure.

The alkyl groups at the radical centers (radicals **10**, **11** and **12**) also increase the reactivities of the radicals which are in the order of tertiary > secondary > primary radicals. As the order of the alkyl radical stability is considered, it can be seen that the effect of the radical stabilization is not important in the cyclization reactions of 5-hexenyl radicals. The fact that the tertiary radical cyclized faster than the secondary radical suggests that the electron donating effect of the alkyl groups on the ring closure is the dominant one in the transition states.

Table 1-5. Absolute rate constants for cyclization of electronic Acceptor or Donor-substituted 5-hexenyl radicals at 298<sup>0</sup>K.

Radicals	$k_{c5} \text{ s}^{-1} (\times 10^{-5})$
<b>1</b> 	2.5 <sup>a</sup>
<b>15</b> 	4.1 <sup>b</sup>
<b>16</b> 	667 <sup>b</sup>
<b>17</b> 	1000 <sup>b</sup>

<sup>a</sup> ref. 32 b) <sup>b</sup> Calculated from the Arrhenius parameters given in ref. 36.

The presence of an electron acceptor group (like CN) at the terminal end of the olefinic bond increases the reactivity of the radicals dramatically as is shown in Table 1-5, radical **16**.<sup>36</sup> The electron donating methoxy group at the same position (radical **15**)

increases the rate but the effect is small. Seung-Un et al rationalized the kinetic effects of the substituents with the frontier molecular orbital theory.<sup>36</sup> In alkyl radical addition reactions to substituted alkenes the interaction of the SOMO-LUMO is the most dominant, and the one from the SOMO-HOMO is next dominant.<sup>22,26b,39</sup> Thus, the lower LUMO energy of the  $\pi$ -bond in radical **16** (the acceptor group lowering the MO energy of the olefins<sup>39</sup>) leads to stronger SOMO-LUMO interaction, while a less important, increased SOMO-HOMO interaction in radical **15** is introduced by the methoxy substituent.

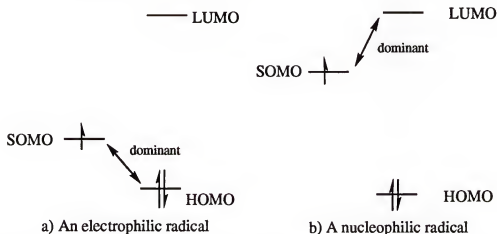




Figure 1-6. The dominant interactions for the electrophilic a) and nucleophilic b) radicals with the HOMO or LUMO of the alkenes<sup>22</sup>.

Substituents on the radical center of 5-hexenyl radicals also can influence the interactions of SOMO-LUMO, or SOMO-HOMO (Figure 1-6). Briefly, an electrophilic radical (the radical attached the electron withdrawing groups) will have a lower SOMO leading to a stronger SOMO-HOMO interaction. On the other hand, a nucleophilic radical (the radical attached the electron donating groups) will have a higher SOMO leading to a stronger SOMO-LUMO interaction. However, when the radical centers are substituted by electron withdrawing groups (Table 1-6, radical **19**)<sup>35a,35b</sup> or a phenol group, the polar effects have been obscured; either by steric effects or by the reversibility<sup>35</sup> of the cyclization for the radicals stabilized by the electron withdrawing groups. Table 1-6 shows that the

major products are 6-endo products (thermo products) for the cyclization of stabilized radicals **18,19**, which have been used for the evidence of the reversibility of the cyclization for the substituted 5-hexenyl radicals.<sup>41</sup>

Table 1-6. Cyclization of stabilized 5-hexenyl radicals.

	Radicals	5-exo product (%)	6-endo product (%)
18		32.3 <sup>a</sup>	77.1
19		16 <sup>b</sup>	84

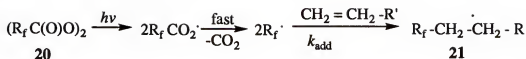
<sup>a</sup> ref. 35 c) <sup>b</sup> ref. 35 a).

#### Methods for Determination of Rate Constants of Cyclization of 5-Hexenyl radicals

Basically, there are two kinds of methods<sup>42,43</sup> to measure rate constants of cyclization of 5-hexenyl radicals; Direct methods and Indirect competition methods.

#### The Direct Method: Laser Flash Photolysis (LFP)

In LFP, radical intermediates are generated by laser pulse and the results of radical reactions are monitored by UV-visible spectroscopy. Recently, the rate constants of perfluoro-n-alkyl radicals addition to alkenes have been measured by Ingold and Dolbier research groups.<sup>42</sup> In this experiment, perfluoro-n-alkyl radicals were generated "instantaneously" by photolysis of the parent diacyl peroxide **20** using a laser pulse. The perfluoro-acyloxyl radicals produced initially were decarboxylated rapidly to yield the perfluoro-n-alkyl radicals. The addition of perfluoroalkyl radicals to alkenes (excess under



pseudo-first-order conditions) were monitored directly *via* observation of the pseudo-first-order growth of the absorption which resulted from the formation of the adducts **21**. Based on the experimental growth curves, the  $k_{\text{exptl}}$  can be obtained. The relationship between  $k_{\text{exptl}}$  and  $k_{\text{add}}$  can be expressed by equation (13).<sup>42</sup> Thus,  $k_{\text{add}}$  can be determined by measuring

$$k_{\text{exptl}} = k_0' + k_{\text{add}} [\text{alkene}] \quad 1-13$$

$k_{\text{exptl}}$  with varying the concentration of alkenes. For example, the rate constant of the perfluoro-*n*-heptyl ( $\text{R}_f = \text{C}_7\text{F}_{15}$ ) radical's addition to 1-hexene is  $7.9 \times 10^6 \text{ s}^{-1}\text{M}^{-1}$  at  $25^\circ\text{C}$  which is the fundamental number which was necessary for the determination of the rate constants of hydrogen abstraction of perfluoroalkyl radicals from  $\text{R}_3\text{MH}$  hydrides using the indirect method.

### Indirect Methods: Competition Kinetics

The competition kinetic<sup>43</sup> method requires partitioning of a radical intermediate between two reaction pathway (Figure 1-7), the reaction 1 of interest with an unknown rate constant  $k_1$  while the competitive reaction 2 has a known rate constant  $k_2$ .

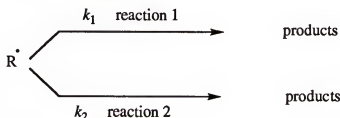
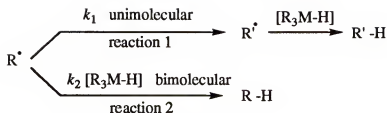
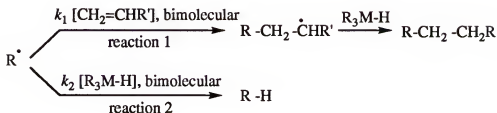


Figure 1-7. Competition Kinetics





$$\text{A: } \frac{k_1}{k_2} = \frac{[\text{R}'\text{-H}]}{[\text{R-H}]} [\text{R}_3\text{M-H}] \quad 1-14$$



$$\text{B: } \frac{k_1}{k_2} = \frac{[\text{R-CH}_2\text{-CH}_2\text{R}']}{[\text{R-H}]} \frac{[\text{CH}_2=\text{CHR}']}{[\text{R}_3\text{M-H}]} \quad 1-15$$

Figure 1-8 The Competition Kinetic Methods

The reactions 1 and 2 can be either unimolecular (like cyclization of 5-hexenyl radicals) or bimolecular (like alkene addition or hydrogen abstraction) reactions. In the case where  $k_1$  is a first order rate constant being measured and  $k_2$  is the known rate constant (Figure 1-8, A), the initial radical  $\text{R}^\bullet$  can either undergo the unimolecular reaction 1 to form radicals  $\text{R}'^\bullet$  which forms products ( $\text{R}'\text{-H}$ ) or react with radical trap agents ( $\text{R}_3\text{M-H}$ ) via reaction 2 pathway to yield products ( $\text{R-H}$ ). Under the condition where the radical trap agent ( $\text{R}_3\text{M-H}$ ) is in excess (greater than fivefold excess respect to the radical precursor) to fit the pseudo-first order process for reaction 2, the ratio of rate constants ( $k_1/k_2$ ) can be obtained directly from the product distribution by equation (1-14) in which reaction 1 is irreversible.<sup>44</sup> In the case where  $k_1$  is also second order, two bimolecular reactions will be in the competition process (Figure 1-8, B), the equation (1-15) will be used to calculate the ratio of the rate constants ( $k_1/k_2$ ) from the product distribution. It is important that both

reagents ( $R_3M-H$ ) and ( $CH_2=CHR'$ ) should be in excess to fit the requirement of a pseudo-first order process according to equation (1-15).

In the event that more precise kinetic values are desired, a series of competition reactions can be run in which the concentrations of the radical trap agents are varied. For example, in using equation (1-14), the ratio of the rate constants ( $k_1/k_2$ ) is found by the slope of a plot of  $[R'-H]/[R-H]$  as a function of the trap agent's concentration.

The competition method must involve a partitioning of a radical between two processes (reactions 1 and 2) and both processes should be competent steps in a radical chain sequence that permits high conversions of the radical precursors. Figure 1-9 shows the competition process consisting of two bimolecular reactions used by the Dolbier group<sup>42</sup> to determine for the first time the rate constant of reaction of tributyl tin hydride with perfluoroalkyl radicals. The initial step is photolysis of radical precursors ( $R_f-I$ ) to generate

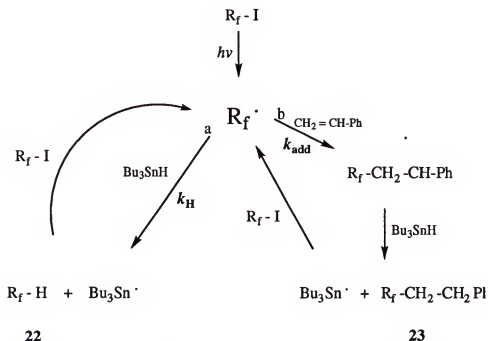


Figure 1-9. The Rate  $k_H$  Determination<sup>42</sup> for Hydrogen Abstraction of  $R_f \cdot$  with Tin Hydrides

perfluoro-radicals  $R_f^{\cdot}$  which have two different chain processes to continue the reactions: Path a, to form reduced product **22** and regenerate  $R_f^{\cdot}$ , or Path b, to form adduct **23** and regenerate  $R_f^{\cdot}$ . The rate constant  $k_{add}$  is known as measured by the LFP method.<sup>42</sup> As a result,  $k_H$  can be determined according to the kinetic relationship of equation (1-14) where  $(CH_2=CHR^{\cdot})$  is  $CH_2=CH-Ph$  and  $(R_3M-H)$  is the  $Bu_3SnH$ .

### Conclusion

The absolute rate constants for reduction of alkyl radicals by  $R_3MH$  ( $M = Si, Ge$  and  $Sn$ ) have been measured as shown in Table 1-1, and such rates have been used as fundamental data in designing synthetic radical reactions as well as in kinetic studies. The reactivities of metal hydrides towards alkyl radicals increase as  $R_3M-H$  bond strengths decrease along the series  $M = Si < Ge < Sn$ . The reaction of *t*-butoxyl radicals towards the  $R_3MH$  hydrides are much faster than the alkyl radicals, which are attributed to the polar effect lowering the activation energies of the reactions. The constants of the Evans-Polanyi equation ( $\alpha/RT$ ) for alkyl and *t*-butoxyl radicals are 0.5 and 0.22, respectively. Thus, a smaller value of  $\alpha/RT$  seems to indicate a stronger polar effect in the transition state.

Some reduction reactions which involve fluorinated radicals are discussed in Chapter 2, but there had been no quantitative data, especially no data on the rate constants for perfluoro-*n*-alkyl radicals with the various hydrides, before this work.

Alkyl groups increase the rates of the 5-exo cyclization of 5-hexenyl radicals except when alkyl groups are on the olefinic bond at  $C_5$ . This presence retards the rates of the ring closure of the radicals. Alkyl groups introduce a steric effect which becomes an important effect in the cyclization reactions, but a polar influence can be observed when alkyl groups are at the radical centers. Electron donors and acceptors introduce polar effects which can be rationalized by the FMO theory. Reversibility of the ring closure of substituted 5-hexenyl radicals has been observed but only in the cases where radicals are highly stabilized.

Fluorinated 5-hexenyl radicals have been less studied and we present a quantitative study of their cyclizations in Chapter 4. There had been no quantitative data in this area before our work.

## CHAPTER 2

### FLUORINE AS SUBSTITUENTS IN THE RADICAL ADDITION AND CYCLIZATION REACTIONS

#### Introduction

The effects exhibited by fluorine as a substituent are due to three inherent characteristics of the fluorine atom: 1) small relative size, 2) extreme electronegativity and 3) non-bonded electron pairs.

Fluorine is the most electronegative of all elements with a Pauling scale value of 4.10 as compared with oxygen (3.50), chlorine (2.83), bromine (2.74), carbon (2.50), and hydrogen (2.20).<sup>5a</sup> Strong polarization of fluorinated molecules through the  $\sigma$  bonding framework and through space (field effects) are an artifact of fluorine's large electronegativity. On the other hand, similar dimension in the orbitals makes it more efficient to accommodate three lone pair electrons to the p orbitals on carbon.<sup>5b</sup> Because of these two factors, fluorine exhibits an interesting donor/acceptor contradiction under certain circumstances in which the strong removal of electron density from a bonded atom (e.g. carbon) can be offset due to back donation of density from the non-bonded electrons. The Van der Waals radii size of fluorine is 1.47 Å as compared with hydrogen (1.20 Å), carbon (1.70 Å), chlorine (1.73 Å), bromine (1.84 Å) and iodine (2.01 Å). Thus, fluorine should exhibit minimal or no effect on the steric environment in a hydrocarbon upon substitution of C-F for C-H.

The potentially strong electronic influences of fluorine, its negligible size, and its NMR-active nucleus that has a very broad range on chemical shifts make it unique as a substituent and particularly effective for use in a probing mechanism.

## The General Effect of the Fluorine Substituent in Organic Chemistry

### Fluorine Substituents in $sp^3$ Carbon Systems

The strengthening and incremental shortening of the C-F bond in the series of fluoromethanes <sup>45</sup> are shown in Table 2-1. This trend of bond strengthening with increased fluorines as substitution is unique to fluorine among the halogens. The series of chlorinated methanes exhibit a similar bond shortening but it is accompanied by an incremental weakening: 83.7 kcal mol<sup>-1</sup> down to 72.9 kcal mol<sup>-1</sup> per first C-Cl bond homolysis in transcending from CH<sub>3</sub>Cl to CCl<sub>4</sub>.<sup>45</sup>

Table 2-1. C-F bond lengths and dissociation energies in fluoromethanes <sup>45</sup>

Fluoromethane	$r$ (C-F) (Å)	$D^0$ (C-F) (kcal mol <sup>-1</sup> )	$D^0$ (C-H) (kcal mol <sup>-1</sup> )
CH <sub>3</sub> F	1.385	109.0	101.2
CH <sub>2</sub> F <sub>2</sub>	1.358	122	103.2
CHF <sub>3</sub>	1.332	128.0	106.7
CF <sub>4</sub>	1.317	129.7	--

The fluorination also affects the C-C bond lengths, and strengths in fluoroethanes are shown in Table 2-2.<sup>46</sup> Geminal fluorination leads to strengthening and shortening of C-C bond in the series CH<sub>3</sub>-CH<sub>3</sub> to CF<sub>3</sub>-CF<sub>3</sub>, but the C-C bond lengths increase and the C-C bond strength decreases upon vicinal fluorination from CH<sub>3</sub>-CF<sub>3</sub> to CF<sub>3</sub>-CF<sub>3</sub>. The trends in C-C bond strengths and lengths with various degrees of fluorination have not been fully understood; however, valence bond arguments have been used to rationalize the observed trends in C-F bonding in alkanes. It is rationalized for carbon substituted with two or more fluorines, that negative hyperconjugation, as shown in the classical sense by Figure 2-1, leads to increased bond order between the carbon and fluorine

Table 2-2. Bond lengths and dissociation energies in fluoroethanes

Fluoroethane	$r$ (C-C) ( $\text{\AA}$ )	$D^0$ (C-C) ( $\text{kcal mol}^{-1}$ )	$D^0$ (C-F) ( $\text{kcal mol}^{-1}$ )
$\text{CH}_3\text{-CH}_3$	1.532	90.4	--
$\text{CH}_3\text{-CH}_2\text{F}$	1.502	91.2	107.7
$\text{CH}_3\text{-CHF}_2$	1.498	95.6	unknown
$\text{CH}_3\text{-CF}_3$	1.494	101.2	124.8
$\text{CH}_2\text{F-CF}_3$	1.501	94.6	109.4 ( $\text{CH}_2\text{F}$ )
$\text{CF}_3\text{-CF}_3$	1.545	98.7	126.8

Figure 2-1. Fluorine hyperconjugation leads to shortened bond C-F<sup>47,48</sup>

in which the non-bonded electron pairs on fluorine overlap with the orbital of carbon.<sup>47,48</sup> As the degree of geminal fluorination increases, the number of valence bond structures involving doubly bonded fluorines increases and the C-F bond becomes increasingly shorter and stronger. Theoretical calculations at the ab initio level have confirmed such a bonding scheme where it is found that the stabilizing interaction arises from back-donation of a fluorine lone pair into an antibonding  $\sigma^*_{\text{C-F}}$  orbital.<sup>47,48</sup> On the other hand, the argument which inherently does not involve the non-bonding electrons on fluorine suggests that when carbon is bonded to more electronegative elements, atomic p character concentrates in orbitals directed towards the electronegative species since p electrons are less tightly bonded than s electrons.<sup>49,50a</sup> Carbon rehybridization then assists in accounting for bonding and geometry trends in fluoro-organics. The other argument based on

Coulombic interactions between oppositely charged fluorine and carbon predicts an increase in C-F bond ionic character meaning an increase of positive charge on carbon as the degree of fluorination increases.<sup>50b</sup>

The variety of rationalizations for C-F bonding in such simple systems illustrates the complexities in theoretically, and certainly quantitatively explaining bonding trends in saturated fluoro-organics.

### Fluorine as Substituents in $sp^2$ Carbon Systems

Fluorine substitution at a vinylic carbon leads to substantial changes in alkene geometry and reactivity. The data in Table 2-3 reveal that fluoroethylenes have shorter C=C bonds than ethylene and the C-F bond lengths are shorter than geminal or vicinal fluorinated alkenes.<sup>45,46</sup> The bond angles (F-C-F) in geminal difluorinated olefins which are much smaller than ethylene can be rationalized by non-bonded attraction of lone pair electrons on the geminal fluorines.<sup>51,52</sup> The C=C and C-F bonds shortening can be attributed to the effect of fluorine on a planar molecule: Perfluoro effect.<sup>53</sup>

Table 2-3. Structural aspects of fluoroethylenes<sup>45,46</sup>

	CH <sub>2</sub> =CH <sub>2</sub>	CH <sub>2</sub> =CHF	CH <sub>2</sub> =CF <sub>2</sub>	CHF=CF <sub>2</sub>	CF <sub>2</sub> =CF <sub>2</sub>
r(C-C) Å	1.339	1.333	1.315	1.309	1.311
r(C-F) Å	-	1.348	1.323	1.32	1.319
H-C-H <sub>deg</sub>	117.8	120.4	121.8	-	-
H-C-F <sub>deg</sub>	-	115.4	-	116.2	-
F-C-F <sub>deg</sub>	-	-	109.3	112.2	112.5
D <sup>0</sup> <sub>π(C=C)<sub>deg</sub></sub>	59.1	Unknown	62.1	Unknown	52.3

Brundle and co-workers<sup>53</sup> have proposed a perfluoro effect based on the study of the successive ionization potentials (IP.) in fluorinated ethylenes (Table 2-4). They stated:



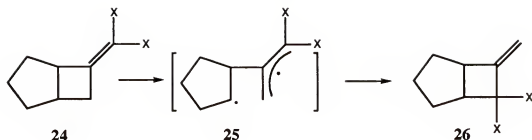
Table 2-4. Vertical Ionization Potentials (IP) and Electron Affinities (EA) of Ethylene and Fluoroethylenes

Fluoroethylenes	IP. ( $\pi$ , eV) <sup>a</sup>	EA. ( $\pi$ , eV) <sup>b</sup>	IP. ( $\sigma$ , eV) <sup>c</sup>
CH <sub>2</sub> =CH <sub>2</sub>	10.51	1.78	12.85
CH <sub>2</sub> =CHF	10.56	1.91	13.79
CH <sub>2</sub> =CF <sub>2</sub>	10.69	2.18	14.79
cis-CHF=CHF	10.44	1.84	13.97
trans-CHF=CHF	10.38	2.39	13.90
CF <sub>2</sub> =CHF	10.54	2.45	14.64
CF <sub>2</sub> =CF <sub>2</sub>	10.56	3.00	15.95

<sup>a</sup> Ref. 54, <sup>b</sup> Ref. 55, <sup>c</sup> Ref. 53

" the substitution of fluorine for hydrogen in a planar molecule has a much larger stabilizing effect on the  $\sigma$  MO's than the  $\pi$  MO's." (p. 1451) The data of vertical IP of ethylene and the fluoro-ethylenes in Table 2-4 show that there is only a slight variation of the IP ( $\pm 0.20$  eV) throughout the fluoroethylene series, whereas the  $\sigma$  IP is progressively shifted upward over 3 eVs from ethylene to tetrafluoroethylene. Analysis of the wave functions<sup>53</sup> shows that in the perfluoro compounds, the  $\sigma$  MOs are appreciably delocalized over the fluorine atoms, and are strongly stabilized by the high effective nuclear charge of that atom. In the  $\pi$  MOs, the delocalization onto the fluorine atoms is much less, and its stabilizing effect is counteracted by a strong  $\pi$  antibonding between the fluorine atom and the carbon atom to which it is  $\sigma$  bonded. It is noteworthy that electron affinities of fluoroethylenes are also increased as the degree of fluorination increases on the double bond, which indicates that fluorination of ethylene destabilizes the  $\pi^*$  anions with respect to that of ethylene.<sup>55</sup>

In the study of thermal rearrangement of **24** to **26**, Dolbier *et al*<sup>56</sup> have found that



activation parameters are almost identical when  $X = H$  or  $F$ . This has been the evidence that the overall effect of fluorination on the stability of free radicals would seem to be minimal. But it should also be the evidence of the perfluoro effect on the fluorinated allyl radical (25) which has similar reactivity with respect to the unfluorinated allyl radical. It is noteworthy that the perfluoro effect should be stronger with the increase of fluorine substituents on the double bond. The thermodynamic study<sup>57</sup> on the mono-fluoropropene 27 and the difluoro propene 28 as shown in Figure 2-2 has indicated that a single fluorine substituent actually stabilizes a  $\pi$  system, while the geminal difluoro substitution leads to the  $CF_2$  group which is stabilized in the  $sp^3$  orbitals.

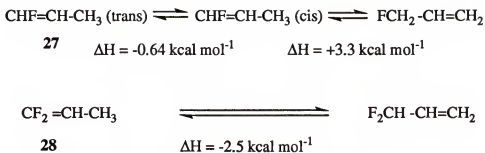


Figure 2-2. Thermodynamic Study on the Mono and Difluoro Propenes

### Fluorine Non-bonded Electron Interaction

Interaction of fluorine non-bonded electrons has related precedent in the case of  $\alpha$ -fluoro carbanions. Such systems are found to be destabilized in situations where the carbon bearing the negative charge and fluorine are planar.<sup>58</sup> Figure 2-3 illustrates the

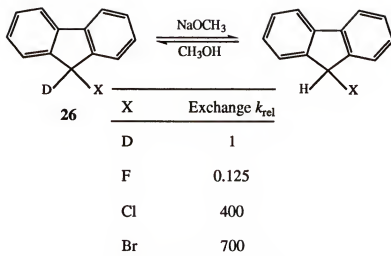


Figure 2-3. Destabilization in Planar  $\alpha$ -Fluorocarbanions<sup>59</sup>

rate inhibition in isotope exchange in 9-fluorofluorene relative to fluorene-9- $d_2$  (26) and other 9-halogenofluorenes.<sup>59</sup> Conjugative destabilization is invoked in this case between the fluorine non-bonded electron pairs and the planar carbanion.

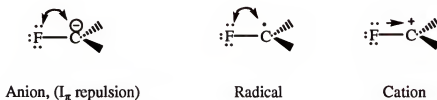
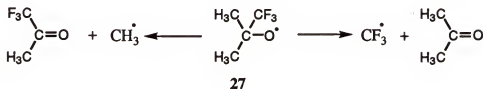


Figure 2-4.  $\alpha$ -fluoro interaction of anion, radical and cation

Destabilization in planar  $\alpha$ -fluorocarbanions is rationalized by the  $I_\pi$  repulsion<sup>58</sup> (Figure 2-4), first proposed by Tedder and by Burdon. It is considered simply as repulsion between lone pairs of electrons around fluorine and centers of high electron density. The repulsion is not to say the overall electron attraction of fluorine is overcome, but it is just the result of the strong electron withdrawing effect of fluorine and its comparable size with carbon. For the anion, the repulsion will be stronger when fluorine substitution is increased. For the cation, however, any fluorine substitution at  $\alpha$  carbon can stabilize it. Direct evidence for the stabilization of carbocations by  $\alpha$  substituted

fluorine has been obtained and the ascending order of stability in the series of fluoromethyl cabocations is  ${}^+\text{CH}_3 < {}^+\text{CF}_3 < {}^+\text{CH}_2\text{F} < {}^+\text{CHF}_2$ .<sup>60,61</sup>



In the case of the radical, it becomes complicated. However, one still can expect that with strong repulsion, the trifluoromethyl radical  $\text{CF}_3^\bullet$  would be destabilized with respect to the methyl radical  $\text{CH}_3^\bullet$ . The experimental support<sup>62</sup> for this proposal is of the evidence in the radical fragmentation of **27** in which the methyl radical is formed ten times as faster than the trifluoromethyl radical. Pasto and co-workers<sup>63</sup> reported the radical stabilization energies (RSEs) of the various fluorine and fluoromethyl substituents which were calculated according to the isodesmic reaction (equation 2-1). A single fluorine is

Table 2-5. Radical Stabilization Energies (RSE) for Substituent Attached to the Methyl Radical ( $\text{RSE} = \Delta\text{H}$  in equation 2-1)<sup>63</sup>

$\text{X}_n \dot{\text{C}}\text{H}_{3-n} + \text{CH}_4 \longrightarrow \text{X}_n \text{CH}_{4-n} + \dot{\text{C}}\text{H}_3$		$\Delta\text{H} \quad (2-1)$	
X	RES (kcal mol <sup>-1</sup> )	X	RES (kcal mol <sup>-1</sup> )
F	+1.64	CH <sub>3</sub>	+3.27
F <sub>2</sub>	+0.56	CH <sub>3</sub> O	+5.30
F <sub>3</sub>	-4.21	CN	+5.34
FCH <sub>2</sub>	+1.46	HS	+5.66
F <sub>2</sub> CH	+0.16	H <sub>2</sub> S <sup>+</sup>	-3.17
F <sub>3</sub> C	-1.34	H <sub>3</sub> N <sup>+</sup>	-4.07
		H <sub>3</sub> P <sup>+</sup>	-0.42

slightly radical stabilizing (relative to hydrogen). Increased fluorine substitution results in a decrease in the stabilization of the radical center, with three fluorines having a substantial destabilizing effect. Table 2-5 also shows the effect of  $\beta$  - fluorine substitution on the stability of radicals. Again, increasing fluorine substitution at the  $\beta$  - position of the radicals results in decreasing stability of radicals; the mono and difluoromethyl groups are slightly stabilizing the radicals but the trifluoromethyl group is destabilizing the radical. The destabilizing effect of  $\text{CF}_3$  could appear to be due to an inductive effect,<sup>63</sup> which will also be evident with several other functional groups ( $\text{H}_2\text{S}^+$ ,  $\text{H}_3\text{N}^+$  and  $\text{H}_3\text{P}^+$ ).

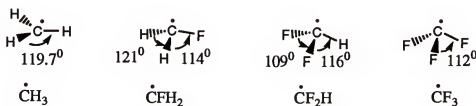


Figure 2-5. The Structures of the Methyl and Fluoromethyl Radicals in the Ground State<sup>64b</sup>

Table 2-6. SOMO Energies of the Fluoromethyl Radicals<sup>64</sup>

Structure	$E_{\text{SOMO}}$ (eV)	Ref.
$\text{CH}_3$	-9.8	22
$\text{CH}_2\text{F}$ planar	-10.645	63
nonplanar	-10.994	
$\text{CHF}_2$ planar	-10.845	63
nonplanar	-12.088	
$\text{CF}_3$ planar	-11.100	63
nonplanar	-19.550	

Fluorine's non-bonded interaction also affect the structure of the fluoromethyl radicals in the ground state. Table 2-6 shows the structures of the methyl and the fluoro methyl radicals.<sup>64</sup> The methyl radical has a planar structure and it is a  $\pi$ -type<sup>65</sup> radical with the free electron located in a carbon p orbital. The  $\text{CH}_2\text{F}$  radical is nearly planar, but the  $\text{CF}_2\text{H}$  and  $\text{CF}_3$  radicals have pyramidal structures and they are considered to be of the  $\sigma$ -type radicals

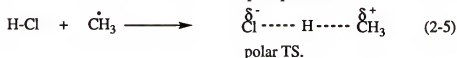
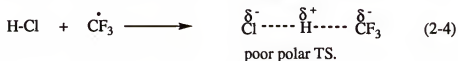
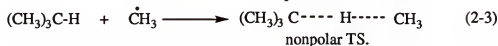
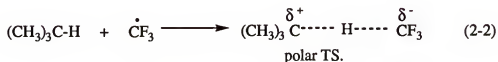
with the free electron located in the carbon  $sp^3$  hybridized orbital.<sup>65</sup> The nonplanar fluoromethyl radicals are all lower in energy than the planar structures because of the fluorine non-bonded interaction. The SOMO energies of the fluoromethyl radicals in planar and non-planar structures are calculated by Pasto<sup>63</sup> as shown in Table 2-6.

### The Effect of Fluorine Substitution on H-atom Transfer Reactions

The electronic nature of fluorine substituents and its small size make polar effects very important in the way that fluorine substituents affect reaction transition states. For example, in the hydrogen abstraction by  $\text{CH}_3^\cdot$  and  $\text{CF}_3^\cdot$  from alkanes, the reaction for  $\text{CF}_3^\cdot$

Table 2-7. Arrhenius Parameters<sup>10</sup> for Hydrogen Abstraction by  $\text{CH}_3^\cdot$  and  $\text{CF}_3^\cdot$

H-donor	$\text{CH}_3^\cdot$		$\text{CF}_3^\cdot$	
	logA	$E_a$	logA	$E_a$
$\text{CH}_3\text{-H}$	8.8	14.2	8.9	11.3
$\text{CH}_3\text{CH}_2\text{-H}$	8.8	11.8	8.4	6.9
$(\text{CH}_3)_2\text{CH-H}$	8.8	10.1	8.1	6.5
$(\text{CH}_3)_3\text{C-H}$	8.3	8.0	7.7	4.9
$\text{H-Cl}$	-	2.5	-	5.0



is always faster than for  $\text{CH}_3\cdot$  (Table 2-7). An important factor is that the height of the energy barrier is lowered by polar forces in the transition state. The fluorine substituents in  $\text{CF}_3\cdot$  make the radical be a 'electrophilic' one in comparison with the methyl radical which is a 'nucleophilic' species. When alkanes are the hydrogen donors, the electrophilic species, trifluoromethyl radical, will facilitate the formation of a polar transition state (equation 2-2) in comparison with the nucleophilic methyl radical (equation 2-3).

The polar effect do not always make fluorinated radicals more reactive than hydrocarbon radicals. It depends on the electronic nature of both the radical and the hydrogen donor. In the case of hydrogen abstraction from hydrogen chloride (Table 2-7), the polar effect retards the reaction of trifluoromethyl radicals with the hydrogen chloride while the reaction of methyl radicals with the hydrogen chloride is enhanced by the polar effect (equations 2-4 and 2-5). The electronegative chlorine atom with the electrophilic trifluoromethyl radical will form a 'poor polar transition state' with a higher energy barrier, while the nucleophilic methyl radical will release electron in forming the transition state to facilitate the formation of a polar transition state.

### The Effects of Fluorine Substituents on Radical Addition Reactions

#### Intermolecular Addition Reactions

The rate constant of trifluoromethyl radical's addition to ethylene has been measured by Tedder and Walton<sup>66</sup> and his coworkers as shown in Table 2-8. In comparison with the rate constants of  $\text{CH}_3\cdot$  and  $\text{CF}_3\cdot$  radicals addition to ethylene, it shows that the fluorinated radical reacts faster with ethylene than the methyl radical, in which trifluoromethyl radicals behave as "electrophiles," and thus add rapidly to nucleophilic double bonds such as ethylene. For trifluoromethyl radicals, however, addition to tetrafluoroethylene as shown in Table 2-9, is slower than that of methyl radicals,<sup>14</sup> In this case, trifluoromethyl radicals are adding to the electrophilic double bond of tetrafluoroethylene. Such reactions are all influenced by the polar effect which is induced

Table 2-8. Absolute Rate Constants for  $\text{CH}_3$  and  $\text{CF}_3$  radicals addition to Ethylene<sup>66</sup>

Radical	$\log k$ (164 <sup>0</sup> C)	$\log A$	$E_a$ kcal mol <sup>-1</sup>
$\text{CH}_3^\bullet$	4.7	8.5	7.7
$\text{CF}_3^\bullet$	6.6	8.0	2.9

Table 2-9. Relative Parameters for Addition  $\text{CH}_3$  and Fluorinated Methyl Radicals to Ethylenes and Tetrafluoroethylenes<sup>14</sup>

Radical	$k_{\text{C}_2\text{F}_4} / k_{\text{C}_2\text{H}_4}$	$E_{\text{C}_2\text{F}_4} / E_{\text{C}_2\text{H}_4}$
$\text{CH}_3^\bullet$	6.0	-2.5
$\text{CH}_2\text{F}^\bullet$	3.4	-1.3
$\text{CHF}_2^\bullet$	1.1	-0.2
$\text{CF}_3^\bullet$	0.1	+1.7

Table 2-10. Absolute Rate Constants for the Reactions of perfluoro-n-alkyl Radicals with Various Unsaturated Substrates at 298K<sup>42</sup>

Substrate	$k_{\text{add}} \times 10^{-6} \text{ M}^{-1} \text{ s}^{-1}$			
	$\text{C}_2\text{F}_5^\bullet$	$\text{n-C}_3\text{F}_7^\bullet$	$\text{n-C}_7\text{F}_{15}^\bullet$	$\text{n-C}_8\text{F}_{17}^\bullet$
Styrene	-	43	46	46.2
$\alpha$ -methyl styrene	94	78	89	89.3
4- $\text{CF}_3$ - $\text{C}_6\text{H}_4$ CH=CH <sub>2</sub>	-	29	24	24.3
1-hexene	16	6.2	<b>7.9</b>	-
CH <sub>2</sub> =CH-CN	3.2	2.2	1.6	2.0



by fluorine substitution in the transition state of the radical addition reactions. Table 2-8 shows that with the increase of electrophilicity of radicals (increase of the degree of fluorination), addition to ethylene is more facilitated while addition to tetrafluoroethylene becomes more retarded.

The discussion above has shown that the trifluoromethyl radical is more reactive toward ethylene than is the methyl radical. Thus, it would be expected that the absolute reactivities of perfluoro-n-alkyl radicals and alkyl radicals should be significantly different. Ingold and Dolbier *et al*<sup>42</sup> have measured the absolute kinetics of the addition of perfluoro-n-alkyl radicals to alkenes using LFP and conventional competitive kinetics. The results are shown in Table 2-10. In comparing the alkyl radical with the perfluoro-n-alkyl radical, one can see that the electrophilicity of the perfluoro-n-alkyl radical is an important factor in giving rise to their high reactivities. The frontier molecular orbital theory has been applied to explain such a polar effect<sup>42</sup> in the addition reactions, in which the SOMO-HOMO interaction is expected to be a dominant factor because of the low-lying SOMO orbital for the perfluoro-n-alkyl radical.

The data in Table 2-10 show that the  $C_2F_5\cdot$  is a little more reactive than the  $n-C_3F_7\cdot$  toward alkenes, but there is little or no difference in the rate of addition of  $n-C_3F_7\cdot$ ,  $n-C_7F_{15}\cdot$  and  $n-C_8F_{17}\cdot$  to alkenes. Thus, it seems likely that the reactivities of all homologous perfluoro-n-alkyl radicals ( $n-C_nF_{2n+1}\cdot$ ,  $n > 3$ ) can be defined by the reactivities of the  $n-C_3F_7\cdot$  and  $n-C_7F_{15}\cdot$  radicals. In rationalizing the different reactivities of the perfluoroethyl and perfluoro-n-propyl radicals, it has been said<sup>42</sup> that the extra  $\beta$ -fluorine substituent in  $C_2F_5\cdot$  provides greater electron withdrawing power (via fluorine hyperconjugation) than the  $CF_3$  group in  $n-C_3F_7\cdot$ .

The effects of fluorine atoms or perfluoroalkyl groups on the bonded carbon are different, in which the fluorine substituent introduces both the inductive and the electron donating effects on the bonded carbon while the perfluoroalkyl group (like  $CF_3CF_2\cdot$  group) introduces the electron withdrawing power as the major effect. This has been proved by the hydrogen isotope exchange experiment<sup>67</sup> in which the acidity of the  $CF_3(CF_2)_3CF_2-H$  is


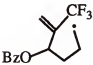
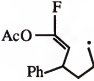
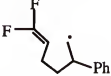
about 10 times greater than that of  $\text{CF}_3\text{-H}$ . Based on this, the trifluoromethyl radical should be a less electrophilic species relative to the perfluoro-*n*-alkyl ( $n > 3$ ) radicals.

Lloyd and Rogers<sup>68</sup> and Frusic and Krusic<sup>69</sup> studied the structures of perfluoroalkyl radicals through ESR experiment and they found that the non-planarity of fluorinated radicals depends most on the number of  $\alpha$ -fluorine atoms. That is, the geometry of the perfluoroethyl, perfluoro-isopropyl and perfluoro-*t*-butyl radicals are almost the same as those of the difluoromethyl, monfluoromethyl and methyl radicals, respectively. Thus, it is expected that perfluoro-*n*-alkyl radicals will have the same nonplanar geometry as that of the difluoromethyl radical.

#### Intramolecular Addition Reactions: 5-Hexenyl Radical Cyclization

The quantitative study on the effect of the fluorine substituent on the 5-hexenyl radical cyclization has not been seen in the literature, but some synthetic use of fluorinated 5-hexenyl radical cyclizations has been reported.<sup>70</sup> The regiochemistry of cyclization of

Table 2-11. Regiochemistry of Cyclization of Fluorinated 5-hexenyl Radicals<sup>70</sup>

Radical	5 exo product %	6 endo product %	Ref.
	83	undetected	70a
	8	86	70b
	88	undetected	70c
	77	undetected	70c

fluorinated 5-hexenyl radicals is similar to that of hydrocarbon systems, in which the cyclization is mostly cyclized through the 5-exo pathway to produce 5-exo products as shown in Table 2-11. However, in the case of the trifluoromethyl group at C<sub>5</sub> (the vinyl position), that the 6-endo product is the major one indicates that the 6-endo ring closure ( $k_{C_6}$ ) is faster than the 5-exo pathway, which is the same as for the methyl group at the same position.

### Conclusion

Fluorine is both the smallest and the most electronegative atomic substituent, and it is the best  $\pi$  donor of the halogen substituents. Its high electronegativity and effective orbital overlap combine to result in a C-F  $\sigma$  bond which is both strong and short, and its non-bonded electron interaction destabilizes the anion as well as the radical; however, it stabilizes the cation respect to hydrocarbon analogues. The combination of electronegativity with the  $\pi$  donor effect of fluorine results in the perfluoro effect, the influence of fluorine on the  $\sigma$  bond being stronger than the  $\pi$  bond, which reflects the effect of fluorine substituents on the reactivity of a planar molecule.

The polar effect is a dominant factor for the fluorine effects regarding the abstraction of an H-atom from alkyl hydrogen donors by trifluoromethyl radicals as well as for the addition of trifluoromethyl radicals to alkenes, wherein the reactivities of trifluoromethyl radicals are higher than alkyl radicals. The fact that a perfluoro-n-alkyl radical ( $C_nF_{2n-1}^{\cdot}$ ;  $n \geq 3$ ) is a more reactive species towards alkenes than a trifluoromethyl radical indicates that the trifluoromethyl radical is a less electrophilic species relative to the perfluoro-n-alkyl radical. Based on the result that the rate of the perfluoro-n-alkyl radical with the tin hydride is about 100 times as fast as that of alkyl radical with the tin hydride, one can expect that the other metal hydrides (Table 1-1) will react faster with perfluoro-n-alkyl radicals than alkyl radicals.

There has not been any quantitative study reported on fluorinated 5-hexenyl radical before this work, however, some results in Table 2-11 show that the ring closure of

fluorinated 5-hexenyl radical give 5-exo product as the major product except the one where the trifluoromethyl group is at the C<sub>5</sub> of the radical.

The polar effect in the perfluoro-radical system could be rationalized readily by the lower-lying SOMO of the radical which interacts with HOMO of M-H in hydrides or HOMO of olefinic bonds in alkenes more efficiently leading to dramatic rate enhancements.

## CHAPTER 3

### THE REACTIVITY OF PERFLUOROALKYL RADICALS WITH SOME H-ATOM DONORS IN LIQUID SOLUTION

#### Introduction

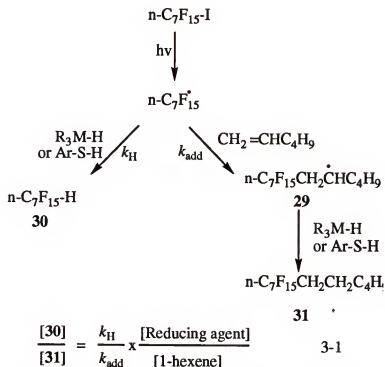
Radicals have become very important intermediates for use in carbon-carbon bond forming reactions. Most productive radical-based synthetic processes are chain reactions in which one of the key propagation steps involves transfer of a hydrogen atom from some reducing agent such as tributyltin hydride (Scheme 1-2, steps 8 and 9). In such cases, identification of the most efficacious reducing agent is always a critical aspect of the reaction, often determining the success or failure of the desired radical addition, cyclization, rearrangement and fragmentation processes which will be taking place in competition with the radical reduction.

When the radical in question is an alkyl radical there generally is no problem in finding a suitable reducing agent with an appropriate reduction rate constant for the situation, since there exists a vast spectrum of H-atom donors<sup>43</sup> with accurately determined bimolecular rate constants for reduction ranging between  $6.4 \times 10^2 \text{ M}^{-1} \text{ s}^{-1}$  for  $\text{Et}_3\text{SiH}$  and  $2.3 \times 10^9 \text{ M}^{-1} \text{ s}^{-1}$  for  $\text{PhSeH}$  at room temperature. In contrast, a similar arsenal of kinetically-well-defined reducing agents has not heretofore been available for studies of fluorinated radicals. Based on the higher reactivity of trifluoromethyl radicals with respect to methyl radicals (Table 2-7), one would expect that a perfluoro-n-alkyl radical with its high electrophilicity should exhibit significantly modified kinetic behavior towards reducing agents relative to its nucleophilic alkyl radical counterpart. With the recent laser flash photolysis experiments<sup>42,71</sup> providing absolute rate constants for a large number of

perfluoro-n-alkyl radicals to alkenes, it has now become possible to determine such rates of hydrogen abstraction using competition experiments.

### Absolute Rate Determination of Hydrogen Abstraction for Perfluoro-n-alkyl Radicals

Making use of the competition kinetic method, we have successfully measured the absolute rate constants of hydrogen atom abstraction by perfluoro-n-alkyl radicals <sup>72,73</sup> for a series of hydrides ( $R_3M-H$ ,  $M=Si, Ge, Sn$ ) as well as for a series of arene thiols at room temperature. In order to use the competition kinetic method,<sup>43</sup> one must first choose the perfluoro-n-alkyl radical precursor which will generate free radicals with reducing agents in the chain processes, after which one must design the two competing channels for the perfluoro-n-alkyl radical; one channel should be the hydrogen abstraction reaction with an unknown rate constant  $k_H$  being determined and the other should be the reaction with a known absolute rate constant  $k$ , where the radical will be converted to products which will be stable under the kinetic conditions.



Scheme 3-1. Rate Determination of Hydrogen Abstraction for Perfluoroalkyl Radicals

A typical designed experiment is shown in Figure 3-1. Perfluoro-n-heptyl iodide ( $\text{n-C}_7\text{F}_{15}\text{-I}$ ) is chosen as the radical precursor.<sup>42,74</sup> It has a strong UV absorption at 276.5 nm which can be used for photoinitiation. The competing channels are the reactions in which hydrogen abstraction with the unknown  $k_{\text{H}}$  competes with the radical addition to 1-hexene with the rate constant  $k_{\text{add}}$  which has been measured by LFP to be  $7.9 \times 10^6 \text{ M}^{-1} \text{ s}^{-1}$  at  $298^\circ\text{K}$ .<sup>42,71</sup> The reduced product **30** and the addition product **31** are stable to the reaction conditions and they can be determined quantitatively by  $^{19}\text{F}$  NMR analysis of the  $\text{CF}_2\text{H}$  peak ( $\delta$  -138.1ppm, d) of **30** and the  $\text{CF}_2\text{CH}_2$  peak ( $\delta$  -114.4 ppm, t) of **31**. In a series of rate determinations using various reducing agents, the products analyzed by  $^{19}\text{F}$  NMR are the same, the reduced product, **30**, and the addition product, **31**, since the only component changed in the whole competition system from one determination to another one is the reducing agent being used for rate determination. The final analysis of the data, obtained for varied concentrations of 1-hexene and the reducing agent which both are at least nine-fold in excess with respect to the radical precursor, is based on equation 3-1 deduced from equation 1-12; the ratio of the rate constants ( $k_{\text{H}} / k_{\text{add}}$ ) is found by the slope of a plot of the ratio, **30/31**, as a function of the ratio,  $[\text{Reducing agent}]/[\text{1-hexene}]$ . Since the value for  $k_{\text{add}}$  for  $\text{n-C}_7\text{F}_{15}\cdot$  to 1-hexene is known, it is thus possible to convert the ratio of rate constants ( $k_{\text{H}} / k_{\text{add}}$ ) to the values for  $k_{\text{H}}$ , the absolute rate constant of hydrogen atom abstraction for perfluoro-n-alkyl radicals.

#### The Rates Determination for Perfluoroalkyl Radicals ( $\text{R}_\text{f}\cdot$ ) with *tris*(trimethylsilyl)silane $(\text{TMS})_3\text{Si-H}$

In Scheme 3-1, if  $\text{R}_3\text{M-H} = (\text{TMS})_3\text{Si-H}$ , it will represent the competition kinetic method for the rate determination for perfluoroalkyl radicals with *tris*(trimethylsilyl)silane. However, when one starts to design a set of competition reactions, it is important to estimate the rate constant being measured so that one can find the best kinetic condition for the competition process. For the reason of the product analysis (the ratio of **30/31** being

Table 3-1. Data for the Reaction of Perfluoro-n-heptyl Radicals with (TMS)<sub>3</sub>SiH

No. of rxn <sup>a</sup>	C <sub>7</sub> F <sub>13</sub> I (M)	(TMS) <sub>3</sub> SiH (M)	1-Hexene (M)	[(TMS) <sub>3</sub> SiH]/[1-Hexene]	30/31	Y <sup>c</sup> %
Fts-R31	0.094	1.813	3.344	0.542	3.440	97
Fts-R32	0.094	1.693	3.684	0.460	2.955	98
Fts-R33	0.094	1.541	4.052	0.380	2.295	100
Fts-R34	0.094	1.360	4.494	0.303	1.840	98
Fts-R35	0.094	1.148	5.010	0.229	1.416	96
Fts-R36	0.094	1.907	5.600	0.162	1.001	94

a: The total volume of each reaction was kept at 0.548 ml during photo-reaction, and 0.25ml of

C<sub>6</sub>D<sub>6</sub> was added in for NMR analysis.

b: From <sup>19</sup>F NMR; the ratio of integral of CF<sub>2</sub>-H (-138.1 ppm) to that of CF<sub>2</sub>-CH<sub>2</sub> (-114.4 ppm).

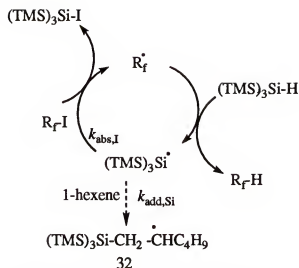
c: From <sup>19</sup>F NMR; Ph-CF<sub>3</sub> as internal standard.

closer to unity), the value of  $k_{\text{add}}$  [1-hexene] should be closer to the value of  $k_{\text{H}}$  [(TMS)<sub>3</sub>Si-H]. As the rate for the *tris*(trimethylsilyl)silane with hydrocarbon n-alkyl radicals is about 6 times as slow as with tributyltin hydride (Table 1-1), it is expected that the rate for *tris*(trimethylsilyl)silane with perfluoroalkyl radicals will be slower than that of the tributyltin hydride ( $2.02 \times 10^8 \text{ M}^{-1} \text{ s}^{-1}$ ). Based on this expectation, the concentrations of the *tris*(trimethylsilyl)silane and 1-hexene were designed as shown in Table 3-1. To fit the requirement of equation 3-1 (pseudo-first-order condition for both reactions), the concentration of the radical precursor, perfluoro-n-heptyl iodide, is at least ten-fold less than that of the *tris*(trimethylsilyl)silane and 1-hexene.

It is also important to have close to a quantitative conversion (or recovery) of the radical precursor. The overall yield for 30 and 31 combined in Table 3-1 indicates that except for the competing channels in which the reactions take place for the radicals, there is no other significant, undesirable reaction taking place for the radicals. This is a necessary requirement for getting a set of accurate data in competition reactions.

Because there are at least three compounds in the reaction system, during the chain process some side-reaction might take place. For example, in the propagation steps for the





Scheme 3-2. Propagation Steps for Reduction Reaction of Perfluoro-n-alkyl radicals

reduction reaction of perfluoro-n-alkyl radicals as shown in Scheme 3-2, the formed *tris*(trimethylsilyl)silyl radical might have chance to react with 1-hexene (in a high concentration)  $k_{\text{add,Si}}$  and form radical 32, which would compete with the next chain step  $k_{\text{abs,I}}$  where the silyl radical reacts with the radical precursor to generate new perfluoro-n-alkyl radicals. As a result, the influence of such a side-reaction on the propagation steps would depend on the relative values of the rate constants  $k_{\text{abs,I}}$  and  $k_{\text{add,Si}}$ . However, there are no absolute rate constants for the reactions of *tris*(trimethylsilyl) silyl radicals with 1-hexene and with perfluoro-n-heptyl iodide. Table 3-2 shows some available absolute rate

Table 3-2. Absolute Rate Constants for Some Reactions of Metal Radicals at Room Temperature ( $k$ ,  $\text{M}^{-1} \text{s}^{-1}$ )

Substrate	$\text{Me}_3\text{SiSiMe}_2^\bullet$ <sup>a</sup>	$\text{Et}_3\text{Si}^\bullet$ <sup>a</sup>	$\text{Bu}_3\text{Ge}^\bullet$ <sup>b</sup>	$\text{Bu}_3\text{Sn}^\bullet$ <sup>b</sup>
1-hexene	$3.9 \times 10^6$	$4.8 \times 10^6$	--	--
n-propyl iodide	--	$4.3 \times 10^9$	$>> 3 \times 10^7$	--
n-propyl bromide	$1.6 \times 10^8$	$5.4 \times 10^8$	$4.6 \times 10^7$	$3.2 \times 10^7$

<sup>a</sup>: Ref. 75a, <sup>b</sup>: Ref. 75b.

constants which may give some qualitative guide for comparison with those reactions. Fortunately, it does not cause any perfluoro-n-heptyl radical to form the radical **32** from the side-reaction  $k_{\text{add, Si}}$ , plus large excess of the *tris*(trimethyl-silyl)silane and 1-hexene, meaning that reaction  $k_{\text{add, Si}}$  does not interfere with the rate constant determination. Nevertheless, such is not always the case, and there are times when such processes affect the rate determination if the radical generated from the radical precursor takes part in the side-reactions (see the discussion in Chapter 4).

The product ratios of **30**/**31** in Table 3-1 were obtained from a series of  $^{19}\text{F}$  NMR analyses (the ratios of the integral of the  $\text{CF}_2\text{H}$  peak to that of the  $\text{CF}_2\text{CH}_2$  peak) for a group run which contained six reactions which differed only in the concentrations of *tris*(trimethylsilyl)silane and 1-hexene. The Figure 3-1 shows a typical  $^{19}\text{F}$  NMR spectrum for one of the reactions. The peak at  $\delta = -138.1$  and the peak at  $\delta = -114.4$  represent the reduced product **30** and the addition product **31**, respectively. Figure 3-2 shows the plot of the ratio of the products vs the ratio of the concentrations of the *tris*(trimethylsilyl)silane and 1-hexene. Thus, with a slope of 4.47 and a standard error of 0.18, the rate constant  $k_{\text{H}}$  for  $(\text{TMS})_3\text{SiH}$  with  $\text{R}_t^{\cdot}$  is

$$k_{\text{H}} = 5.11 (\pm 0.14) \times 10^7 \text{ M}^{-1} \text{ s}^{-1} \quad \text{at } 30^\circ\text{C}$$

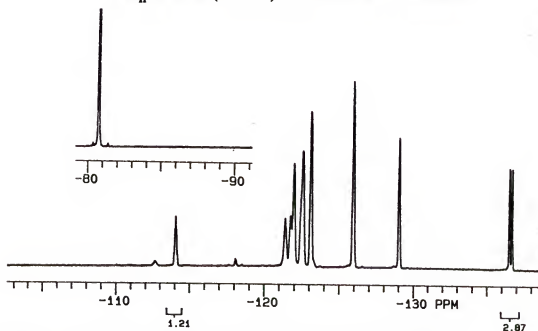


Figure 3-1. A typical  $^{19}\text{F}$  NMR for Analysis of the Product Distribution

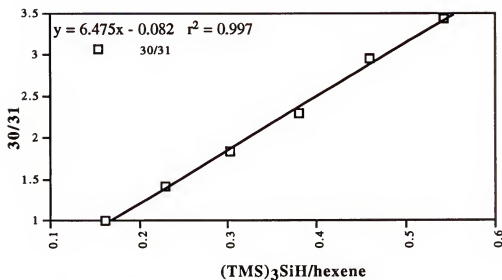


Figure 3-2. The Plot for Rate  $k_H$  Determination for  $(\text{TMS})_3\text{Si-H}$  with  $\text{R}_t^\cdot$

The Rate Determinations for  $(\text{Me}_3\text{Si})_2\text{SiH}$ ,  $\text{Et}_3\text{SiH(D)}$  and  $\text{Bu}_2\text{GeH}$  with  $\text{R}_t^\cdot$

Basically the procedures for rate determinations of the title hydrides (the metal system) with perfluoro-*n*-alkyl radicals ( $\text{R}_t^\cdot$ ) were similar to that used for the *tris*(trimethylsilyl)silane. The results<sup>72</sup> of the rate constants measured in this work are listed in the Table 3-3. The data for those rate determinations can be found in Chapter 5.

Table 3-3. Rate Constants for  $\text{R}_3\text{M-H}$  ( $\text{M} = \text{Si, Ge and Sn}$ ) with  $\text{R}_t^\cdot$

$\text{R}_3\text{M-H}$	$k_H \text{ M}^{-1} \text{ s}^{-1} \quad 30^\circ\text{C}$
$\text{Et}_3\text{SiH}$	$7.5(\pm 0.17) \times 10^5$
$\text{Et}_3\text{SiD}^a$	$3.1(\pm 0.14) \times 10^4$ ; $k_D = 2.4(\pm 0.06) \times 10^5$
$(\text{Me}_3\text{Si})_2\text{SiMeH}$	$1.6(\pm 0.04) \times 10^7$
$\text{Bu}_3\text{GeH}$	$1.5(\pm 0.03) \times 10^7$
$(\text{TMS})_3\text{SiH}$	$5.1(\pm 0.14) \times 10^7$
$\text{Bu}_3\text{SnH}^b$	$2.0(\pm 0.03) \times 10^8$

<sup>a</sup> H-atom and D-atom abstractions were observed when  $\text{Et}_3\text{SiD}$  being used as the reducing agent, both rates  $k_H$  and  $k_D$  were determined (see the discussion following).

<sup>b</sup> Ref. 42

When the rate constant for the  $\text{Et}_3\text{SiD}$  with  $\text{R}_i^\cdot$  was measured, both H-atom and D-atom abstractions by  $\text{R}_i^\cdot$  were detected with the observation of both a  $\text{CF}_2\text{D}$  peak and a  $\text{CF}_2\text{H}$  peak in the  $^{19}\text{F}$  NMR analysis. The well separated  $\text{CF}_2\text{D}$  peak ( $\delta = -137.3$  ppm, singlet) from the  $\text{CF}_2\text{H}$  peak ( $\delta = -136.2$  ppm, doublet) makes it possible to produce a ratio of  $\text{CF}_2\text{D}/\text{CF}_2\text{H} = 7.5$ . From this kinetic and product ratio data one could readily calculate that  $k_D = 2.4 \times 10^5$  and  $k_H = 3.1 \times 10^4$  for this system. It is obvious that the rate constant  $k_H$  for  $\text{Et}_3\text{SiD}$  must represent the rate for the H-atom abstraction by  $\text{R}_i^\cdot$  from its ethyl groups, and that therefore one can readily calculate that about 96% of the hydrogen from  $\text{Et}_3\text{SiH}$  ( $k_H = 7.5 \times 10^5$ ) in its reduction of n- $\text{C}_7\text{F}_{15}\text{I}$  derives from the Si-H bond. In contrast, in the reactions with hydrocarbon radicals, it has been found that as much as 40 % of the hydrogen which comes from  $\text{Et}_3\text{SiH}$  derives from its ethyl groups<sup>11e</sup>. The other difference is that the kinetic isotope effect for H-atom abstraction from  $\text{Et}_3\text{SiH}$  by  $\text{R}_i^\cdot$ , is  $k_H/k_D = 3.1$ , such value being significantly larger than the values of 2.2 to 2.3 which were observed for reductions of alkyl radicals by  $\text{Et}_3\text{SiH}$ ,<sup>11e</sup>  $(\text{TMS})_3\text{SiH}$ <sup>11a</sup> and  $\text{Bu}_3\text{SnH}$ .<sup>6</sup> Such results suggest that the enhanced reactivity of *the hydrogen bound to the silicon* in  $\text{Et}_3\text{SiH}$  towards the  $\text{R}_i^\cdot$  with respect to the hydrocarbon alkyl radical is what leads largely to the rate enhancement for  $\text{Et}_3\text{SiH}$  with perfluoroalkyl radicals.

#### The Rate Determinations for Arene Thiols ( $\text{ArSH}$ ) with $\text{R}_i^\cdot$

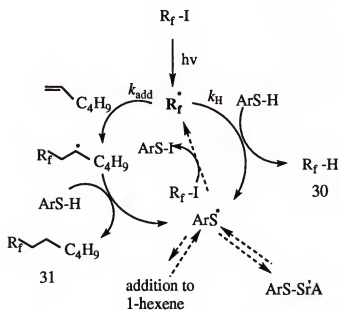
When the hydrogen donors in Scheme 3-1 are a series of  $\text{ArS-H}$  (the Benzene thiol system), the rates for a series of  $\text{ArS-H}$  with  $\text{R}_i^\cdot$  can be measured. Table 3-4 shows the results of the rate constants measured in this work.<sup>72,73</sup>

Based on the rate for  $\text{PhS-H}$  with hydrocarbon radicals ( $\text{R}^\cdot$ ),  $k_H = 1.1 \times 10^8$  being faster than  $\text{Bu}_3\text{SnH}$  with  $\text{R}^\cdot$ , the conditions used for the tin hydride system were chosen to be used. However, the amount of reduced product **30** was too little to be detected accurately by  $^{19}\text{F}$  NMR. In fact, a rate determination could not be made until the Table 3-4. Rates of H-Atom Abstraction from Arene thiols at  $30^\circ\text{C}$  in  $\text{C}_6\text{D}_6$ .

ArS-H	$k_H \times 10^5 \text{ M}^{-1} \text{ s}^{-1} \text{ } 30^\circ\text{C}$	$\sigma^+{}^a$
<i>p</i> -CH <sub>3</sub> O-Ph-S-H	9.9(±0.9)	-0.78
<i>p</i> -CH <sub>3</sub> -Ph-S-H	6.6(±0.6)	-0.31
Ph-S-H	3.3(±0.3) <sup>b</sup>	0
<i>m</i> -CH <sub>3</sub> O-Ph-S-H	3.0(±0.3)	+0.12
<i>p</i> -CF <sub>3</sub> -Ph-S-H	1.8(±0.2)	+0.61

<sup>a</sup> Ref. 76; <sup>b</sup> if PhS-H as solvent,  $k_H = 2.8(\pm 0.3) \times 10^5 \text{ M}^{-1} \text{ s}^{-1}$ .

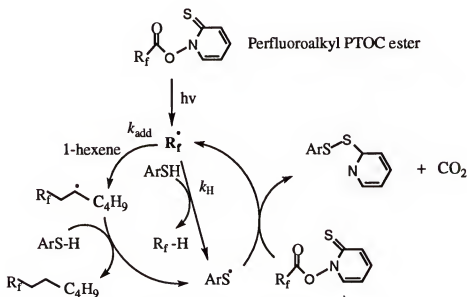
concentration of the benzene thiol was as high as approximately 50 times relative to the radical precursor, which implies a slow rate for hydrogen abstraction by  $R_f^\cdot$  from ArS-H.



Scheme 3-3. Rates Determination for Benzene thiol system

The other feature for this system is that much longer time is required to complete reactions in comparison to the metal system, which means that the chain processes in the competition reactions are quite poor. As shown in Scheme 3-3, the competition steps ( $k_{add}$  and  $k_H$ ) for perfluoroalkyl radicals  $R_f^\cdot$  in the benzene thiol system generate benzene thiyl radicals (ArS·) which are supposed to react with radical precursors ( $R_f-I$ ) to continue the chain processes. Unfortunately, this step does not appear to be as favorable in comparison

with the metal hydride ( $R_3M-H$ ) systems for kinetic and thermodynamic reasons, including a poor polar transition state:  $R_f^{\delta-} \cdots I^{\delta+} \cdots \delta-SAr$  and the weak S-I bond. On the other hand, the reactions of  $ArS^{\cdot}$  adding to 1-hexene and coupling to  $ArS-SAr$  would compete with the iodide abstraction from the radical precursor  $R_f-I$ .<sup>77</sup> Although there are poor radical chain processes in the benzene thiol system, this fact should not affect the results for the rate determination, which is based on the factors: a) the poor step takes place after the competing reactions ( $k_{add}$  with  $k_H$ ), meaning that the perfluoroalkyl radicals after being generated (e.g. via photolysis of the radical precursor  $n-C_7F_{15}-I$ ) could only pass the competing channels to continue their reactions leading to reduced **30** and addition **31** products, which is the same process as in the Nitroxyl Radical Couplings method,<sup>43</sup> and b) the concentrations of **30** and **31** in equation 3-1 are not necessary to be those sampled after reactions finish. In principle, they can be the concentrations sampled at any time during the reaction processes.



Scheme 3-4. A Designed Competition Process; Perfluoroalkyl Barton's PTOT ester as Radical precursors

It has been believed that the use of Barton's PTOT esters<sup>78</sup> rather than alkyl halides as radical precursors can improve the radical chain processes. The designed chain reaction

sequence involved is shown in Scheme 3-4 for the case where a radical addition competes with hydrogen abstraction by perfluoroalkyl radicals from ArS-H. Radicals ArS $\cdot$  produced by reactions of ArS-H with R $_t\cdot$  and R $_t$ -CH $_2$ CH $\cdot$ -C $_4$ H $_9$  propagate the chain reaction by addition to the PTOC ester. Unfortunately, attempts to isolate perfluoroalkyl Barton's PTOC esters at room temperature have failed because of their instability.

### Solvent Effects on the Rate Constants

Effects of the solvent polarity on the rates for Et $_3$ SiH and PhSH systems were briefly studied. The results demonstrated that an important assumption which is inherent to this study, that of solvent nondependence of rates, is not strictly correct!

First, it was noticed that the ratio of  $k_H/k_{add}$  for the Et $_3$ SiH system varied progressively from 0.123 to 0.151 to 0.179 as one progressed from C $_6$ D $_6$  to the more polar media CH $_3$ CN/C $_6$ D $_6$  (2.6:1) and CH $_3$ OH, respectively. On the other hand, the ratio of  $k_H/k_{add}$  for the PhSH system decreased from 0.081 to 0.069 with increase of the polarity of the solvent from C $_6$ D $_6$  to DMF.

Secondly, preliminary LFP results indicate an approximate 2.5-fold increase in rate for addition of n-C $_3$ F $_7\cdot$  to styrene when changing solvent from Freon 113 to acetonitrile.<sup>80</sup> Since all of the rate data presented in this work utilize a  $k_{add}$  value for 1-hexene which was obtained in Freon 113, and most of the competition experiments were run in C $_6$ D $_6$ , there may be some error introduced into our deduced "approximate" rates which would derive from an expected small difference in  $k_{add}$  value for solvents C $_6$ D $_6$  and Freon 113.

An interesting conclusion that one can reach, since the value for  $k_H/k_{add}$  changes as solvent polarity changes, is that the H-abstraction process must be more sensitive to changes in solvent polarity than the addition process.

### The Effects of Fluorine Substituents on H-atom Abstraction Reactions

As can be seen (Table 3-3), all of the silane, germanium and stannane reducing agents exhibit substantial rate enhancements in their transfer of a hydrogen atom to the perfluoro-*n*-alkyl radical relative to an analogous hydrocarbon radical (Table 1-1). Such enhancements range from a factor of 75 for the most reactive  $\text{Bu}_3\text{SnH}$  to 880 for the least reactive  $\text{Et}_3\text{SiH}$ . Why are perfluoroalkyl radicals so much more reactive with such H-atom donors? Certainly the observed hydrogen atom abstractions by  $\text{R}_f^\cdot$  are much more exothermic than those by an analogous *n*-alkyl radical ( $\text{R}_f\text{-H BDE} = 107 \text{ kcal mol}^{-1}$  versus  $98 \text{ Kcal mol}^{-1}$  for  $\text{R-H}^{\text{81b}}$ , and greater rates for such processes, from that point of view, were to be expected. However, that this cannot be the entire explanation was evident from a study of rates of hydrogen atom abstraction from benzene thiol and its substituted derivatives. In this case, benzene thiol (Table 3-4) was found to be a relatively poor H-atom transfer agent to perfluoro-*n*-alkyl radical, exhibiting a rate of  $3.3 \times 10^5 \text{ M}^{-1} \text{ s}^{-1}$  (in 1:1  $\text{PhSH/C}_6\text{D}_6$ ), which is  $\sim 420$  times slower than its rate of reduction of *n*-alkyl radicals ( $k_{\text{H}} = 1.1 \times 10^8$ ).<sup>79</sup> Since the same relative exothermicities prevail for this reduction as for those of the  $\text{R}_3\text{M-H}$  hydrides, for example, the BDE of S-H bond in  $\text{PhS-H}^{\text{81a}}$  is  $82.0 \text{ kcal mol}^{-1}$  and those of the M-H bonds in the  $\text{R}_3\text{M-H}$  are in the range from  $73.7$  to  $90.1 \text{ kcal mol}^{-1}$  (Table 1-1), it is obvious that relative heats of reaction cannot be the complete story regarding the differences in reactivity between  $\text{R}^\cdot$  and  $\text{R}_f^\cdot$ .

### The Evans-Polanyi Relationship in $\text{R}_3\text{M-H}$ Systems

As mentioned in Chapter 1, the Evans-Polanyi equation<sup>10,17</sup> can be used not only to represent the relationship between the activation energy and the BDE but also to study the polar effect in reactions. First, if the relationship does not hold well, it would indicate the interaction of varying polarity effect from reaction to reaction. Secondly, if the relationship of the Evans-Polanyi type is observed, it could be either no polarity in a series of reactions or a constant polarity from reaction to reaction, which can be analyzed based on the change



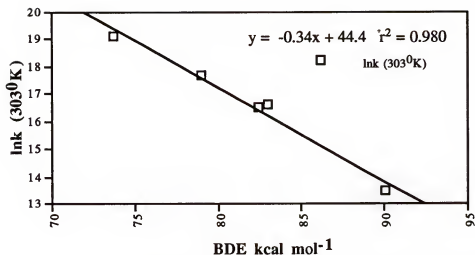


Figure 3-4. The Evans-Polanyi Relationship for the H-atom Abstraction of  $R_3M-H$  by  $R_f^\cdot$

of the constant  $\alpha/RT$  (at certain temperature) in equation (1-12). For example, in the  $R_3M-H$  systems it could be assumed that there is no polarity in H-atom abstraction of the series of  $R_3M-H$  hydrides by alkyl radicals. Thus, there might be a polar effect in the system with a smaller  $\alpha/RT$  value and with a rate enhancement. The straight line (in Figure 3-4) has an  $\alpha/RT = 0.34$  which is smaller than that (0.50, Table 3-5) for alkyl radicals which indicates that there must be a constant polar effect enhancing the rates in H-atom transfers from the series of the  $R_3M-H$  hydrides to perfluoro-n-alkyl radicals. The other feature for

Table 3-5. The Analysis of equation 1-12

$R_3M-H + X^\cdot \longrightarrow X-H + R_3M^\cdot$ $\ln k_T = -(\alpha/RT)[D(M-H)] + (\ln A - \beta/RT)$		
$X^\cdot$	$\alpha/RT$	$\ln A - \beta/RT$
$R^\cdot$	0.50	52
$R_f^\cdot$	0.34	44
$t-BuO^\cdot$	0.22	36

$R_f^{\cdot}$  systems is that the value  $\alpha/RT$  (0.34) is larger than that for  $t\text{-BuO}^{\cdot}$  (0.22) as shown in Table 3-5. The difference might indicate that the "electrophilicity" of perfluoroalkyl radicals is relatively stronger than that of the hydrocarbon alkyl radicals but not so strong as that of  $t\text{-BuO}^{\cdot}$ . The conclusion is that there are strong and constant polar effects in the perfluoro-alkyl radical systems, which results from electrophilicity of perfluoroalkyl radicals.

### The Polar Effect in H-atom Abstraction by $R_f^{\cdot}$

As discussed above, the contrasting relative reactivities of electropositive H-atom donors such as silanes, germanium and stannanes, and a relatively electronegative H-atom donor such as arene thiols are undoubtedly a reflection of the importance of transition state polar effects in such hydrogen atom transfer reactions, and of the fact that perfluoroalkyl radicals are very electron poor. If one includes the BDE for PhSH in the Fig. 3-4, one will find that the point of  $k_H$  for PhSH is far away off the line, which indicates the different polarities in the transition states between the benzene thiol  $-R_f^{\cdot}$  and  $R_3M\text{-H}-R_f^{\cdot}$  systems. One can attempt to examine such transition-state polarization effects more quantitatively by making a comparison of the "absolute" or Mulliken electronegativities for the respective radicals which are reacting and being formed in the hydrogen transfer processes in question. Absolute electronegativities,  $\chi$ , of radicals are defined by the following equation:  $\chi = (IP + EA)/2$ , and such values are available for a number of radicals<sup>82</sup>, unfortunately perfluoro-n-alkyl radicals not being among them. A typical "nucleophilic" radical,  $t\text{-Bu}^{\cdot}$ , for example, has an  $\chi$  value of 3.31 eV, while the value for  $C_6H_5S^{\cdot}$  and  $C_6H_5O^{\cdot}$  are 5.5 and 5.6 eV, respectively.  $\chi$  for  $^{\cdot}OH$  is 7.5 (the value for  $t\text{-BuO}^{\cdot}$  should be closed to that for  $^{\cdot}OH$ ). One might realistically expect the value for  $R_f^{\cdot}$  to lie between 5.5 and 7.5, while the values for the series of  $R_3M^{\cdot}$  radicals should lie below that of  $t\text{-Bu}^{\cdot}$ .

Abstraction of H-atom by  $R_f^{\cdot}$  from  $Et_3Si\text{-H}$ , for example, would give rise to an excellent match-up of electronegativities which should facilitate the reasonable nature of

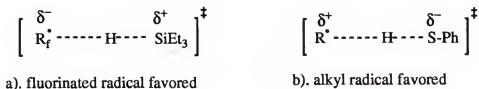
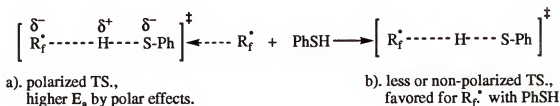


Figure 3-4. Polarized Transition States Favored for H-atom Transfers

Figure 3-5. Polar Effects for the H-atom Transfer from Benzene Thiols to  $R_f^\bullet$ 

polarization which is depicted in Figure 3-4,(a). While, in contrast, a more nucleophilic alkyl radical should give rise to a similarly favorable, but inverted, match-up of electronegativities in its H-atom abstraction process with benzene thiol (Figure 3-4, (b)). In both transition states, the heights of the energy barriers is lowered by such polar effects<sup>10</sup> so that the rates of H-atom transfers are enhanced relative to the less or non-polarized transition states. However, not all polar effects enhance the rates of H-atom transfers. In the case of perfluoroalkyl radicals with benzene thiols, if one considers the BDE's for the S-H bond in PhSH (82.0 kcal mol<sup>-1</sup>) and for the Si-H bond in Et<sub>3</sub>SiH (90.1 kcal mol<sup>-1</sup>), it would be expected that PhSH is more reactive than Et<sub>3</sub>SiH towards to  $R_f^\bullet$ . However, the polar effect in the transition state for PhSH with  $R_f^\bullet$  increases the activation energy in the polarized transition state as shown in Figure 3-5,(a), and forces the reaction to pass through a less or non-polarized transition state (Figure 3-5.(b)). It results that the rate for H-atom abstraction of the benzene thiol by  $R_f^\bullet$  diminishes to the value of  $3.3 \times 10^5 \text{ M}^{-1} \text{ s}^{-1}$  which is close to the value of the Et<sub>3</sub>SiH with  $R_f^\bullet$  ( $7.5 \times 10^5 \text{ M}^{-1} \text{ s}^{-1}$ ). This is not to say that there is no polar effect, but it just emphasizes the result of the polar effects in the benzene thiol - $R_f^\bullet$  system.

That transition state polar effects intervene importantly in hydrogen atom abstraction reactions of perfluoroalkyl radicals should not be surprising.  $R_f\cdot$  abstracts hydrogen from PhSH [ $R_f\cdot + \text{PhSH} \rightarrow R_f\text{-H} + \text{PhS}\cdot$ ] with  $\Delta H^\circ = -24 \text{ kcal mol}^{-1}$ <sup>43</sup>, and the  $E_a$  for this reaction must be very low (i.e.  $\leq 3 \text{ kcal mol}^{-1}$ ).<sup>43</sup> Such a large exothermicity combined with a relatively small activation energy should give rise to a reactant-like transition state with little bond-breaking and little transfer of radical character. It is in such transition states that FMO interactions should be most important and where polar effects would be expected to play their most important role. Certainly, as was found, the relative stabilities of the product arene thiyl radicals should not greatly influence the rates of a reaction with such an early transition state.

#### A Hammett Study on a Series of Arene Thiols

To confirm the important role of polar effects, a Hammett study was carried out for the reduction of  $n\text{-C}_7\text{F}_{15}\text{-I}$  by a series of arene thiols. As can be seen from the data in Table 3-4, there is a definite correlation between the rates of reduction and the "electron-richness" or "electron-poorness" of the arene thiol with the electron-rich *p*-methoxy derivative being 5.5 times more reactive than the most electron-poor *p*- $\text{CF}_3$  derivative.

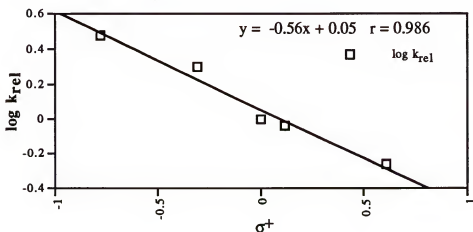


Figure 3-6. Hammett Plot of Arene Thiol Rates

In attempts to correlate the rate data with various types of  $\sigma$ - values, it was found that, as in the case of a related study of H-atom abstraction from arene thiols by the electrophilic *t*-butoxyl radical<sup>84</sup>, the best correlation was with  $\sigma^+$ , as shown in Figure 3-6. Much poorer correlations were observed when  $\log k_{\text{rel}}$  was plotted against  $\sigma$  or  $\sigma^-$ .

In our case a  $\rho^+$  value of -0.56 ( $r = 0.986$ ) was observed as compared to that observed for *t*-butoxyl [ $\rho^+ = -0.30$  ( $r = 0.987$ ) in  $\text{C}_6\text{H}_6$ ]. Interestingly, perfluoroalkyl radicals are less reactive than the *t*-butoxyl radical towards the arene thiols. This might be caused by the relatively comparable electronegativities between  $\text{R}_f^\cdot$  and  $\text{PhS}^\cdot$ , and by the extremely electrophilicity of the *t*-BuO $^\cdot$ . Although the relatively slow rate of H-atom abstraction from benzene thiol by perfluoroalkyl radicals can clearly be rationalized in term of the polar effect in the transition state, such a slow rate is nevertheless still a curious result since a similar diminution in rate does not seem to derive from the similarly mismatched transition states for H-atom abstraction by the electronegative *t*-butoxyl radical.<sup>85</sup>

Unfortunately, the absolute rate of reaction of *t*-butoxyl radicals with benzene thiol has not yet been reported. The rates of H-atom abstraction from phenol ( $3.3 \times 10^8 \text{ M}^{-1} \text{ s}^{-1}$ ) and substituted phenols have been measured and are among the fastest yet observed for *t*-butoxyl radicals.<sup>85</sup> In our attempts to measure rates of reduction of perfluoroalkyl radicals by phenol, it was found that aromatic addition processes competed with H-atom abstraction, making accurate rates impossible to obtain thus far.

### Conclusion

Using competitive methods, and based on the data of perfluoroalkyl radical addition to 1-hexene ( $7.9 \times 10^6 \text{ M}^{-1} \text{ s}^{-1}$ ).<sup>42</sup> rates of hydrogen atom abstraction by a typical perfluoroalkyl radical,  $\text{n-C}_7\text{F}_{15}^\cdot$ , have been determined for a series of the metal hydrides  $\text{R}_3\text{MH}$  ( $\text{M} = \text{Si}, \text{Ge}$  and  $\text{Sn}$ ). The results are shown in Table 3-3, all of which exhibited substantial rate enhancements relative to their analogous reductions of hydrocarbon radicals. The reduction by benzene thiol is, in contrast, ~400 times slower than for hydrocarbon radicals (as shown in Table 3-4). Transition state polar effects are invoked to

rationalize the relative reactivity of perfluoro versus hydrocarbon radicals in these hydrogen-transfer reactions. A Hammett study for H-atom transfer from arene thiols ( $\rho^* = -0.56$ ) provided further substantiation for this conclusion.

In any event, the observed kinetic results indicate that triethylsilane reduced perfluoroalkyl radicals efficiently and at a rate which should make it a very useful agent for relatively slow chain processes involving fluorinated radicals. Moreover, the whole group of the metal hydrides ( $R_3MH$ ) makes available a series of good, chain-carrying reductants with sufficient range of reactivities to allow most addition, rearrangement or cyclization reactions of fluorinated radical systems to be carried out efficiently under competitive reductive conditions. In the following chapter, Chapter 4, we present some applications for these data in the determination of the rates of cyclization reactions for fluorinated 5-hexenyl radicals.

From the electronegativity point of view, perfluoroalkyl radicals are the only carbon-based radicals which would appear to approach the reactivity/selectivity characteristics of the *t*-butoxyl radical, which has been utilized as a model for biologically-significant oxygen-based radicals. In our continuing study, it may be that specially-designed perfluoro-alkyl radicals may have some utility as reactivity mimics of  $HO^\cdot$  in biological systems.

## CHAPTER 4

### THE REACTIVITY OF FLUORINATED 5-HEXENYL RADICALS

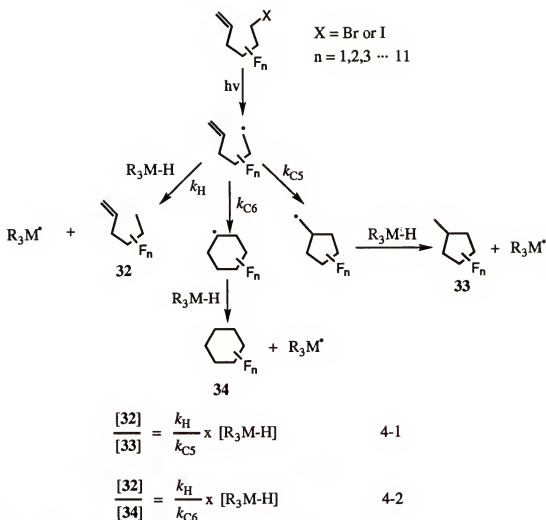
#### Introduction

Since it was first reported in 1963,<sup>29a</sup> the ring closure reactions of the 5-hexenyl radical and its non-fluoro-substituted analogs by intramolecular addition have been extensively investigated.<sup>29-39</sup> The cyclizations to give 5-exo products have been widely accepted as a mechanistic probe which is characteristic of a free radical intermediate<sup>86</sup> and have been used as standards for the determination of the absolute rates of a wide variety of competitive free radical reactions.<sup>43</sup> With an understanding of the mechanism of these cyclization reactions, their use as standard synthetic methodology has rapidly been established.<sup>2,3</sup>

For fluorinated 5-hexenyl radicals, however, very little was known about the absolute rates of cyclization leading to 5-exo products or 6-endo ones. Since the study of such cyclizations could provide fundamental insight into the reactivity of fluorinated radicals, our attention was attracted to the study of these reactions. In the present work we have employed competition methods to measure the absolute rates of cyclization of fluorinated 5-hexenyl radicals using the data in Table 1-1, the rate constants ( $k_H$ ) of primary alkyl radicals with  $R_3MH$  hydrides, and the data in Table 3-3, the rate constants ( $k_H$ ) of perfluoro radicals with  $R_3MH$  hydrides discussed in Chapter 3. A series of fluorinated radical precursors have been synthesized for the kinetic studies.

#### The Results of Determination of Absolute Rates of Cyclization Reactions for Fluorinated 5-Hexenyl Radicals

The design of a typical experiment is shown in Figure 4-1. The fluorinated radical precursors, bromides or iodides, are photolyzed<sup>6b</sup> to give initial fluorinated 5-hexenyl



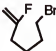

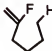
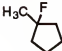


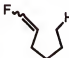
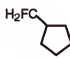
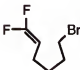
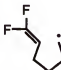
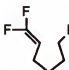
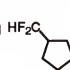

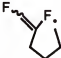
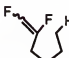
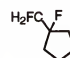
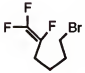
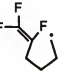
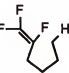
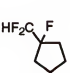
Scheme 4-1. Rate Determination of Cyclization Reactions for Fluorinated 5-Hexenyl Radicals

radicals and then, through two or three radical chain reactions ( $k_H$ ,  $k_{C5}$  or  $k_{C6}$ ) the radicals are converted to reduced and cyclized products competitively. The formed metal radical  $R_3M^\bullet$  will then react with the bromides or iodides to generate fluorinated 5-hexenyl radicals to continue the chain. In the competing steps, the reduction ( $k_H$ ) of radicals with  $R_3MH$  is the basis reaction with a known rate constant ( $k_H$ ) and the cyclization reactions of fluorinated 5-hexenyl radicals are the reactions for which the rate constants ( $k_{C5}$  or  $k_{C6}$ ) are measured. The reduced product **32**, cyclized products (5-exo) **33** and (6-endo) **34** are stable under the reaction conditions and they can be determined quantitatively by  $^{19}\text{F}$  NMR analysis. It should be pointed out that the  $^{19}\text{F}$  NMR analysis will be different for each of the



different fluorinated radical systems (see the experimental section in Chapter 5), which is unlike the situation for rate determination of reduction of  $R_f^{\cdot}$  with  $R_3M-H$  hydrides where the products were eventually the same from one determination to another one. The final analysis of the data, obtained for varied concentrations of reducing agents ( $R_3M-H$ ) which are at least nine-fold excess in respect to radical precursors, is based on equation 4-1

Table 4-1. Absolute Rate Constants of Cyclization Reactions for Fluorinated 5-Hexenyl Radicals at 30°C

Precursor <sup>a</sup>	Radical	Products			$k_{C5} \times 10^{-5} s^{-1}$	$k_{C6} \times 10^{-5} s^{-1}$
		reduced	5-exo	6-endo		
				UD <sup>b</sup>	0.28 (± 0.04)	--
35	35-1	35-1	35-2			
				UD	1.3 (± 0.16)	--
36	36-1	36-1	36-2			
				UD	1.6 (± 0.16)	--
37	37-1	37-1	37-2			
				UD	1.5 (± 0.15)	--
38	38-1	38-1	38-2			
				UD	4.7 (± 0.14)	--
39	39-1	39-1	39-2			

<sup>a</sup>. The precursor and the radical are named by the same number.

<sup>b</sup>. Undetected, which is less than 4% in the total yield and could not be detected accurately.

Table 4-1. *continued*

Precursor	Radical	Products			$k_{C5} \times 10^{-5} \text{ s}^{-1}$	$k_{C6} \times 10^{-5} \text{ s}^{-1}$
		reduced	5-exo	6-endo		
					440 ( $\pm 46$ )	52 ( $\pm 6.4$ )
<b>40</b>	<b>40-1</b>	<b>40-1</b>	<b>40-2</b>	<b>40-3</b>		
					107 ( $\pm 17$ )	35 ( $\pm 4.4$ )
<b>41</b>	<b>41-1</b>	<b>41-1</b>	<b>41-2</b>	<b>41-3</b>		
				UD	4.3 ( $\pm 0.75$ )	—
<b>42</b>	<b>42-1</b>	<b>42-1</b>	<b>42-2</b>			
				UD	4.9 ( $\pm 0.79$ )	—
<b>43</b>	<b>43-1</b>	<b>43-1</b>	<b>43-2</b>			
				UD	35 ( $\pm 6.3$ )	—
<b>44</b>	<b>44-1</b>	<b>44-1</b>	<b>44-2</b>			

for  $k_{C5}$  and equation 4-2 for  $k_{C6}$ . The ratio of the rate constants ( $k_H / k_{C5}$  or  $k_H / k_{C6}$ ) is found by the slope of a plot of the ratio, **32/33** or **32/34**, as a function of the concentrations of reducing agents  $[R_3M-H]$ . Since the value of  $k_H$  is known, it is thus possible to convert the ratio of rate constants ( $k_H / k_{C5}$  or  $k_H / k_{C6}$ ) to the value of  $k_{C5}$  or  $k_{C6}$ , the absolute rate constants of 5-exo or 6-endo cyclization reactions of fluorinated 5-hexenyl

radicals. The results of the determination of rates of cyclization reactions for fluorinated 5-hexenyl radicals are shown in Table 4-1. The error estimates reported here reflect both the least squares fit of the line and the error in  $k_H$ , and largely derive from the error in  $k_H$ .

#### Discussion on Determination of Absolute Rates of Cyclization Reactions for Fluorinated 5-Hexenyl Radicals

In the course of determination of such rate constants the problems most often met are: a) the choice of the reducing agent ( $R_3M-H$ ), which is based on the knowledge of how fast the ring closure of a fluorinated radical being studied might be; and b) the addition of formed metal radicals  $R_3M^\cdot$  to the double bonds of 5-hexenyl radicals or reduced products, which will cause errors in determination of  $k_{C5}$  and  $k_{C6}$  (it has been reported that the ease of addition of  $R_3M^\cdot$  radicals to hydrocarbon double bonds follows the order:<sup>75a,75b</sup>  $Et_3Si^\cdot > Bu_3Ge^\cdot > (TMS)_3Si^\cdot \sim Bu_3Sn^\cdot$ ). On the other hand, from the present work it has been found that the ease of addition of  $R_3M^\cdot$  radicals to fluorinated (especially to the perfluorinated) double bonds follows the order:  $(TMS)_3Si^\cdot \sim Bu_3Sn^\cdot > Bu_3Ge^\cdot > Et_3Si^\cdot$ ; lastly, c) choosing peaks for the  $^{19}F$  NMR analysis of reaction mixtures to represent reduced and cyclized products, which often require the preparation of pure compounds which are formed in the competition reactions. For most situations, the peaks chosen for reduced and cyclized products in  $^{19}F$  NMR spectra should be as close as possible provided there is no overlap of peaks with each other or others.

#### Determination of Rate Constants for 5-hexenyl radicals with a Perfluoro Radical Center

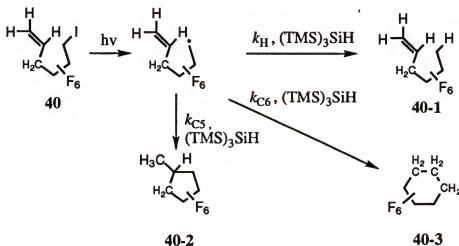
The radicals with a perfluorinated radical center are those of radicals: **40**, **41**, **43** and **44** in Table 4-1. In order to measure the rate constants ( $k_C$ ) of the cyclization reactions of those radicals by the competition method, the reduction rate constants ( $k_H$ ) have to be these of the reactions in which metal hydrides ( $R_3M-H$ ) reduce the radicals with a perfluorinated radical center, such as those reported in Table 3-3. In the determination of the rate constants ( $k_{C5}$  or  $k_{C6}$ ), all kinds of metal hydrides,  $Bu_3SnH$ ,  $(TMS)_3SiH$ ,  $Bu_3GeH$

and  $\text{Et}_3\text{SiH}$ , were tried to find the best fit so as to give comparable amounts of reduced and cyclized products under competition conditions for accurate  $^{19}\text{F}$  NMR analysis. For example, radical **43** (the perfluoro 5-hexenyl radical) only reacted with the  $\text{Et}_3\text{SiH}$  to give a comparable ratio of reduced to cyclized products; and any of the other hydrides gave too much reduced products to provide an accurate  $^{19}\text{F}$  NMR analysis of the reaction mixtures. The rates of the reactions ( $k_{\text{H}}$  and  $k_{\text{C}}$ ) are the first factor which must be considered in choosing an appropriate reducing agents for study of a particular radical, but the problem of addition of metal radicals ( $\text{R}_3\text{M}^\cdot$ ) to double bonds of radicals (or reduced products) also plays an important rule in designing conditions for competition reactions. For example, at the beginning of working with radical **44**,  $(\text{TMS})_3\text{SiH}$  was chosen as the reducing agent because it gave a ratio of reduced to cyclized products close to unity. However, after  $^{19}\text{F}$  NMR analysis of the reaction mixture, it was apparent that there were considerable addition products present, deriving from  $(\text{TMS})_3\text{Si}^\cdot$  adding to the perfluoro vinyl ether. By changing to the  $\text{Bu}_3\text{SnH}$ , the situation became worse, not only too much reduced products but also an increase of the addition products. The  $\text{Bu}_3\text{GeH}$  has a comparable rate constant and less ability to add to fluorinated double bond in comparison to the  $(\text{TMS})_3\text{SiH}$ , and it thus was found to be the best reducing agent for the study of radical **44**. The addition of metal radicals ( $\text{R}_3\text{M}^\cdot$ ) to double bonds was not important for radicals **40** and **41** since the fast reduction ( $5.1 \times 10^7 \text{ M}^{-1} \text{ s}^{-1}$  for  $(\text{TMS})_3\text{SiH}$  with perfluoro radicals  $\text{R}_f^\cdot$ ) and cyclization ( $k_{\text{CS}} > 10^7 \text{ s}^{-1}$ ) minimized addition problems.

The concentrations of radical precursors are important too, and normally, the lower concentration is good for avoiding intermolecular addition reactions. However, working with very low concentration solutions would give rise to a weak ratio of signal to noise in  $^{19}\text{F}$  NMR analysis and introduce a large systematic error. Thus, the concentrations of radical precursors had to be controlled within the range of  $0.019 \sim 0.12 \text{ M}$  (see the experimental section in Chapter 5).

Choosing peaks in  $^{19}\text{F}$  NMR spectra of reaction mixtures to represent reduced and cyclized products is complicated and varies with the specific radical being studied. All of

the data used for determination of the rate constants of cyclization are reported in Chapter 5. Here, radical **40** will be taken as an example to show the procedure of the data accumulation and processing.



Scheme 4-2. The Competition Reaction of Radical **40** with  $(\text{TMS})_3\text{SiH}$

Under photo-conditions (Rayonet lamps), radical precursor **40** reacts with  $(\text{TMS})_3\text{SiH}$  to give three compounds competitively, **40-1**, **40-2**, and **40-3** as shown in Scheme 4-2. **40-1** is the reduced product while **40-2** and **40-3** are the 5-exo and 6-endo cyclization products, respectively. In the determination of the rate constants ( $k_{C5}$  and  $k_{C6}$ ), a series of samples containing a certain amount of precursor **40**, varied in the concentration of the  $(\text{TMS})_3\text{SiH}$ , were prepared as shown in Table 4-2. With the changes of the concentration of reducing agent  $(\text{TMS})_3\text{SiH}$ , the distribution of the products from radical **40** would vary in the series of samples and could be detected quantitatively by  $^{19}\text{F}$  NMR. Figure 4-1 shows one of the  $^{19}\text{F}$  NMR spectra of the reaction mixtures in which the peak at  $\delta = -137.89$  represents the reduced product ( $\text{CF}_2\text{H}$ ), the peak at  $\delta = -120.97$  (A-B system) the 5-exo cyclization product (one fluorine from the ring) and the peak at  $\delta = -117.53$  the 6-endo product (four fluorines from the ring). Based on this  $^{19}\text{F}$  NMR analysis, the ratios of **40-1**/ **40-2** and **40-1**/ **40-3** could be obtained (as shown in Table 4-2), and then the combination of the data of the concentrations of the  $(\text{TMS})_3\text{SiH}$  would

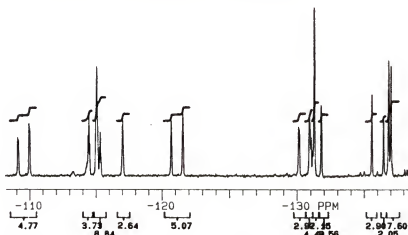
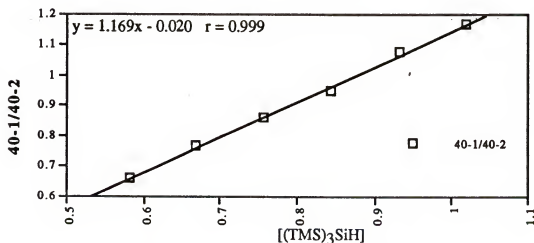
Table 4-2. Competition Data for the Reaction of Radical **40** with  $(\text{TMS})_3\text{SiH}^a$ 

[Precursor], M	$[(\text{TMS})_3\text{SiH}]$ , M	[Reduced]/ $[\text{C}_5]^b$	[Reduced]/ $[\text{C}_6]^c$	Yield
0.058	0.582	0.66	5.15	96
0.058	0.669	0.77	6.08	100
0.058	0.756	0.86	6.68	100
0.058	0.844	0.95	7.68	97
0.058	0.931	1.08	8.45	100
0.058	1.018	1.17	9.48	100

<sup>a</sup> The samples were photolyzed with Rayonet lamps for 20 min.

<sup>b</sup> Obtained by  $^{19}\text{F}$  NMR analysis;  $\text{C}_5$ , the 5-exo product.

<sup>c</sup> Obtained by  $^{19}\text{F}$  NMR analysis;  $\text{C}_6$ , the 6-endo product.

Figure 4-1. One of the  $^{19}\text{F}$  NMR Spectra of the Reaction Mixtures from Radical **40**Figure 4-2. The Determination of Rate Constant  $k_{\text{C}_5}$  for Radical **40**

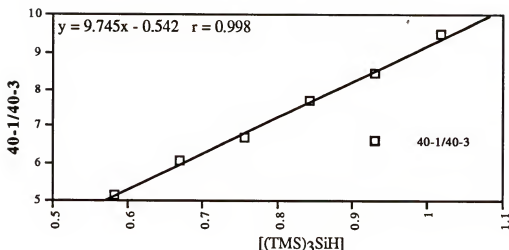
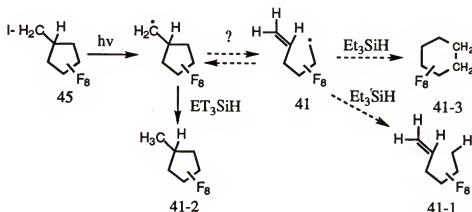


Figure 4-3. The Determination of Rate Constant  $k_{C6}$  for Radical **40**

give the plots of **40-1/40-2** ~  $[(TMS)_3SiH]$  and **40-1/40-3** ~  $[(TMS)_3SiH]$  as shown in Figure 4-2 and 4-3, respectively. On the basis of equations 4-1' and 4-2, the slope of the line depicted in Fig. 4-2 is  $k_H/k_{C5}$  and it equals 1.169, and the slope of the line in Fig. 4-3 is  $k_H/k_{C6}$  and it equals 9.745. Since  $k_H$  for the  $(TMS)_3SiH$  reacting with perfluoro radicals is  $5.1 \times 10^7 M^{-1} s^{-1}$  at  $30^\circ C$ , the rate constant,  $k_{C5}$ , is  $4.4 \times 10^7 s^{-1}$ , and  $k_{C6}$  is  $5.2 \times 10^6 s^{-1}$  at  $30^\circ C$ .

The control reactions have been run to confirm the results. For example, 6-endo products were only observed in the studies of radicals **40** and **41** which have the perfluorinated radical centers and the hydrocarbon double bonds, and the question thus arises



Scheme 4-3. The Reversibility of the Ring Closure of Radical **41**

whether the ring closures of radicals **40** and **41** were irreversible or reversible under such conditions? That is, if the fluorine substituents at radical center would cause the ring closures of radical **40** and **41** to be reversible, just as that the groups CN and COOEt in radical **19** (Table 1-6) cause the ring closure of the radical to be reversible, the amount of 6-endo product should increase dramatically. The control reaction (Scheme 4-3) was that the mixture of the  $\text{Et}_3\text{SiH}$  and 1-iodomethyl-2,2,3,3,4,4,5,5-octafluorocyclopentane **45** (2:1, respectively) in  $\text{C}_6\text{D}_6$  was photolyzed till the iodide disappeared. The  $^{19}\text{F}$  NMR analysis of the resultant mixture indicated that there were no other compounds except the one formed by direct reduction of the iodide, that is, 1-methyl-2,2,3,3,4,4, 5,5-octafluorocyclopentane **41-2**. This result directly demonstrates that the ring closure of radical **41** was irreversible under the competition conditions, and that the rate constants ( $k_{\text{C5}}$  and  $k_{\text{C6}}$ ) which were measured are reliable.

#### The 5-Hexenyl Radicals with a Hydrocarbon Radical Center ( $-\text{CH}_2^{\cdot}$ )

The radicals belonging to this classification are those in Table 4-1: **35**, **36**, **37**, **38**, **39** and **42**. To determine the rate constants for the cyclization reactions of those radicals by the competition method, the normal "Tin hydride" method should be satisfactory if the ring closures of the radicals are not too slow in comparison with the rate constant  $k_{\text{H}}$  for tributyltin hydride reduction of primary radicals. Actually, except for radical **35** with a single fluorine at the vinyl position, all of others gave satisfactory results with the "Tin hydride" method in the determination of the rate constants. Radical **35** gave the reduced **35-1** as the major product, and the cyclized product **35-2** was too little to be detected accurately by  $^{19}\text{F}$  NMR analysis, which meant that the ring closure of radical **35** is too slow to use  $\text{Bu}_3\text{SnH}$  as the reducing agent.  $\text{Bu}_3\text{GeH}$  reduces a primary radical with a rate constant of the order of  $1 \times 10^5$  (Table 1-1) which is about 20 times slower than  $\text{Bu}_3\text{SnH}$  at room temperature. Another problem for radical **35** was that the fluorine at the vinyl position facilitates the addition of metal radicals  $\text{Bu}_3\text{Ge}^{\cdot}$  to the double bond. This problem



was solved by lowering the concentration of the radical precursor **35** and controlling the time period during which the samples were photolysed.

To check out the reliability of rate constants measured in this work, a control reaction has been run in which the radical precursor **41** was reacted with PhS-H under competition conditions. In this case the rate constants,  $k_{C5}$  and  $k_{C6}$ , were taken as the known rate constants while the rate constant,  $k_H$ , of reduction for PhS-H with perfluoro radicals was the one being determined. Under competition conditions used for determination of the rate constants, the results show that the  $k_H$  is  $4.7 \times 10^5$  or  $3.5 \times 10^5 \text{ M}^{-1} \text{ s}^{-1}$  based on the  $k_{C5}$  or  $k_{C6}$ , respectively. In comparison with the value of  $k_H$  ( $3.3 \times 10^5 \text{ M}^{-1} \text{ s}^{-1}$ ) in Table 3-4 for PhS-H as measured from the  $R_t$ -I/ Hexene system, the results are similar and are within experimental errors ( the error is at least 8.9% introduced by the  $k_{add}$  measured by the FLP method.<sup>42</sup>

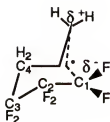
#### The Fluorine Substituent Effects on the Cyclization Reaction of 5-Hexenyl Radicals

As discussed in Chapter 1, substituents on the olefin moiety and/or the alkyl fragment of the 5-hexenyl radical might exert steric as well as electronic effects in the transition states for the cyclization reactions, which are dependent on the nature of substituents. Basically, the alkyl groups replacing any hydrogen in the 5-hexenyl radical system will enhance the rate of the ring closure except for the one at the vinyl position where the alkyl groups will retard the reaction dramatically (Table 1-3 and 1-4). The overall effects of the fluorine substituents are similar to those of alkyl groups, that is, the radical with the fluorine at vinyl position has the slowest rate (about 10 times as slow as the unsubstituted 5-hexenyl radical **1**), and this is only one that has a rate slower than that of **1** (see Table 4-1). The radicals **36**, **37** and **38** might cyclize a little bit slower than **1**, but in consideration of errors by the competition method, it is really hard to tell the difference between them. With the fluorine substituents connected to the saturated carbons, like radicals **40** to **44**, the rates of ring closures are all faster than the radical **1**.

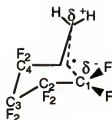
However, the substantial enhancement of the rates for radicals **40**, **41** and **44** indicates that the effects of the fluorine substituents must be different from the alkyl groups as well as those groups, like CN, MeO, COOEt, and so on. The fluorine substituents, as discussed in Chapter 2, will introduce a dramatic electronic effect, such as the strong electron withdrawing effect on the reaction. Based on the discussions in Chapter 1 and 2, the reactivity of fluorinated 5-hexenyl radicals will be discussed and the effects of the fluorine on the ring closures of the radicals will also be analyzed in the following discussions.

### The Radicals **40** and **41**

The radicals **40** and **41** were designed to test that how the polar effect would influence the reactivities of the 5-hexenyl radical system. As we have known that the polar effect cause the intermolecular addition of perfluoro radicals to hydrocarbon double bonds ( $k_{\text{add}} = 7.9 \times 10^6$ ) to be much faster than that of alkyl radicals<sup>42</sup>, it is not surprising that the ring closures (5-exo) of the radicals **40** and **41** are much faster than that of the unsubstituted radical **1** (Table 4-1). Based on the similarity between these two systems, we will consider that the SOMO-HOMO interaction is a dominant factor in the addition of perfluoro-n-alkyl radicals to alkenes<sup>42</sup> in order to explain the polar effects on the reactivities of the radicals **40** and **41**. The other factor that contributes to the rate enhancement would be the  $\sigma$ -type radical center of the perfluoro-alkyl radical since the geometry of an attacking radical center in the transition state (see Fig. 1-5) should be non-planar, and the perfluoro-alkyl radicals with the non-planar radical center already fits this requirement. On the other hand, as discussed in Chapter 2, the non-planar radicals are lower in the energy which are shown in the SOMO energies (see Table 2-5 as reference). Therefore, as discussing the effects of low-lying SOMO orbital of the perfluoro radical on the ring closures, the effects of the  $\sigma$ -type radical center of  $R_f^\cdot$  should be included. The low-lying SOMO of  $R_f^\cdot$  makes the SOMO-HOMO interaction be a dominant factor in the cyclization reactions of the radicals **40** and **41**, and therefore the charge separation in the



A, TS for 40



B, TS for 41

transition state would be expected as above,<sup>26b</sup> A and B. The negative charge  $\delta^-$  at  $C_1$  would be delocalized by the inductive effect of the perfluoroalkyl group so that the height of the activation barrier will be lowered by the polar effect, and thus the cyclization reactions will be facilitated. A further comparison between the radical 40 and 41 shows that varying groups at  $C_4$  ( $\text{CH}_2$  or  $\text{CF}_2$ ) make the reactivities of the radicals significantly different, that is, the ring closure of 40 is about 4 times faster than that of 41. The reason for this could also be explained by the polar effect, the  $\text{CH}_2$  at  $C_4$  in radical 40 separating the perfluoroalkyl group from the double bond so that it becomes electron richer relative to the double bond in the radical 41 which is connected directly to the perfluoroalkyl group. The electron richer double bond of 40 has a higher HOMO which interacts with SOMO of the perfluoroalkyl radical more efficiently.<sup>26b,26c</sup> Therefore, the polarized transition state A shown above in which the  $\delta^+$  at the terminal carbon could be considered as being stabilized indirectly by the  $\text{CH}_2$  group is the most favored one for the radicals in Table 4-1, which makes the radical 40 the most reactive one among the radicals which were studied.

The other feature for the radicals 40 and 41 is that the rates,  $k_{C6}$ , for the 6-endo cyclization are unusually fast, and it is even more than 10 times faster relative to the rate,  $k_{C5}$ , for the 5-exo ring closure of the radical 1. The polar effect must play some role, but definitely can not be the only reason for the rate enhancement since the ratio of the  $k_{C6}/k_{C5}$  for the radical 40 is 0.12 while it is 0.33 for the radical 41, meaning that the rate enhancement of  $k_{C6}$  for 41 is larger than that for 40. The relative stabilities of forming radicals (6-membered ring radicals) are not relevant because the 6-membered ring radical from 41 should not be more stable than the one from 40 (see Table 2-5 for the stability of

radicals). Based on the discussion of transition states (Fig. 1-5), the attacking angle  $\theta$  would be important in the regio-selectivity of the ring closure of 5-hexenyl radicals. Thus, it might be possible that a 'twist' exo-chair transition state caused by 1,3-repulsion between fluorines in the perfluoro-n-alkyl fragment <sup>87</sup> of the radicals facilitates the formation of 6-endo product. However, it is not possible at this time to give a solid evidence to prove it.

It should be pointed out that **40** and **41** are the first examples of cyclization where a substantial increase in rate is caused by lowering the SOMO of radicals without increasing the reversibility of 5-exo ring closures in the 5-hexenyl radical systems. The reason is that the perfluoro-n-alkyl radical has a lower SOMO in relative to the 'alkyl radical, but it is not more stable than an alkyl radical (Table 2-5).

### The Vinyl Fluoro-radical **35**

As mentioned before, this is the only radical, among the radicals which were studied, which has the rate ( $k_{C5}$ ) retarded by presence of a fluorine substituent in the 5-exo ring closure. Actually, a similar situation was observed in the studies on alkyl group effects on the cyclization reaction of 5-hexenyl radicals (Tables 1-3 and 1-4), that is, the rates are retarded only when the alkyl group (methyl or isopropyl) is at the vinyl position ( $C_5$ ) of the radicals, a result which was rationalized as deriving from the B-strain effect engendered at the  $C_5$  of the radical by its change from  $sp^2$  to  $sp^3$  hybridization.<sup>32b</sup> Thus, the fluorine effect at  $C_5$  on the ring closure can be similarly rationalized by the B-strain effect caused by the replacement of hydrogen by the fluorine at vinyl position ( $C_5$ ). The most interesting results were that for the alkyl system, with the rates of 5-exo cyclization being retarded, the rates of 6-endo cyclization were increased so that  $k_{C6}$  was larger than  $k_{C5}$  (Table 1-4). For our fluorinated radical **35**, however, there was no similar obvious change for the 6-endo cyclization reaction. There are some relevant arguments in the explanation of the regio-selectivity change for alkyl systems. Beckwith has pointed out<sup>4,32b</sup> a purely steric reason which is due to the non-bonded interaction between the alkyl group at  $C_5$  and the radical center. Canadell disagreed with such an explanation and argued that the

important factor for that should be the stability of forming radicals (6-membered ring),<sup>38b</sup> that is, an alkyl group at C<sub>5</sub> would stabilize the forming radical. Since there is no reliable data on the stability of radical  $R^1-\dot{C}F-R^2$ , it is hard to tell what is the real reason to make the radical **35** cyclize only via 5-exo pathway.

### The Radicals with a Perfluoro-double Bond System: **43**, **44**, **42** and **39**

Radical **43** is a perfluoro-5-hexenyl radical, the mysterious system which could not be fully understood. For example, based on the perfluoro effect discussed in Chapter 2, the reactivity of the double bond in **43** were expected as the one in **41**, and thus the rate of the ring closure of **43** should have been as fast as that of **41**. On the other hand, the electrophilic perfluoro-radical adding to the electrophilic perfluoro-double bond in **43** should be similar to the system in which trifluoromethyl radicals add to tetrafluoroethylene (Table 2-8). Thus, such radical cyclization should have been slower than that of the radical **1**. Nevertheless, **43** has the rate which is about twice as fast as the radical **1**.

With a  $\pi$  electron donor group (e.g. oxygen) connected to the perfluoro-double bond (**44**), the reactivity of the radical is enhanced relative to **43**, which can be understood by the polar effect, like the CH<sub>2</sub> group increasing the reactivity in **40**. The  $\pi$  electron donor, oxygen, makes the perfluoro-double bond in **44** electron richer than the one in **43**, and thus the transition state for **44** will be stabilized by delocalization of the  $\delta^+$  charge on the double bond through the oxygen.

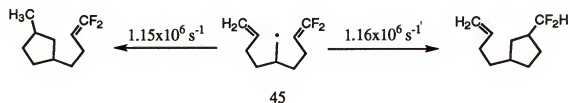
Radicals **42** and **39** are designed as the reverse systems as those of **40** and **41**, respectively. It was expected that the rates of the ring closures of **42** and **39** would be as fast as those of **40** and **41** by the polar effects. However, it was surprising that the dramatic rate enhancements which were observed in the systems, **40** and **41**, were not observed for **42** and **39**, but that both radicals gave similar rates which were close to the value of **43**, the perfluoro-5-hexenyl radical. Although the reasons for that are not clear, the observations that the cyclization of a perfluorinated radical to a hydrocarbon double

bond is much faster than that of a hydrocarbon radical to a perfluoro-double bond can be used in the synthesis of fluorinated polymers.

It is noteworthy that except for **44**, with a oxygen connected to the double bond, all of other radicals, **43**, **42** and **39**, with the perfluoro-double bonds have similar rates which seem not affected by that what difference is at the alkyl fragment. Thus, it looks as if there are some factors from the perfluoro-double bond that override the polar effects so that they all have similar reactivities. However, the similarity of these rates may just be fortuitous and derive from various combinations of factors for the individual systems.

### Radicals with Fluorinated Double Bonds 36, 37 and 38

Based on the perfluoro effect, the fluorine substituents connected to an alkene have less effect on the  $\pi$  bond than the  $\sigma$  bond. This should also lead to a lack of effect of fluorine on the reactivity of the ring closure of 5-hexenyl radicals, which are shown by the radicals **36**, **37** and **38**. These are consistent with the results reported by our group<sup>88</sup> in

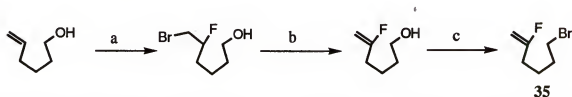


which a bifurcated system (**45**) permitted direct comparison of rates of cyclization to a hydrocarbon and a fluorine-substituted olefinic component via intramolecular competition.

These results were unexpected in view of the earlier-reported work of Tedder and Walton.<sup>14,66</sup> However, it is found by careful examination of those data reported that there were no data on the difluorinated ethylene systems ( $\text{CF}_2=\text{CH}_2$  or trans/cis isomers  $\text{CFH}=\text{CFH}$ ). Therefore, their conclusion that the reactivity of alkyl radicals with fluorine-substituted ethylene was greater than with ethylene should not include the difluorinated ethylene systems.

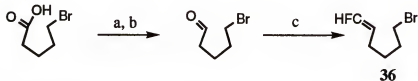
### Synthesis of Radical Precursors **35** to **40**

The radical precursors from **35** to **40** in Table 4-1 were synthesized in this work, and those from **41** to **44** were supplied by Bruce Smart (CR & D, DuPont) or C.-M. Hu (Shanghai Inst. of Organic Chemistry, China). In this section, only reaction schemes are shown, with the more detailed procedures for the synthesis of **35** to **40** as well as the preparation of the competition products (reduced and cyclized) from those radical precursors (**35** to **44**) being reported in the experimental section, Chapter 5.



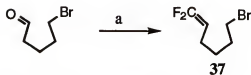
a), HF/pyridine,  $\text{CH}_2\text{Cl}_2$ , RT. b), Na/*t*-butyl alcohol,  $50^\circ\text{C}$ . c), TsCl/pyridine,  $0^\circ\text{C}$ , and then LiBr/DMF, RT.

Scheme 4-4. Synthesis of 2-Fluoro-6-bromo-1-hexene **35**



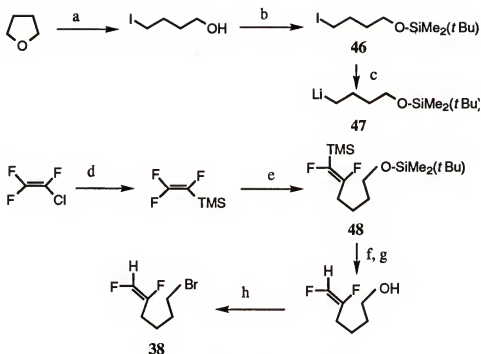
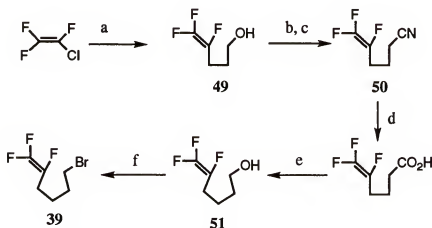
a), Borane-dimethyl sulfide,  $\text{Et}_2\text{O}$ , RT. b), Pyridinium chlorochromate,  $\text{CH}_2\text{Cl}_2$ , reflux. c),  $\text{Bu}_3\text{P}/\text{CFCl}$ ,  $\text{CH}_2\text{Cl}_2$ ,  $0^\circ$  to RT.

Scheme 4-5. Synthesis of 1-Fluoro-6-bromo-1-hexene **36**

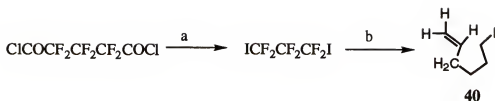


a),  $\text{P}[\text{N}(\text{CH}_3)_2]_3/\text{CF}_2\text{Br}_2$ , THF,  $0^\circ$  to  $45^\circ\text{C}$ .

Scheme 4-6. Synthesis of 1,1-Difluoro-6-bromo-1-hexene **37**

Scheme 4-7. Synthesis of 1,2-difluoro-6-bromo-1-hexene **38**Scheme 4-8. Synthesis of 1,1,2-Trifluoro-6-bromo-1-hexene **39**





a), KI, 480 psi by argon at RT, 200<sup>0</sup>-250<sup>0</sup>C. b), allylbromide/(Bu<sub>3</sub>Sn)<sub>2</sub>, C<sub>6</sub>H<sub>6</sub>, hv.

Scheme 4-9. Synthesis of 4,4,5,5,6,6-hexafluoro-6-iodo-1-hexene **40**

### Conclusion

Based on the rate constants of reduction of hydrocarbon alkyl and perfluoro-*n*-alkyl radicals by metal hydrides (R<sub>3</sub>MH, Tables 1-1 and 3-3), the rate constants of intramolecular cyclization of the series of fluorinated 5-hexenyl radicals have been measured using the competition methods as shown in Table 4-1. The regioselectivity of cyclization indicates that 5-exo cyclization is most favored for the fluorinated 5-hexenyl radicals being studied. The effects of fluorine on the reactivity of cyclization are varied with differing degrees of fluorination of the radicals.

The vinyl fluorinated radical **35** is the only one for which the fluorine substituent makes the rate of 5-exo ring closure slower (about 10 times) without affecting the 6-endo ring closure relative to unsubstituted 5-hexenyl radical (**1**), results which have been rationalized as deriving from B-strain at C<sub>5</sub> of the radical during the ring closure. If radicals have a fluorine-substituted olefinic component and an alkyl radical center (such as **36**, **37** and **38**), the fluorine-substitution has negligible effect on the rate of cyclization of the 5-hexenyl radical. However, if radicals have a perfluoro-radical center and a hydrocarbon olefinic component (such as **40** and **41**), the rates of 5-exo and 6-endo cyclization increase dramatically (up to 170 times as fast as that of radical **1**). Based on the low-lying SOMO of the perfluoro-alkyl radical, the SOMO-HOMO interaction is a dominant factor on which the polar effects are invoked to explain the rate enhancement of fluorine substituents on the ring closure of radicals **40** and **41**. Although they have different radical centers (alkyl or perfluoro-alkyl), those radicals having a perfluoro-olefinic

component (such as 39, 42 and 43) give similar rates (about twice as fast as that of radical 1).

The results obtained in this work can be used to provide some guidelines in the synthesis of compounds containing 5-membered ring with fluorines. For example, the "Tin hydride" method can be used for the fluorinated 5-hexenyl radicals in which fluorine substituents are on the olefinic bond since these radicals have a reactivity similar to that of hydrocarbon systems. Furthermore, the dramatically fast cyclization of the perfluoro-alkyl radical center to hydrocarbon olefins can override the cyclization of the alkyl radical center to hydrocarbon or fluorinated olefins so that one can design a system in which the perfluoro-alkyl radical generated in a chain reaction cyclizes (or adds) to a hydrocarbon olefin without being interfered with by other processes.

Within the continuing study of the effects of fluorine substituents on the cyclization of 5-hexenyl radicals, the results obtained in this work are just like an initiator which will open our mind in this field to search for the answers to many remaining mysteries.

## CHAPTER 5

### EXPERIMENTAL

#### General Methods

Nuclear magnetic resonance (NMR) chemical shifts are reported in parts per million (ppm) downfield ( $\delta$ ) from internal reference TMS for  $^1\text{H}$  and  $^{13}\text{C}$  spectra, and in ppm upfield ( $\delta$ ) from internal standard  $\text{CFCl}_3$  for  $^{19}\text{F}$  spectra. All NMR spectra were obtained on Varian VXR-300, Gemina-300 or Varian XL-200 instruments. The format (field strength, solvent, reference) is included for all NMR spectra reported.

Gas chromatographic separations were performed by gas-liquid phase chromatography (GLPC) on packed columns. Quantitative GLPC was performed on a Hewlett Packed 5890 Series II gas chromatograph with a flame ionization detector and a Hewlett Packed 3396a integrator. Preparative GLPC was performed on a Varian Aerograph A-90 gas chromatograph equipped with a thermal conductivity detector. Conditions and columns used are discussed in relevant experimental sections.

Mass spectra and exact masses were determined on a Finnigan MAT-95 high resolution spectrometer.

Ultraviolet (UV) spectra were obtained on a Perkin-Elmer Lambda 9 UV/VIS/NIR spectrophotometer.

Experimental text discussing a "dry" solvent indicates such material was purified (distilled) off the appropriate drying agent and stored under an inert atmosphere. The following solvents and drying agents were used: dimethylformamide ( $\text{CaH}_2$ ,  $\sim 80^\circ\text{C}$  over night and then  $50^\circ\text{C}/15\text{ mmHg}$  distillation), tetrahydrofuran (sodium/potassium benzophenone ketyl), diethyl ether (sodium benzophenone ketyl), methylene chloride ( $\text{CaH}_2$ ). All other special preparations are discussed in the appropriate experimental section.

### Experimental Procedures for those in Chapter 3

#### Materials

Arene thiols (except for *p*-trifluoromethylbenzene thiol), triethylsilane, *tris* (trimethylsilyl)silane and 1-hexene were obtained commercially (Aldrich) and used as received. Perfluoro-*n*-heptyl iodide was obtained from PCR, Inc. The  $(\text{TMS})_2\text{SiMeH}$  was obtained from C. Chatgililoglu. The  $\text{Et}_3\text{SiD}$ , *p*- $\text{CF}_3\text{PhS-H}$  and  $\text{Bu}_3\text{GeH}$  were prepared in this work as described by Stary<sup>89</sup>. All compounds used in this work were > 98% pure.

#### General Procedure for the Rate Constant of H-atom Transfers ( $k_H$ ) Determination

Samples of the reaction mixtures were degassed (freeze and thaw) three times and sealed with rubber septa under argon in Pyrex NMR tubes and then photolyzed using a Rayonet reactor for 12 hours or longer (monitored by  $^{19}\text{F}$  NMR). The products (reduction **30** and addition **31**) of the reactions were analyzed by  $^{19}\text{F}$  NMR, and in most cases,  $\text{PhCF}_3$  was used as the internal standard to calculate the NMR yield of the reactions. The ratios of reduced products to addition products were obtained by measuring the integral of the corresponding peaks in the  $^{19}\text{F}$  NMR ( $\text{CF}_2\text{-H}$ ,  $\delta = -138.1$  for the reduced product;  $\text{CF}_2\text{-CH}_2$ ,  $\delta = -114.4$  for the addition product). In the case of  $\text{Et}_3\text{SiD}$ , the two reduced products ( $\text{C}_7\text{F}_{13}\text{D}$  and  $\text{C}_7\text{F}_{13}\text{H}$ ) were identified and quantified by  $^{19}\text{F}$  NMR: a singlet peak at  $\delta = -137.3$  represented  $\text{CF}_2\text{D}$ , and a doublet peak ( $J = 54$  Hz) at  $-136.2$  is the one for  $\text{CF}_2\text{H}$ . The ratios of **30/31**, obtained for varied concentrations of 1-hexene and reductant, combined with the respective ratios of reductant to 1-hexene, allowed the determination of the ratio  $k_H/k_{\text{add}}$  according to equation 3-1. It should be pointed out that the accuracy of the values for  $k_H$  can, of course, be no better than those reported for  $k_{\text{add}}$ , which was  $\pm 8.9\%$ <sup>42,71</sup>. Thus the error estimates reported in the Table 3-3 and Table 3-4 reflect both the least squares fit of the line and the error in  $k_{\text{add}}$ , and largely derive from the error in  $k_{\text{add}}$ .

### Preparation of Et<sub>3</sub>SiD<sup>89</sup>

10.0 g (0.067 mol) of Et<sub>3</sub>SiCl (Aldrich) was added to a 250 mL, 3-neck, round bottom flask equipped with a magnetic stirrer, in which 100 mL of diethyl ether and 0.84 g (0.080 mol) of LiAlD<sub>4</sub> were charged under nitrogen. The addition of Et<sub>3</sub>SiCl was dropwise through a addition funnel at room temperature. After addition, the mixture was stirred for 0.5 hr., and then 100 mL of water was added to the reaction mixture. The aqueous mixture was extracted with diethyl ether (3 x 150 mL). The ether solution was dried over anhydrous MgSO<sub>4</sub>, and distilled by rotary evaporator to yield 8g of crude material which was purified by distillation under normal pressure to give 5.8 g of Et<sub>3</sub>SiD (78% yield).

### Preparation of Bu<sub>3</sub>GeH

The procedure was the same as that for preparation of Et<sub>3</sub>SiD, only the yield was 70%.

### Preparation of *p*-trifluoromethylbenzenethiol (*p*-CF<sub>3</sub>PhSH)

*p*-Trifluoromethylbenzenethiol was prepared by the procedure described by Holm and co-workers<sup>91</sup>. The product was identified by comparison of its <sup>19</sup>F NMR and <sup>1</sup>H NMR with those of the authentic material in the literature.<sup>91</sup>

### Preparation of 1-Hydo-perfluoro-n-heptane.30

Under photolysis conditions, 1-iodo-perfluoro-n-heptanes were reduced by Bu<sub>3</sub>SnH to yield the designated compound 30. Thus, 1.2 equiv. of Bu<sub>3</sub>SnH was added to a 50 mL flask in which 20 ml of benzene and 1.0 g of C<sub>7</sub>F<sub>15</sub>I were charged. The mixture was stirred at room temperature for 30 min. after the addition of Bu<sub>3</sub>SnH. The product 30 and solvent C<sub>6</sub>H<sub>6</sub> were separated from the reaction mixture by reduced pressure (~15 mm Hg) distillation at RT, and further purification was by preparative GC.(SE-30 column)

1-hydro-perfluoro-n-heptane, **30**:  $^{19}\text{F}$  NMR ( $\text{CDCl}_3$ ,  $\text{CFC}_l_3$ ), -80.6 (s,3F), -121.7 (s, 2F), -122.3 (s,2F), -122.7(s,2F), -128.9 (s, 2F), -138.1 (d,  $J = 54$  Hz, 2F), -125.7 (s, 2F);  $^1\text{H}$  NMR, 6.89 (t of t,  $J = 52$  and 4 Hz, 1 H); HRMS, Calculated for  $\text{C}_7\text{F}_{15}\text{H}$ , 369.9839; found, 369.9912.

### Preparation of 1-n-hexyl-perfluoro-n-heptane.31

$\text{C}_7\text{F}_{15}\text{I}$  underwent addition to 1-hexene under  $\text{Et}_3\text{B}$  catalysis.<sup>90</sup> 0.1 equiv  $\text{Et}_3\text{B}$  (0.2 mL of 1 M hexane solution solution) was added to a 25 mL 3-necked flask in which 1.0 g of  $\text{C}_7\text{F}_{15}\text{I}$  and 1.2 equiv. of 1-hexene were charged. The mixture was stirred at RT for 6 hr, and then 2 equiv of  $\text{Bu}_3\text{SnH}$  was added via syringe and stirred for 30 min. The reaction mixture was distilled under reduced pressure (~2 mmHg) to get rid of tin compounds. Further purification was by preparative GC (SE-30 column).

1-n-Hexyl-perfluoro-n-heptane, **31**.  $^{19}\text{F}$  NMR, -81.26 (s, 3F, -114.4 (t,  $J = 12$  Hz, 2F), -121.80 (s, 2F), -122.14 (s, 2F), -122.90 (s, 2F), -123.5 (s, 2F), -126.3 (s,2F);  $^1\text{H}$  NMR, 1.69 (m, 2H), 1.32 (m, 2H), 1.12 (m, 2H), 0.98 (m, 4H), 0.83 (t,  $J = 4.9$  Hz, 3H); HRMS, calculated for  $\text{C}_{13}\text{H}_{13}\text{F}_{15}$ , 454.0777, found, 454.0774.

Table 5-1. Competition Data for the Reaction of Perfluoro-n-heptyl Radical with 1-Hexene and *tris*-(Trimethylsilyl)silane at 303K

[1-hexene]	[Silane]/[1-hexene]	30/31	Yield
3.34	0.54	3.44	97
3.68	0.46	2.96	98
4.05	0.38	2.30	99
4.49	0.30	1.84	98
5.01	0.23	1.42	96
5.06	0.16	1.00	94

Table 5-2. Competition Data for the Reaction of Perfluoro-n-heptyl Radical with 1-Hexene and *bis*-(Trimethylsilyl)methylsilane at 303K

[1-hexene]	[Silane]/[1-hexene]	30/31	Yield
0.71	1.90	4.16	94
0.87	1.47	3.14	92
1.00	1.16	2.55	94
1.19	0.86	2.02	93
1.29	0.67	1.55	93
1.44	0.50	1.23	99

Table 5-3. Competition Data for the Reaction of Perfluoro-n-heptyl Radical with 1-Hexene and Tributyl Germanium hydride at 303K

[1-hexene]	[Bu <sub>3</sub> GeH]/[1-hexene]	30/31	Yield
1.76	0.31	0.74	94
1.51	0.44	0.97	96
1.26	0.63	1.31	99
1.01	0.90	1.79	99
0.75	1.37	2.66	100
0.58	1.97	3.94	97

Table 5-4. Competition Data for the Reaction of Perfluoro-n-heptyl Radical with 1-Hexene and Triethylsilane at 303K

[1-hexene]	[Et <sub>3</sub> SiH]/[1-hexene]	30/31	Yield
0.78	6.85	0.71	98
1.16	4.36	0.48	93
1.56	3.06	0.34	94
1.94	2.31	0.29	95
2.32	1.80	0.24	94
2.72	1.43	0.20	91

Table 5-5. Competition Data for the Reaction of Perfluoro-n-heptyl Radical with 1-Hexene and Triethylsilane-d<sub>1</sub> at 303K

[1-hexene]	[Et <sub>3</sub> SiD]/[1-hexene]	30-D/31	30-H/31	Yield
0.74	7.49	0.235	0.035	93
0.87	6.28	0.202	0.030	92
0.98	5.49	0.172	0.028	92
1.05	4.77	0.156	0.024	96
1.23	4.20	0.138	0.019	94
1.35	3.74	0.124	--	93

Table 5-6. Competition Data for the Reaction of Perfluoro-n-heptyl Radical with 1-Hexene and *p* methoxybenzenethiol at 303K

[1-hexene]	[Thiol]/[1-hexene]	30/31	Yield
0.61	6.06	0.86	90
0.73	4.70	0.70	92
0.85	3.74	0.54	90
0.97	3.03	0.48	90
1.21	2.02	0.36	90

Table 5-7. Competition Data for the Reaction of Perfluoro-n-heptyl Radical with 1-Hexene and *p* methylbenzenethiol at 303K

[1-hexene]	[Thiol]/[1-hexene]	30/31	Yield
0.61	6.01	0.53	95
0.85	3.74	0.35	89
0.97	3.01	0.28	94
1.08	2.49	0.24	92
1.21	1.99	0.19	94



Table 5-8. Competition Data for the Reaction of Perfluoro-n-heptyl Radical with 1-Hexene and *m*-methoxybenzenethiol at 303K

[1-hexene]	[Thiol]/[1-hexene]	30/31	Yield
0.61	6.00	0.25	87
0.73	4.66	0.21	91
0.85	3.71	0.18	92
0.97	3.00	0.14	94
1.08	2.48	0.12	94
1.21	2.00	0.10	94

Table 5-9. Competition Data for the Reaction of Perfluoro-n-heptyl Radical with 1-Hexene and benzenethiol at 303K

[1-hexene]	[Thiol]/[1-hexene]	30/31	Yield
0.61	7.26	0.34	89
0.85	4.49	0.23	89
0.97	3.63	0.19	95
1.07	3.00	0.17	94
1.21	2.42	0.13	99

Table 5-10. Competition Data for the Reaction of Perfluoro-n-heptyl Radical with 1-Hexene and *p*-Trifluoromethylbenzenethiol at 303K

[1-hexene]	[Thiol]/[1-hexene]	30/31	Yield
0.61	6.02	0.19	91
0.73	4.68	0.17	96
0.86	3.72	0.14	95
0.98	3.01	0.13	94
1.08	2.48	0.11	97
1.22	2.00	0.09	94

## Experimental Procedures for those in Chapter 4

### Synthesis of 2-Fluoro-6-bromo-1-hexene 35

The vinyl fluorination involved two steps: a) the *in situ* generation of bromine fluoride (BrF) and subsequent addition to an olefin<sup>92</sup>, and b) elimination of hydrogen bromide (HBr) under basic conditions. 1.4 g (0.014 mol) of 5-hexenol (Aldrich) was mixed with 3.0 g of N-bromosuccinimide in 10 mL methylene chloride in a poly-ethylene container at RT. 1.4 mL (0.042 mol) of HF/ pyridine (PCR, 70% HF in 30% pyridine) was slowly added to the mixture at RT, and then stirred for 2 hr. The reaction mixture was poured into 100 mL of saturated NaHCO<sub>3</sub> solution and extracted with CHCl<sub>3</sub> (3 x 100 mL). The dark red mixture was distilled under reduced pressure (0.5 mmHg, 70°C) to obtain 2.8 g (45% yield) of 6-bromo-5-fluorohexanol.

Elimination of hydrogen bromide from 6-bromo-5-fluorohexanol took place as following: 5 equiv of sodium metal was added to *t*-butyl alcohol in a round bottom flask and stirred until that the sodium was dissolved completely. Setting the temperature to 50°C, 2.8 g (6.3 mmol) of 6-bromo-5-fluoro-1-hydroxy-hexane was added through a syringe. After stirring for about 0.5 hr at 50°C, the mixture was distilled under reduced pressure (0.5 mmHg, 50°C) to remove *t*-butyl alcohol. To the residue 50 mL of saturated NaHCO<sub>3</sub> was added and extracted by diethyl ether (3 x 50 mL). Then, 2-fluoro-6-hydroxy-hexene was obtained, which was through tosylation (TsCl/pyridine) and bromination (LiBr/ DMF) converted to the title compound. The final purification was by column chromatography.

2-Fluoro-6-bromo-1-hexene **35**: <sup>1</sup>H NMR (300 Mhz, CDCl<sub>3</sub>, TMS), 1.70 (m, 2H) 1.93 (m, 2H), 2.24 (m, 2H), 3.44 (t, J = 7 Hz, 2H), 4.26 (m of d, J = 51 Hz, 1H), 4.54 (d of d, J = 18 Hz, 3 Hz, 1H); <sup>13</sup>C NMR (75 Mhz, CDCl<sub>3</sub>, TMS) 24.5, 30.7, 31.1, 31.7, 33.17, 90.0 (d); <sup>19</sup>F NMR (282 MHz, CDCl<sub>3</sub>, CFCl<sub>3</sub>) -95.39 (q of d, J = 51 Hz, 17 Hz, 1F); HRMS, calcd for C<sub>6</sub>H<sub>10</sub>BrF, 179.9950, found, 179.9950.

### Preparation of 2-fluoro-1-hexene 35-1

Reduced compound **35-1** was obtained by reduction of **35** by  $\text{Bu}_3\text{SnH}$  under photolytic conditions. 0.067 g of **35** was mixed with 1.1 equiv of the tin hydride in 0.4 mL of  $\text{C}_6\text{H}_6$  and sealed in a Pyrex NMR tube. Photolyzed in a Rayonet reactor for 12 hr, the reaction mixture was distilled under reduced pressure (0.5 mmHg, RT) to remove tin compounds. Further purification was by preparative GC.

2-Fluoro-1-hexene **35-1**:  $^1\text{H}$  NMR (300 Mhz,  $\text{CDCl}_3$ , TMS) 0.93 (t,  $J = 7$  Hz, 3H), 1.36 (m, 2H), 1.48 (m, 2H), 2.18 (m, 2H), 4.20 (m of d,  $J = 51$  Hz, 1H), 4.48 (d of d,  $J = 18$  Hz, 3 Hz, 1H);  $^{13}\text{C}$  NMR (75 MHz,  $\text{CDCl}_3$ , TMS) 13.7, 22.0, 28.1, 31.34, 31.7, 89.2 (d);  $^{19}\text{F}$  NMR (282 MHz,  $\text{CDCl}_3$ ,  $\text{CFCl}_3$ ) -95.13 (q of d,  $J = 51$  Hz, 17 Hz, 1F); HRMS, calcd for  $\text{C}_6\text{H}_{11}\text{F}$ , 102.0845, found, 102.0861.

### Preparation of 1-fluoro-1-methylcyclopentane 35-2

**35-2** could be obtained by cyclization of **35** under photolytic conditions, in which  $\text{Bu}_3\text{GeH}$  was the radical conductor. 0.067 g of **35** was mixed with 1.1 equiv of the  $\text{Bu}_3\text{GeH}$  in 0.4 mL of  $\text{C}_6\text{H}_6$  and sealed in a Pyrex NMR tube. Photolyzed in a Rayonet reactor for 12 hr, the reaction mixture was distilled under reduced pressure (0.5 mmHg, RT) to separate **35-2** and  $\text{C}_6\text{H}_6$  from the reaction mixture. Further purification was by preparative GC.

1-Fluoro-1-methyl-cyclopentane **A-2**:  $^1\text{H}$  (300 MHz,  $\text{CDCl}_3$ , TMS) 1.29 (d,  $J = 20.6$  Hz, 3H), 1.16-1.42 (m, 4H), 1.76-1.97 (m, 4H);  $^{19}\text{F}$  NMR (282 MHz,  $\text{CDCl}_3$ ,  $\text{CFCl}_3$ ) -134.66 (m, 1F); HRMS, calcd for  $\text{C}_6\text{H}_{11}\text{F}$ , 102.0845, found, 102.0860.

### Synthesis of 1-fluoro-6-bromo-1-hexene 36

5-Bromopentanoic acid (Aldrich) could be converted to 1-fluoro-6-bromo-1-hexene through 2 steps: a) the conversion of carboxylic acids to aldehydes<sup>93</sup>, and b) fluorine-containing Wittig olefination of the aldehyde<sup>94</sup>.

5-Bromopentanal. 10.8 g (60 mmol) of 5-bromopentanoic acid and 75 mL of diethyl ether were mixed in a dry 250 mL round-bottom flask under nitrogen. The mixture was stirred vigorously and borane-dimethyl sulfide (BMS, Aldrich; 6.12 mL, 60 mmol) was added dropwise using a syringe. Following the addition of the initial 2-3 mL of BMS, when the gas evolution had ceased, the mixture was heated under gentle reflux to complete the evolution of gas (hydrogen). The remainder of the BMS was added at such a rate as to maintain a gentle reflux. After the addition, the mixture was heated under reflux for 2 hr. The solvent and dimethyl sulfide were removed under vacuum and 20 mL of methylene chloride was introduced to dilute the product. This solution was added dropwise to a well-stirred suspension of pyridinium chlorochromate (14.3 g, 66 mmol, PCC, Aldrich) in 100 mL of methylene chloride in a 500 mL flask. The stirred mixture was heated under reflux for 1 hr and then diluted with 150 mL of diethyl ether. The supernatant liquid was filtered and dried over  $\text{MgSO}_4$ . The colorless filtrate was concentrated and distilled under reduced pressure to give 5-bromopentanal; yield 6.8 g (70%),  $^1\text{H}$  NMR (300 MHz,  $\text{CDCl}_3$ , TMS), 1.84 (m, 4H), 2.51 (t, 2H), 3.43 (t,  $J = 7$  Hz, 2H), 9.78 (t, 1H);  $^{13}\text{C}$  NMR (75 MHz,  $\text{CDCl}_3$ , TMS), 20.3, 31.6, 32.9, 42.4, 183.2.

1-Fluoro-6-bromo-1-hexene. A 300 mL three-necked flask was charged with 22.4 mL (0.090 mol) of tri-*n*-butylphosphine and 30 mL of methylene chloride. The solution was cooled in an ice bath, and 2.8 mL (0.030 mol) of trichlorofluoromethane was added via syringe. The resultant mixture was stirred at  $0^\circ\text{C}$  for 1 hr and then at RT for 6 hr. To this phosphoranium salt solution was added 3.9 g (0.024 mol) of 5-bromopentanal via syringe. The reaction was stirred for 8 hr at RT. 40 mL of 10% NaOH was added slowly to the reaction mixture followed by stirring at RT for 18 hr. The resultant organic layer was acidified and then was extracted with methylene chloride (2 x 50 mL), followed by washing with 40% sodium bisulfite (2 x 50 mL) and water (2 x 50 mL), and the organic portion dried with magnesium sulfate. Purification was by reduced pressure distillation ( $60^\circ\text{C}$ , 0.5 mmHg) to give 1.3 g (30% yield) and the major product was *Z*-isomer (>98%).

1-Fluoro-6-bromo-1-hexene:  $^1\text{H}$  NMR (300 MHz,  $\text{CDCl}_3$ , TMS), 1.14 (m, 2H), 1.35 (m, 2H), 1.86 (q, 2H), 3.04 (t,  $J = 7$  Hz, 2H), 4.25 (m of d,  $J = 43$  Hz, 1H), 6.11 (d of d,  $J = 85$  Hz, 5 Hz, 1H);  $^{13}\text{C}$  (75 MHz,  $\text{CDCl}_3$ , TMS), 24.5, 30.7, 32.1, 32.7, 33.5, 90.2 (d);  $^{19}\text{F}$  NMR (282 MHz,  $\text{CDCl}_3$ ,  $\text{CFCl}_3$ ), -130.44 (q,  $J = 43$  Hz, 1F); HRMS, calcd for  $\text{C}_6\text{H}_{10}\text{BrF}$ , 179.9950, found, 179.9927.

#### Preparation of 1-fluoro-1-hexene 36-1

1-Fluoro-1-hexene **36-1** was obtained with reduction of 1-fluoro-6-bromo-1-hexene **36** by the tributyltin hydride under photolytic conditions. 0.1 g (0.6 mmol) of **36** was mixed with the tributyltin hydride in 0.3 mL of pentane and sealed in a Pyrex NMR tube. The mixture was photolyzed in a Rayonet reactor for 12 hr. Both reduced product **36-1** and cyclized product **36-2** were obtained (about 50% to 50%). The reaction mixture was distilled under reduced pressure (0.5 mmHg, RT) to separate the tin compounds from the products. Further purification of both **36-1** and **36-2** was by preparative GC. It is noteworthy that the double bond was isomerized to give Z and E isomers of **36-1** after photolysis.

Z, 1-Fluoro-1-hexene **36-1**:  $^1\text{H}$  NMR (300 MHz,  $\text{CDCl}_3$ , TMS), 0.82 (t,  $J = 7$  Hz, 3H), 1.20 (m, 4H), 2.05 (q, 2H), 4.46 (m of d,  $J = 43$  Hz, 1H), 6.19 (m of d,  $J = 85$  Hz, 1H);  $^{19}\text{F}$  NMR (282 MHz,  $\text{CDCl}_3$ ,  $\text{CFCl}_3$ ), -130.92 (q,  $J = 43$  Hz, 1F); HRMS, calcd for  $\text{C}_6\text{H}_{11}\text{F}$ , 102.0845, found, 102.0861.

E, 1-Fluoro-1-hexene **36-1-1**:  $^1\text{H}$  NMR (300 MHz,  $\text{CDCl}_3$ , TMS), 0.81 (t,  $J = 7$  Hz, 3H), 1.11 (m, 4H), 1.59 (q, 2H), 5.21 (m, 1H), 6.25 (d of d,  $J = 85$  Hz, 12 Hz, 1H);  $^{19}\text{F}$  NMR (282 MHz,  $\text{CDCl}_3$ ,  $\text{CFCl}_3$ ), -130.34 (d of d,  $J = 85$  Hz, 19 Hz, 1F); HRMS, calcd for  $\text{C}_6\text{H}_{11}\text{F}$ , 102.0845, found, 102.0868

#### Preparation of monofluoromethylcyclopentane 36-2

Cyclized compound **36-2** from **36** was isolated from the reaction mixture as described above in preparing **36-1**, by preparative GC.

Monofluoromethylcyclopentane **36-2**:  $^1\text{H}$  NMR (300 MHz,  $\text{CDCl}_3$ , TMS), 1.32-1.42 (m, 4H), 1.5-1.58 (m, 4H), 3.04 (m, 1H), 3.99 (d of d,  $J = 48$  Hz, 7 Hz, 2H);  $^{19}\text{F}$  NMR (282 MHz,  $\text{CDCl}_3$ ,  $\text{CFCl}_3$ ), -215.9 (d of t,  $J = 48$  Hz, 17 Hz, 1F); HRMS, calcd for  $\text{C}_6\text{H}_{11}\text{F}$ , 102.0845, found, 102.0843.

### Synthesis of 1,1-difluoro-6-bromo-1-hexene **37**

Fluorine-containing Wittig olefination<sup>95</sup> of 5-bromopentanal which had been made in the synthesis of 1-fluoro-6-bromo-1-hexene will give the title product. To a dry 300 mL 3-necked flask under nitrogen were added 100 mL of THF and 4.2 g (0.02 mol, 3.6 mL) of dibromodifluoromethane and the mixture then cooled to  $0^\circ\text{C}$ . 13.2 g (0.04 mol) of  $\text{P}[\text{N}(\text{CH}_3)_2]_3$  was dissolved in 15 mL of THF and added dropwise to the mixture. The resultant suspensant of white solid was stirred at  $0^\circ\text{C}$  for 1 hr, and 3.3 g (0.02 mol) of 5-bromopentanal dissolved in 20 mL of THF was added dropwise via a syringe. The mixture was stirred at  $0^\circ\text{C}$  for 0.5 hr and warmed to  $45^\circ\text{C}$  for 2 hr. To the resultant mixture was added 10 mL of water to stop the reaction. The organic portion was concentrated by rotary evaporator to get rid of the THF. The residue was dissolved in 150 mL of diethyl ether and washed with water (2 x 100 mL), and then dried over  $\text{MgSO}_4$ . Purification was by column chromatography yielding 2.8 g (71% yield).

1,1-Difluoro-6-bromo-1-hexene **37**:  $^1\text{H}$  NMR (300 MHz,  $\text{CDCl}_3$ , TMS), 1.56 (m, 2H), 1.90 (m, 2H), 2.03 (m, 2H), 3.43 (t,  $J = 7$  Hz, 2H), 4.14 (m of d,  $J = 25$  Hz, 1H);  $^{13}\text{C}$  NMR (75 MHz,  $\text{CDCl}_3$ , TMS), 21.9, 27.4, 28.5, 32.4, 33.5, 156.3 (t);  $^{19}\text{F}$  NMR (282 MHz,  $\text{CDCl}_3$ ,  $\text{CFCl}_3$ ), -89.38 (d,  $J = 47$  Hz, 1F), -91.85 (q,  $J = 25$  Hz, 1F); HRMS, calcd for  $\text{C}_6\text{H}_9\text{BrF}_2$ , 197.9856, found, 197.9834.

### Preparation of 1,1-difluoro-1-hexene **37-1** and difluoromethylcyclopentane **37-2**

The procedure for making these two compounds from **37** was the same as that used in making **36-1** and **36-2** from **36**.

1,1-Difluoro-1-hexene **37-1**:  $^1\text{H}$  NMR (300 MHz,  $\text{CDCl}_3$ , TMS), 0.91 (t,  $J = 7$  Hz, 3H), 1.35 (m, 4H), 1.97 (m, 2H), 4.13 (d of t,  $J = 25$  Hz, 3 Hz, 1H);  $^{19}\text{F}$  NMR (282 MHz,  $\text{CDCl}_3$ ,  $\text{CFCl}_3$ ), -90.41 (d,  $J = 50$  Hz, 1F), -92.83 (q,  $J = 24$  Hz, 1F); HRMS, calcd for  $\text{C}_6\text{H}_{10}\text{F}_2$ , 120.0751, found, 120.0739.

Difluoromethylcyclopentane **37-2**:  $^1\text{H}$  NMR (300 MHz,  $\text{CDCl}_3$ , TMS), 1.53-1.66 (m, 6H), 1.76-1.82 (m, 2H), 2.36 (m, 1H), 5.66 (d of t,  $J = 57$  Hz, 5 Hz, 1H);  $^{19}\text{F}$  NMR (282 MHz,  $\text{CDCl}_3$ ,  $\text{CFCl}_3$ ), -119.44 (d of d,  $J = 57$  Hz, 15 Hz, 2F);<sup>5-8</sup> HRMS, calcd for  $\text{C}_6\text{H}_{10}\text{F}_2$ , 120.0751, found, 120.0713.

### Synthesis of 1,2-difluoro-6-bromo-1-hexene **38**

Part A, 4-*tert*-butyldimethylsilyl-oxy-butyl lithium **47**: the lithium compound was prepared by adaptation of procedures<sup>96,97,98</sup>. To a dry 250 mL round bottom flask was added 50 mL of dry THF, and then 10 g (0.050 mol) of trimethylsilyl iodide was syringed into the THF under nitrogen. At RT, the mixture was stirred for 1 hr before the excess THF was removed by a rotary evaporator. The residue was diluted with diethyl ether (200 mL) and washed with saturated  $\text{NaHCO}_3$  solution (2 x 150 mL). The organic layer was dried over  $\text{MgSO}_4$ , and then diethyl ether was evaporated. To the residue in a 300 mL of round bottom flask were added about 2 equiv (15.5 g, 0.10 mol) of dimethyl-*tert*-butyl silyl chloride and 4 equiv (14.5 g, 0.20 mol) of imidazole in 60 mL of DMF. After stirring for 48 hr at RT, the mixture was poured into 200 mL of diethyl ether, and then the mixture was extracted with  $\text{H}_2\text{O}$  (3 x 100 mL) and dried over  $\text{MgSO}_4$ . The resulting solution was distilled under reduced pressure to give 12.5 g of *t*-butyl-dimethylsilyl 4-iodo-butyl ether **46** (79% yield).  $^1\text{H}$  NMR (300 MHz,  $\text{CDCl}_3$ , TMS), 0.20 (s, 6H), 1.04 (s, 9H), 1.82 (m, 2H), 2.02 (m, 2H), 3.71 (t,  $J = 7$  Hz, 2H), 3.79 (t,  $J = 7$  Hz, 2H). To a dry 500 mL of round bottom flask under argon were added 10 g (0.032 mol) of **46**, dry 120 mL pentane, and 80 mL diethyl ether (pentane/ether = 3/2 by volume). The solution was cooled to -78°C, the stirrer started, and 42 mL (0.070 mol, 1.7 M in pentane, Aldrich) of *tert*-butyl lithium in pentane was then added dropwise via a syringe. Stirring was continued at -78°C

for an additional 5 min following the addition, the cooling bath was then removed, and the mixture was allowed to warm and stand at RT for 2 hr to consume unreacted *t*-BuLi. The solution (200 mL, ~ 0.16 M of **46**) was used at once in Part B.

Part B, *tert*-butyldimethylsilyl 5,6-difluoro-6-trimethylsilyl-5-hexenyl ether **48** was prepared by an adaptation of procedures<sup>99,100</sup>. To 60 mL of diethyl ether in a 300 mL round bottom flask cooled to -110°C was transferred 10 g (0.086 mol) of chlorotrifluoroethylene, and then 45 mL (0.078 mol, 1.7 M in pentane, Aldrich) of *t*-BuLi was added dropwise. The mixture was stirred at -110°C for 0.5 hr before the temperature was allowed to rise to -60°C. To the mixture was added 10 g of trimethylsilyl chloride and the mixture was stirred for 0.5 hr. After warming up to 0°C and remaining at the temperature for 0.5 hr, the reaction mixture was poured into 100 mL of saturated NaHCO<sub>3</sub>. The organic portion was dried over MgSO<sub>4</sub>, filtered and transferred to a dry 300 mL flask (total volume: ~110 mL). The flask was cooled to -78°C, and to it was added all of the solution (prepared in Part A) dropwise. This mixture was stirred at -78°C for 10 min before warming to RT with continued stirring for 1 hr. The reaction mixture was poured into 100mL of saturated NaHCO<sub>3</sub> and washed with H<sub>2</sub>O (3 x 100 mL). The organic layer was dried over MgSO<sub>4</sub>, after removing solvents, 8.7 g crude material was obtained, and was about 85% pure by GC analysis, which was identified as **48** by <sup>19</sup>F NMR analysis. <sup>19</sup>F NMR (282 M Hz, CDCl<sub>3</sub>, CFCl<sub>3</sub>), -145.12 (t of d, J = 128 Hz, 23 Hz, 1F), -173.96 (d, J = 126 Hz, 1F).

Part C, 1,2-difluoro-6-bromo-1-hexene **38**. To a 250 mL round bottom flask were added 100 mL of DMF, 5 mL of H<sub>2</sub>O and 10 g of KF, and the mixture stirred until solids were dissolved in the solution. All of the crude material obtained in Part B was added to the flask and stirred at RT for 12 hr, after which 150 mL of diethyl ether was added to the flask and the solution washed with brine (3 x 100 mL), and then with H<sub>2</sub>O (2 x 50 mL). The organic portion was dried over MgSO<sub>4</sub>, and solvents were removed by rotary evaporator. The residue was placed in a 250 mL round bottom flask, and to it was added 50 mL (2 x 0.024 mol) of Bu<sub>4</sub>NF (Aldrich, 1.0 M in THF) in 100 mL of dry THF, and the



mixture stirred at RT for 24 hr. The THF was removed by rotary evaporator, and the reaction mixture was worked up in the usual manner (as described in Part B). The mixture was purified by distillation under reduced pressure.  $^1\text{H}$  and  $^{19}\text{F}$  NMR analysis of the distillate indicated that it was 5,6-difluoro-5-hexenol:  $^1\text{H}$  NMR (300 M Hz,  $\text{CDCl}_3$ , TMS), 1.61 (m, 4H), 2.41 (m, 2H), 2.62 (br, 1H), 3.61 (t,  $J = 7$  Hz, 2H), 7.08 (d of d,  $J = 117$  Hz, -, 1H);  $^{19}\text{F}$  NMR (282 M Hz,  $\text{CDCl}_3$ ,  $\text{CFCI}_3$ ), -160.73 (t of d,  $J = 192$  Hz, 34 Hz, 1F), -183.78 (d of d,  $J = 192$  Hz, 116 Hz, 1F).

As described in the synthesis of 35, 5,6-difluoro-5-hexenol was converted to 1,2-difluoro-6-bromo-1-hexene 38. The final purification was by column chromatography to give 2.1 g. The overall yield (based on the trimethylsilyl iodide) was 21%.

1,2-Difluoro-6-bromo-1-hexene 38:  $^1\text{H}$  NMR (300 M Hz,  $\text{CDCl}_3$ , TMS), 1.73 (m, 2H), 1.92 (m, 2H), 2.42 (m, 2H), 3.43 (t,  $J = 7$  Hz, 2H), 7.09 (d of d,  $J = 75$  Hz, 3 Hz, 1H);  $^{13}\text{C}$  NMR (75 M Hz,  $\text{CDCl}_3$ , TMS), 23.8, 24.9, 25.2, 31.6, 33.0, 138.1 (d), 141.3 (d);  $^{19}\text{F}$  NMR (282 M Hz,  $\text{CDCl}_3$ ,  $\text{CFCI}_3$ ), -160.37 (t of d,  $J = 128$  Hz, 23 Hz, 1F), -182.81 (d of d,  $J = 128$  Hz, 76 Hz, 1F); HRMS, calcd for  $\text{C}_6\text{H}_9\text{F}_2\text{Br}$ , 197.9856, found, 197.9821.

#### Preparation of 1,2-difluoro-1-hexene 38-1 and 1-monofluoromethyl-1-fluorocyclopentane 38-2

Preparation of 38-1 and 38-2 was carried out by the same procedures as those used for the preparation of 35-2 and 35-3.

1,2-Difluoro-1-hexene 38-1:  $^1\text{H}$  NMR (300 M Hz,  $\text{CDCl}_3$ , TMS), 0.94 (t,  $J = 7$  Hz, 3H), 1.39 (m, 2H), 1.54 (m, 2H), 2.39 (m, 2H), 7.07 (d of d,  $J = 77$  Hz, 3 Hz, 1H);  $^{19}\text{F}$  NMR (282 M Hz,  $\text{CDCl}_3$ ,  $\text{CFCI}_3$ ), -160.12 (t of d,  $J = 130$  Hz, 23 Hz, 1F), -183.79 (d of d,  $J = 128$  Hz, 77 Hz, 1F); HRMS, calcd for  $\text{C}_6\text{H}_{10}\text{F}_2$ , 120.0751, found, 120.0747.

1-Monofluoromethyl-1-fluorocyclopentane 38-2:  $^1\text{H}$  NMR (300 M Hz,  $\text{CDCl}_3$ , TMS), 1.18-1.34 (m, 4H), 1.57 (m, 4H), 4.03 (d of d,  $J = 48$  Hz, 20 Hz, 2H);  $^{19}\text{F}$  NMR

(282 M Hz,  $C_6D_6$ ,  $CFCl_3$ ), -150.44 (br, 1F), -224.51 (d of t,  $J = 48$  Hz, 14 Hz, 1F);

HRMS, calcd for  $C_6H_{10}F_2$ , 120.0751, found, 120.0751.

### Synthesis of 1,1,2-trifluoro-6-bromo-1-hexene 39

The first step in the synthesis of 1,1,2-trifluoro-6-bromo-1-hexene was the key step adapted from a procedure described by Sauvêtre<sup>101</sup>. The complete 7 step synthesis is described as following:

4,5,5-Trifluoro-4-pentenol 49: 300 mL of dry diethyl ether was placed in a dry 1000 mL round bottom flask and cooled to  $-100^{\circ}C$  (liquid nitrogen + diethyl ether). Under argon, to the flask was transferred 53 g (0.455 mol) of chlorotrifluoroethylene. Then, 270 mL (0.459 mol) of *tert*-butyllithium (1.7 M in pentane, Aldrich) was added to the solution dropwise through a additional funnel. After addition of *tert*-butyllithium, the mixture was stirred for 0.5 hr at  $-110^{\circ}C$ , and then 60 g (0.455 mol) of boron trifluoride etherate (Aldrich) was syringed into the solution. 8.8 g (0.152 mol) of trimethylene oxide (Aldrich) was added to the solution slowly in order to keep the temperature at  $-110^{\circ}C$ . After addition of trimethylene oxide, the mixture was stirred for 10min, and then the temperature was allowed to rise to  $-78^{\circ}C$  and stirred for 1 hr more. 250 mL of saturated  $NaHCO_3$  was poured into the reaction mixture and the temperature raised to RT. The organic portion was washed with brine (2 x 200 mL) and dried over  $MgSO_4$ . After distillation, 16.2 g of alcohol was obtained (76% yield)  $^1H$  NMR (300 M Hz,  $CDCl_3$ , TMS), 1.75 (m, 2H), 2.34 (m, 2H), 3.14 (br, 1H), 3.61 (t,  $J = 7$  Hz, 2H);  $^{19}F$  NMR (282 M Hz,  $CDCl_3$ ,  $CFCl_3$ ), -106.03 (d of d,  $J = 89$  Hz, 32 Hz, 1F), -125.11 (d of d,  $J = 116$  Hz, 89 Hz, 1F), 174.76 (m, 1F).

4,5,5-Trifluoro-4-pentenynitrile 50: To a 500 mL dry, round bottom flask was added 16.0 g (0.114 mol) of 4,5,5-trifluoro-4-pentenol (see above) with 200 mL of dry pyridine. The mixture was cooled to  $0^{\circ}C$ , and then 35 g (0.18 mol) of tosyl chloride (Aldrich) was added and the mixture was stirred for 6 hr. The mixture was poured into 50 mL of  $H_2O$  and extracted with methylene chloride (3 x 100 mL). Distillation of the organic

phase gave a light yellow oil (tosylated alcohol) that was used directly in the next step. 30 g (0.45 mol) of potassium cyanide in 500 mL DMSO was placed in a 1000 mL round bottom flask and cooled to 0°C. ~ 0.114 mol of the above tosylated alcohol was syringed into the flask, and the mixture was stirred for 20 min before removing the ice bath. The temperature was allowed to rise to RT, and then the mixture was stirred for 1.5-2 hr (not more than 2.5 hr). 100 mL of H<sub>2</sub>O was poured into the flask and the organic portion was extracted with diethyl ether (4 x 200 mL). All of the ether solutions were combined and washed with brine (4 x 100), and distillation of the resultant solution gave 13.6 g (81% yield based on the alcohol) for the title compound. <sup>1</sup>H NMR (300 M Hz, CDCl<sub>3</sub>, TMS), 1.87 (m, 2H), 2.39 (m, 4H); <sup>19</sup>F NMR (282 M Hz, CDCl<sub>3</sub>, CFCI<sub>3</sub>), -103.91 (d of d, J = 85 Hz, 32 Hz, 1F), -123.38 (d of d, J = 114 Hz, 85 Hz, 1F), -175.29 (m, 1F)

**5.6.6-Trifluoro-5-hexenol 51:** In a 300 mL flask attached to a reflux condenser was placed a mixture of 13.5 g (0.091 mol) of nitrile (made above) and 50 mL of concentrated hydrogen chloride. The mixture was heated to reflux (became dark), and then stirred for 4-5 hr under reflux. 150 mL of H<sub>2</sub>O was added, the solution was extracted with diethyl ether (4 x 100 mL), and distillation of the resultant solution gave 8.5 g (55% yield) of a carboxylic acid. <sup>1</sup>H NMR (300 M Hz, CDCl<sub>3</sub>, TMS), 1.89 (m, 2H), 2.39 (m, 4H), 4.78 (b, 1H); <sup>19</sup>F NMR (282 M Hz, CDCl<sub>3</sub>, CFCI<sub>3</sub>), -104.88 (m, 1F), -124.31 (m, 1F), -176.67 (m, 1F). This carboxylic acid reacted with lithium aluminum hydride to give the title product: To 55 mL of a solution of lithium aluminum hydride (1.0 M in diethyl ether, Aldrich) in a 250 mL round bottom flask was added 8.5 g (0.051 mol) of the acid obtained above. The mixture was stirred at RT for 5 hr. 10 mL of water was added to the flask and the mixture was extracted with diethyl ether (3 x 50 mL), and distillation of the resultant gave the title product (6.5 g, 85% yield). <sup>1</sup>H NMR (300 M Hz, CDCl<sub>3</sub>, TMS), 1.63-1.65 (m, 4H), 2.32 (m, 2H), 2.56 (br, 1H), 3.66 (t, J = 7 Hz, 2H); <sup>19</sup>F NMR (282 M Hz, CDCl<sub>3</sub>, CFCI<sub>3</sub>), -106.77 (d of d, J = 90 Hz, 32 Hz, 1F), -125.82 (d of d, J = 114 Hz, 90 Hz, 1F), -175.25 (m, 1F).

Through tosylation and bromination (see the procedure in the synthesis of 2-fluoro-6-bromo-1-hexene), the above alcohol was converted to 1,1,2-trifluoro-6-bromo-1-hexene **39**. Purification was by column chromatography to give the product 4.8 g (overall yield based on the trimethylene oxide: 15%).

1,1,2-Trifluoro-6-bromo-1-hexene **39**:  $^1\text{H}$  NMR (300 M Hz,  $\text{CDCl}_3$ , TMS), 1.74 (m, 2H), 1.93 (m, 2H), 2.33 (m, 2H), 3.44 (t,  $J = 7$  Hz, 2H);  $^{19}\text{F}$  NMR (282 M Hz,  $\text{CDCl}_3$ ,  $\text{CFCl}_3$ ), -105.21 (d of d,  $J = 88$  Hz, 32 Hz, 1F), -124.54 (d of d,  $J = 114$  Hz, 89 Hz, 1F), -174.53 (m, 1F); HRMS, calcd. for  $\text{C}_6\text{H}_8\text{F}_3\text{Br}$ , 215.9762, found, 215.9772.

#### Preparation of 1,1,2-trifluoro-1-hexene **39-1** and 1-difluoromethyl-1-fluorocyclopentane **39-2**

Preparation of **39-1** and **39-2** was accomplished by the same procedures as those used in the preparation of **36-2** and **36-3**.

1,1,2-Trifluoro-1-hexene **39-1**:  $^1\text{H}$  NMR (300 M Hz,  $\text{CDCl}_3$ , TMS), 0.94 (t,  $J = 7$  Hz, 2H), 1.37 (m, 2H), 1.52 (m, 2H), 2.28 (m, 2H);  $^{19}\text{F}$  NMR (282 M Hz,  $\text{CDCl}_3$ ,  $\text{CFCl}_3$ ), -106.74 (d of d,  $J = 90$  Hz, 32 Hz, 1F), -125.84 (d of d,  $J = 114$  Hz, 90 Hz, 1F), -174.84 (m, 1F); HRMS, calcd. for  $\text{C}_6\text{H}_9\text{F}_3$ , 138.0656, found, 138.0625.

1-Difluoromethyl-1-fluorocyclopentane **39-2**:  $^1\text{H}$  NMR (300 M Hz,  $\text{CDCl}_3$ , TMS), 1.40-1.75 (m, 2H), 1.85-1.96 (m, 4H), 1.97-2.05 (m, 2H), 5.84 (d of t,  $J = 57$  Hz, 5 Hz, 1H);  $^{19}\text{F}$  NMR (282 M Hz,  $\text{CDCl}_3$ ,  $\text{CFCl}_3$ ), -131.50 (d of d,  $J = 56$  Hz, 8 Hz, 2F), -158.30 (br, 1F), -174.53 (m, 1F); HRMS, calcd. for  $\text{C}_6\text{H}_9\text{F}_3$ , 138.0656, found, 138.0664.

#### Synthesis of 4,4,5,5,6,6-hexafluoro-6-iodo-1-hexene **40**

1,3-Diiodoperfluoropropane:  $\text{I}(\text{CF}_2)_3\text{I}$  was prepared from hexafluoroglutaryl chloride ( $\text{CICO}(\text{CF}_2)_3\text{COCl}$ ) by treatment with KI by a reported method<sup>102</sup>. However, there was no detailed procedure in the literature. To a stirred suspension of 36 g KI (0.217 mol, dried at  $200^\circ\text{C}$  for 12 hr) in a 600 mL pressure reactor was added 18.1 g (0.065 mol)

of hexafluoroglutaryl chloride (PCR, Inc.). The reactor was sealed and argon was put into it to increase the pressure to 480 psi. The temperature was increased to 200-250°C (the pressure was as high as 1000 psi at the temperatures) and the reactor stirred for 8 hr. The reactor was cooled to RT and then, at 0°C, the pressure in the reactor was relieved by releasing the argon. 200 mL of H<sub>2</sub>O was added to the reaction mixture in the reactor and total of 300mL of diethyl ether was used to extract this resultant solution. The separated ethereal solution was combined and washed with 40% of sodium thiosulfate (3 x 100 mL, removing iodine from the solution). the resultant mixture was distilled to give 18 g of the title product (68% yield). <sup>19</sup>F NMR (282 M Hz, CDCl<sub>3</sub>, CFCl<sub>3</sub>), -59.45 (s, 4F), -105.43 (s, 2F).

4,4,5,5,6,6-Hexafluoro-6-iodo-1-hexene **40**: Under photolytic conditions, addition of I(CF<sub>2</sub>)<sub>3</sub>I to allyl bromide in the presence of bis(tributyltin) takes place. Following the elimination of Bu<sub>3</sub>SnBr (it was not clear how the elimination happened) in situ, the title product was obtained. The amount of bis(tributyltin) used in the reaction is critical, it could not be over 0.5 equivalent relative to the iodide since any excess bis(tributyltin) would catalyze intramolecular cyclization of the addition product obtained. To a 0.9 mL (10.2 mmol) of allylbromide and 4.12 g (10.02 mL) of 1,3-diiodohexafluoropropane with 50 mL of degassed benzene in a quartz photo-reactor was added 1.23 mL (4.59 mmol) of bis(tributyltin). The mixture was stirred and photolyzed by a medium pressure mercury lamp (ACE glass) for 7 hr. <sup>19</sup>F NMR analysis indicated that the conversion of the iodide was about 50%, any longer photolyzing the reaction mixture caused an increase of the intramolecular cyclization product. The reaction was stopped by removing the lamp, and the mixture was distilled under reduced pressure to remove the tin compounds. The distillate was purified by preparative GC.

4,4,5,5,6,6-Hexafluoro-6-iodo-1-hexene **40**: <sup>1</sup>H NMR (300 M Hz, CDCl<sub>3</sub>, TMS), 2.85 (d of t, J = 18 Hz, 7 Hz, 2H), 5.30-5.34 (m, 2H), 5.81 (m, 1H); <sup>19</sup>F NMR (282 M Hz, CDCl<sub>3</sub>, CFCl<sub>3</sub>), -57.82 (s, 2F), -111.97 (m, 2F), -114.56 (s, 2F); HRMS, calcd for C<sub>6</sub>H<sub>3</sub>F<sub>6</sub>I, 317.9339, found, 317.9327.

Preparation of 4,4,5,5,6,6-hexafluoro-1-hexene 40-1, 1-methyl-2,2,3,3,4,4-hexafluorocyclopentane 40-2 and 1,1,2,2,3,3-hexafluorocyclohexane 40-3

The three compounds were prepared from the reaction of **40** with triethylsilane under the photo-initiation conditions. To 0.8 mL of triethylsilane (5.14 mmol) in a Pyrex NMR tube was added 0.1 mL (0.64 mmol) of **40**, and then the NMR tube was sealed by a rubber septa, and irradiated in a Rayonet photolyzer for 3 days.  $^{19}\text{F}$  NMR analysis indicated that the conversion of the starting material was about 85%. Through preparative GC, the title compounds were isolated.

**4,4,5,5,6,6-Hexafluoro-1-hexene 40-1:**  $^1\text{H}$  NMR (300 M Hz,  $\text{CDCl}_3$ , TMS), 2.84 (d of t,  $J = 19$  Hz, 6 Hz, 2H), 5.29-5.36 (m, 2H), 5.81 (m, 1H), 6.01 (t of t,  $J = 54$  Hz, 6 Hz, 1H);  $^{19}\text{F}$  NMR (282 M Hz,  $\text{CDCl}_3$ ,  $\text{CFCl}_3$ ), -114.92 (m, 2F), -131.69 (s, 2F), -137.89 (d,  $J = 48$  Hz, 2F); HRMS, calcd for  $\text{C}_6\text{H}_6\text{F}_6$ , 192.0374, found, 192.0370.

**1-Methyl-2,2,3,3,4,4-hexafluorocyclopentane 40-2:**  $^1\text{H}$  NMR (300 M Hz,  $\text{CDCl}_3$ , TMS), 1.20 (d,  $J = 7$  Hz, 3H), 1.97 (m, 1H), 2.54 (br, 2H);  $^{19}\text{F}$  NMR (282 M Hz,  $\text{CDCl}_3$ ,  $\text{CFCl}_3$ ), -109.46 (d,  $J = 244$  Hz, 1F), -114.61 (t of d,  $J = 244$  Hz, 18 Hz, 1F), -120.97 (d,  $J = 243$  Hz, 1F), -130.45 (d of d,  $J = 251$  Hz, 19 Hz, 1F), -131.32 (d,  $J = 242$  Hz, 1F), -135.79 (d,  $J = 249$  Hz, 1F); HRMS, calcd for  $\text{C}_6\text{H}_6\text{F}_6$ , 192.0374, found, 192.0368.

**1,1,2,2,3,3-Hexafluorocyclohexane 40-3:**  $^1\text{H}$  NMR (300 M Hz,  $\text{CDCl}_3$ , TMS, RT), 1.59 (s, 1H), 1.82 (m, 2H), 2.18 (br, 3H);  $^{19}\text{F}$  NMR (282 M Hz,  $\text{CDCl}_3$ ,  $\text{CFCl}_3$ , RT), -117.53 (s, 4F), -138.50 (br, 2F); HRMS, calcd for  $\text{C}_6\text{H}_6\text{F}_6$ , 192.0374, found, 192.0362.

3,3,4,4,5,5,6,6-Octafluoro-6-iodo-1-hexene 41

The title compound was provided by M.-H. Hung (DuPont).

**3,3,4,4,5,5,6,6-Octafluoro-6-iodo-1-hexene 41:**  $^1\text{H}$  NMR (300 M Hz,  $\text{CDCl}_3$ , TMS), 4.94 (m, 1H), 5.43 (m, 2H);  $^{19}\text{F}$  NMR (282 M Hz,  $\text{CDCl}_3$ ,  $\text{CFCl}_3$ ), -59.74 (s, 2F), -112.62 (s, 2F), -113.67 (s, 2F), -122.56 (m, 2F); HRMS, calcd for  $\text{C}_6\text{H}_3\text{F}_8\text{I}$ , 353.9151, found, 353.9183.

Preparation of 3,3,4,4,5,5,6,6-octafluoro-1-hexene 41-1, methyl-octafluorocyclopentane 41-2 and 1,1,2,2,3,3,4,4-octafluorocyclohexane 41-3

To 0.55 mL of triethylsilane with 0.3 mL of degassed benzene in a Pyrex NMR tube was added 0.27 mL (1.41 mmol) of **41**. The mixture was photolyzed in a Rayonet photolyzer for 17 hr.  $^{19}\text{F}$  NMR analysis indicated that the reaction was finished. Through preparative GC, the title compounds were isolated.

**3,3,4,4,5,5,6,6-Octafluoro-1-hexene 41-1:**  $^1\text{H}$  NMR (200 M Hz,  $\text{CDCl}_3$ , TMS), 4.98 (m, 1H), 5.21 (t of t,  $J = 52$  Hz, 6 Hz, 1H), 5.44 (m, 2H);  $^{19}\text{F}$  NMR (282 M Hz,  $\text{CDCl}_3$ ,  $\text{CFCl}_3$ ), -113.73 (s, 2F), -125.47 (s, 2F), -129.50 (s, 2F), -137.05 (d,  $J = 57$  Hz, 2F); HRMS, calcd for  $\text{C}_6\text{H}_4\text{F}_8$ , 228.0185, found, 228.0169.

**Methyl-octafluorocyclopentane 41-2:**  $^1\text{H}$  NMR (200 M Hz,  $\text{CDCl}_3$ , TMS), 0.64 (d,  $J = 7$  Hz, 3H), 2.04 (br, 1H);  $^{19}\text{F}$  NMR (188 M Hz,  $\text{CDCl}_3$ ,  $\text{CFCl}_3$ ), -119.49 (d,  $J = 244$  Hz, 2F), -124.84 (d of d,  $J = 252$  Hz, 19 Hz, 2F), -130.76 (d, 250 Hz, 2F), -134.05 (d, 250 Hz, 2F); HRMS, calcd for  $\text{C}_6\text{H}_4\text{F}_8$ , 228.0185, found, 228.0174.

**1,1,2,2,3,3,4,4-Octafluorocyclohexane 41-3:**  $^1\text{H}$  NMR (200 M Hz,  $\text{CDCl}_3$ , TMS, RT), 1.29 (br, 4H);  $^{19}\text{F}$  NMR (188 M Hz,  $\text{CDCl}_3$ ,  $\text{CFCl}_3$ , RT), -118.19 (s, 4F), -135.152 (br, 4F); HRMS, calcd for  $\text{C}_6\text{H}_4\text{F}_8$ , 228.0185, found, 228.0164.

1,1,2,3,3,4,4-heptafluoro-6-bromo-1-hexene 42

The title compound was converted<sup>103</sup> from 1,1,2,3,3,4,4-heptafluoro-6-chloro-1-hexene which was provided by Bruce Smart (CR &D, DuPont). To a mixture of 50 mL DMF, 25 mL  $\text{CH}_2\text{Br}_2$  and 2.16 g (0.0246 mol) LiBr in a 250 mL flask was added 2.45 g (0.0123 mol) of 1,1,2,3,3,4,4-heptafluoro-6-chloro-1-hexene. Setting the oil bath to  $100^\circ\text{C}$ , the reaction mixture was stirred for 6 hr. GC analysis indicated the reaction finished and the reaction mixture was distilled under reduced pressure (20 mmHg, RT). The distillation gave a mixture of  $\text{CH}_2\text{Br}_2$  and the bromide compound. Further separation of the mixture was by preparative GC yielding 1.75 g of the title compound (60% yield).

1,1,2,3,3,4,4-Heptafluoro-6-bromo-1-hexene **42**:  $^1\text{H}$  NMR (300 M Hz,  $\text{CDCl}_3$ , TMS), 2.69 (m, 2H), 3.52 (t,  $J = 8$  Hz, 2H);  $^{19}\text{F}$  NMR (282 M Hz,  $\text{C}_6\text{D}_6$ ,  $\text{CFCl}_3$ ), -89.48 (m, 1F), -106.74 (m, 1F), -115.72 (t,  $J = 17$  Hz, 2F), -119.39 (m, 2F), -187.89 (m of d,  $J = 117$  Hz, 1F); HRMS, calcd for  $\text{C}_6\text{H}_4\text{F}_7\text{Br}$ , 287.9385, found, 287.9374.

Preparation of 1,1,2,3,3,4,4-heptafluoro-1-hexene **42-1** and 1-difluoromethyl-1,2,2,3,3-pentafluorocyclopentane **42-2**

The title compounds were prepared from the bromide **42** following the same procedure as the one used in preparation of **41-1**, **41-2** and **41-3** from **41**.

1,1,2,3,3,4,4-Heptafluoro-1-hexene **42-1**:  $^1\text{H}$  NMR (300 M Hz,  $\text{CDCl}_3$ , TMS), 1.12 (t,  $J = 7$  Hz, 3 H), 2.06 (m, 2H);  $^{19}\text{F}$  NMR (282 M Hz,  $\text{CDCl}_3$ ,  $\text{CFCl}_3$ ), -91.17 (m, 1F), -107.74 (m, 1F), -118.35 (t,  $J = 18$  Hz, 2F), -119.97 (m, 2F), -188.13 (m of d,  $J = 116$  Hz, 1F); HRMS, calcd for  $\text{C}_6\text{H}_5\text{F}_7$ , 210.0279, found, 210.0280.

1-Difluoromethyl-1,2,2,3,3-pentafluorocyclopentane **42-2**:  $^1\text{H}$  NMR (300 M Hz,  $\text{CDCl}_3$ , TMS), 2.27-2.5 (br, 4H), 5.97 (d of t,  $J = 53$  Hz, 7 Hz, 1H); -111.47 (m of d,  $J = 244$  Hz, 1F), -118.98 (d,  $J = 246$  Hz, 1F), -130.03 (d,  $J = 259$  Hz, 1F), -132.89 (d,  $J = 259$  Hz, 1F), -133.68 (t of d,  $J = 53$  Hz, 7 Hz, 1F), -133.98 (t of d,  $J = 53$  Hz, 10 Hz, 1F), -182.24 (s, 1F); HRMS, calcd for  $\text{C}_6\text{H}_3\text{F}_7$ , 210.0279, found, 210.0262.

6-Bromo-perfluoro-1-hexene **43**

The title compound was supplied by W.-Y. Huang, C.-M. Hu (Shanghai Inst. of Organic Chemistry, China). Further treatment with sodium hydride was needed to remove impurities of acids from the sample.

6-Bromo-perfluoro-1-hexene **43**:  $^{19}\text{F}$  NMR (200 M Hz,  $\text{CDCl}_3$ ,  $\text{CFCl}_3$ ), -63.91 (s, 2F), -88.77 (m, 1F), -105.45 (m, 1F), -177.89 (s, 2F), -118.53 (s, 2F), -123.89 (s, 2F), -189.04 (m, 1F); HRMS, calcd for  $\text{C}_6\text{F}_{11}\text{Br}$ , 359.9008, found, 359.9042.



### Preparation of 1,1,2,3,3,4,4,5,5,6,6-undecafluoro-1-hexene 43-1

Under ambient light, the bromide **43** reacted with tributyltin hydride fast and quantitatively to give reduced product **43-1** (as major one) and cyclized product (difluoromethyl-perfluorocyclopentane) **43-2**. To a mixture of 20 mL of benzene and 0.98 g (3.33 mmol) of  $\text{Bu}_3\text{SnH}$  in a 25 mL flask was added 1.0 g (2.78 mmol) of bromide **43** and the mixture was stirred for 30 min. The tin compounds were removed by careful distillation of the reaction mixture ( $\sim 55^\circ\text{C}$  for the oil bath and the receiver for the distillate being cooled to  $0^\circ\text{C}$ ). Further purification was by preparative GC. Because of the close boiling points of compounds **43-1** and **43-2**, the separation of the two compounds was not good enough to isolate them efficiently. Fortunately, the reduction of **43** by tin hydrides is much faster ( $2.03 \times 10^8 \text{ M}^{-1} \text{ s}^{-1}$ ) than the intramolecular cyclization of **43** ( $2.3 \times 10^5 \text{ M}^{-1} \text{ s}^{-1}$ ), and the sample obtained in this manner after preparative GC was  $> 91\%$  pure.

1,1,2,3,3,4,4,5,5,6,6-Undeca-fluoro-1-hexene **43-1**:  $^1\text{H}$  NMR (200 M Hz,  $\text{CDCl}_3$ , TMS), 5.05 (t of t,  $J = 51 \text{ Hz}$ , 5 Hz, 1H);  $^{19}\text{F}$  NMR (200 M Hz,  $\text{CDCl}_3$ ,  $\text{CFCl}_3$ ), -87.82 (m, 1F), -105.08 (m, 1F), -118.53 (s, 2F), -125.47 (s, 2F), -129.77 (s, 2F), -136.97 (d,  $J = 50 \text{ Hz}$ , 2F), -188.66 (m, 1F); HRMS, calcd for  $\text{C}_6\text{H}_1\text{F}_{11}$ , 281.9903, found, 281.9899.

### Preparation of difluoromethyl-perfluorocyclopentane 43-2

The title compound was prepared from the bromide **43** following the same procedure as the one used in preparation of **41-1**, **41-2** and **41-3** from **41**. As mentioned before, **43-2** could not be separated from **43-1** by preparative GC.

Difluoromethyl-perfluorocyclopentane **43-2**:  $^1\text{H}$  NMR (200 M Hz,  $\text{CDCl}_3$ , TMS), 5.26 (d of t,  $J = 50 \text{ Hz}$ , 12 Hz, 1H);  $^{19}\text{F}$  NMR (200 M Hz,  $\text{CDCl}_3$ ,  $\text{CFCl}_3$ ), -124.17 (d,  $J = 285 \text{ Hz}$ , 2F), -128.43 (d,  $J = 265 \text{ Hz}$ , 2F), -130.55 (d,  $J = 290 \text{ Hz}$ , 2F), -131.97 (d,  $J = 273 \text{ Hz}$ , 2F), -135.48 (d,  $J = 54 \text{ Hz}$ , 2F), -200.18 (s, 1F); HRMS, calcd for  $\text{C}_6\text{H}_1\text{F}_{11}$ , 281.9903, found, 281.9917.

(1,1,2,2,3,3-Hexafluoro-3-bromo)propyl trifluorovinyl ether 44

Ether **44** was provided by Bruce Smart (CR & D, DuPont) and no further purification was needed for the sample.

(1,1,2,2,3,3-Hexa-fluoro-3-bromo)propyl trifluorovinyl ether **44**:  $^{19}\text{F}$  NMR (282 M Hz,  $\text{CDCl}_3$ ,  $\text{CFCl}_3$ ), -64.28 (s, 2F), -83.77 (s 2F), -113.39 (d of d,  $J = 83$  Hz, 65 Hz, 1F), -121.20 (s, 2F), 121.62 (d of d,  $J = 112$  Hz, 83 Hz, 1F), -135.11 (d of d,  $J = 112$  Hz, 66 Hz, 1F); HRMS, calcd for  $\text{C}_3\text{F}_9\text{OBr}$ , 325.8989, found, 325.9018.

Preparation of (1,1,2,2,3,3-hexa-fluoro) propyl trifluorovinyl ether **44-1** and 2-difluoromethyl-perfluorooxacyclopentane **44-2**

The title compounds were prepared from the bromides **44** by the same procedure as the one used in preparation of **41-1**, **41-2** and **41-3** from **41**.

(1,1,2,2,3,3-hexa-fluoro) propyl trifluorovinyl ether **44-1**:  $^1\text{H}$  NMR (300 M Hz,  $\text{CDCl}_3$ , TMS), 6.04 (t of t,  $J = 52$  Hz, 5 Hz, 1H);  $^{19}\text{F}$  NMR (282 M Hz,  $\text{CDCl}_3$ ,  $\text{CFCl}_3$ ), -86.56 (s, 2F), -113.08 (d of d,  $J = 83$  Hz, 68 Hz, 1F), -121.45 (d of d,  $J = 110$  Hz, 81 Hz, 1F), 132.44 (s, 2F), -134.71 (d of d,  $J = 112$  Hz, 66 Hz, 1F), -137.26 (m of d,  $J = 58$  Hz, 2F); HRMS, calcd for  $\text{C}_3\text{HF}_9\text{O}$ , 247.9884, found, 247.9888.

2-Difluoromethyl-perfluorooxacyclopentane **44-2**:  $^1\text{H}$  NMR (300 M Hz,  $\text{CDCl}_3$ , TMS), 6.03 (d of t,  $J = 52$  Hz, 7 Hz, 1H);  $^{19}\text{F}$  NMR (282 M Hz,  $\text{CDCl}_3$ ,  $\text{CFCl}_3$ ), -82.89 (d,  $J = 8$  Hz, 1F), -82.99 (t,  $J = 7$  Hz, 1F), -126.18 (d,  $J = 127$  Hz, 1F), -129.16 (d of d,  $J = 262$  Hz, 7 Hz, 1F), -131.63 (d,  $J = 262$  Hz, 1F), -131.38 (s, 1F), -133.40 (m of d,  $J = 312$  Hz, 1F), -135.43 (m of d,  $J = 250$  Hz, 1F), -139.26 (d of d,  $J = 312$  Hz, 52 Hz, 1F); HRMS, calcd for  $\text{C}_3\text{HF}_9\text{O}$ , 247.9884, found, 247.9872.

General Procedure for the Rate Constant ( $k_c$ ) Determination on the Intramolecular Cyclization of Fluorinated 1,5-Hexenyl Radicals

In most of competition experiments, the reaction sample was made by adding a certain amount (5 $\mu\text{L}$ –10 $\mu\text{L}$ ) of radical precursor to benzene- $d_6$  in a Pyrex NMR tube in

which a certain amount of reducing agent was charged. Usually, six of such samples, varied in the amounts of the reducing agent, were needed to complete a rate determination. Samples were sealed in NMR tubes by rubber septa, degassed (freeze and thaw) three times under argon and then photolyzed using a Rayonet reactor or under ambient light for a certain period (monitored by  $^{19}\text{F}$  NMR) at room temperature. The products (reduced and cyclized) of the reactions were analyzed by  $^{19}\text{F}$  NMR, and in most cases,  $\text{PhCF}_3$  was used as the internal standard to calculate the NMR yield of the reactions. The ratios of reduced to cyclized products were obtained by measuring the integral of the corresponding peaks in the  $^{19}\text{F}$  NMR. The ratios of reduced to cyclized products were obtained for varied concentrations of the reductant, which were combined with the respective concentrations of the reductant, allowed the determination of the ratio  $k_{\text{H}}/k_{\text{C}}$  according to equation (4-1) or equation (4-2). All other special operations for each rate determination are discussed following the data table reported respectively. It should be pointed out that the accuracy of the values for  $k_{\text{C}}$  can, of course, be no better than those reported for  $k_{\text{H}}$ . Thus the error estimates reported in the Table 4-1 reflect both the least squares fit of the line and the errors from  $k_{\text{H}}$ , the error in  $k_{\text{C}}$  could be largely derive from the error in  $k_{\text{H}}$ .

Table 5-11. Competition Data for the Reaction of 2-Fluoro-6-bromo-1-hexene **35** with  $\text{Bu}_3\text{GeH}^{\text{a}}$

[Precursor] (M)	$[\text{Bu}_3\text{GeH}]$ (M)	[Reduced]/ $[\text{C}_5]^{\text{b}}$	Yield
0.025	0.233	0.810	94
0.025	0.262	0.953	99
0.025	0.291	1.047	97
0.025	0.320	1.187	97
0.025	0.349	1.271	96
0.025	0.378	1.405	96

<sup>a</sup> The samples were photolyzed for 1 hr to avoid the addition of radicals  $\text{Bu}_3\text{Ge}^{\cdot}$  to the double bond of the precursor. <sup>b</sup> Obtained by  $^{19}\text{F}$  NMR analysis: for the reduced product,  $\delta = -95.13$  ( $\text{CH}_2 = \text{CF}-$ ); for the cyclized  $\text{C}_5$ , 5-exo-product,  $\delta = -134.66$  ( $t-\text{C}-\text{F}$ ).

Table 5-12. Competition Data for the Reaction of 1-Fluoro-6-bromo-1-hexene **36** with  $\text{Bu}_3\text{SnH}^a$ 

[Precursor] (M)	$[\text{Bu}_3\text{SnH}]$ (M)	$[\text{Reduced}]/[\text{C}_5]^b$	Yield
0.026	0.204	2.797	93
0.026	0.233	3.096	94
0.026	0.262	3.452	99
0.026	0.291	4.085	97
0.026	0.320	4.557	98
0.026	0.349	4.948	100

<sup>a</sup> The samples were photolyzed for 28 hr with Rayonet lamps.<sup>b</sup> Obtained by  $^{19}\text{F}$  NMR analysis: for the reduced product,  $\delta = -130.34$  and  $-130.92$  (the *cis* and *trans* isomers,  $\text{FHC}=\text{CH}-$ ); for cyclized  $\text{C}_5$ , 5-*exo*-product,  $\delta = -215.9$  ( $\text{CH}_2\text{F}-$ ).Table 5-13. Competition Data for the Reaction of 1,1-Difluoro-6-bromo-1-hexene **37** with  $\text{Bu}_3\text{SnH}^a$ 

[Precursor] (M)	$[\text{Bu}_3\text{SnH}]$ (M)	$[\text{Reduced}]/[\text{C}_5]^b$	Yield
0.025	0.248	2.781	98
0.025	0.276	3.216	99
0.025	0.304	3.502	100
0.025	0.331	3.941	99
0.025	0.359	4.222	99
0.025	0.386	4.547	97

<sup>a</sup> The samples were photolyzed under ambient light for 14 hr since the Rayonet lamps would cause the addition of radical  $\text{Bu}_3\text{Sn}^\cdot$  to the double bond of the precursor.<sup>b</sup> Obtained by  $^{19}\text{F}$  NMR analysis: for reduced product,  $\delta = -90.41$  and  $-92.83$  ( $\text{CF}_2=\text{CH}-$ ); for the cyclized  $\text{C}_5$ , 5-*exo*-product,  $\delta = -119.44$  ( $\text{CF}_2\text{H}$ ).Table 5-14. Competition Data for the Reaction of 1,2-Difluoro-6-bromo-1-hexene **38** with  $\text{Bu}_3\text{SnH}^a$ 

[Precursor] (M)	$[\text{Bu}_3\text{SnH}]$ (M)	$[\text{Reduced}]/[\text{C}_5]^b$	Yield
0.019	0.248	2.919	93
0.019	0.276	3.302	94
0.019	0.304	3.650	93
0.019	0.331	4.085	90
0.019	0.359	4.390	91
0.019	0.386	4.835	96

<sup>a</sup> The samples were photolyzed under ambient light for 12 hr since the Rayonet lamps would cause the addition of radical  $\text{Bu}_3\text{Sn}^\cdot$  to the double bond of the precursor.<sup>b</sup> Obtained by  $^{19}\text{F}$  NMR analysis: for reduced product,  $\delta = -160.12$ , ( $\text{FHC}=\text{CF}_2-$ ); for cyclized  $\text{C}_5$ , 5-*exo*-product,  $\delta = -150.44$ , (*t*-C-F).

Table 5-15. Competition Data for the Reaction of 1,1,2-Trifluoro-6-bromo-1-hexene **39** with  $\text{Bu}_3\text{SnH}^a$ 

[Precursor] (M)	$[\text{Bu}_3\text{SnH}]$ (M)	[Reduced]/ $[\text{C}_5]^b$	Yield
0.120	0.796	2.919	94
0.120	0.996	3.712	98
0.120	1.137	4.545	95
0.120	1.307	5.141	94
0.120	1.478	5.762	91
0.120	1.649	6.762	94

<sup>a</sup> The samples were photolyzed under ambient light for 18 hr.<sup>b</sup> Obtained by  $^{19}\text{F}$  NMR analysis: for reduced product,  $\delta = -125.84$  (1F from  $\text{E}_2\text{C}=\text{CF}-$ ); for cyclized  $\text{C}_5$ , 5-exo-product,  $\delta = -131.50$  ( $\text{CF}_2\text{H}$ ).Table 5-16. Competition Data for the Reaction of 4,4,5,5,6,6-Hexafluoro-6-iodo-1-hexene **40** with  $(\text{TMS})_3\text{SiH}^a$ 

[Precursor], M	$[(\text{TMS})_3\text{SiH}]$ , M	[Reduced]/ $[\text{C}_5]^b$	[Reduced]/ $[\text{C}_6]^c$	Yield
0.058	0.582	0.66	5.15	96
0.058	0.669	0.77	6.08	100
0.058	0.756	0.86	6.68	100
0.058	0.844	0.95	7.68	97
0.058	0.931	1.08	8.45	100
0.058	1.018	1.17	9.48	100

<sup>a</sup> The samples were photolyzed with Rayonet lamps for 20 min.<sup>b</sup> Obtained by  $^{19}\text{F}$  NMR analysis: for the reduced product,  $\delta = -137.89$  ( $\text{CF}_2\text{H}$ ); for the cyclized  $\text{C}_5$ , 5-exo-product,  $\delta = -120.97$  (1F from the ring); for the cyclized  $\text{C}_6$ , 6-endo-product,  $\delta = -117.53$  (4F from the ring).Table 5-17. Competition Data for the Reaction of 3,3,4,4,5,5,6,6-Octafluoro-6-iodo-1-hexene **41** with  $(\text{TMS})_3\text{SiH}^a$ 

[Precursor], M	$[(\text{TMS})_3\text{SiH}]$ , M	[Reduced]/ $[\text{C}_5]^b$	[Reduced]/ $[\text{C}_6]^b$	Yield
0.076	0.534	2.30	6.43	99
0.076	0.671	2.92	8.35	98
0.076	0.827	3.87	11.08	96
0.076	0.984	4.73	13.52	99
0.076	1.140	5.22	15.11	100
0.076	1.297	5.82	17.31	100

<sup>a</sup> The samples were photolyzed with Rayonet lamps for 4 hr.<sup>b</sup> Obtained by  $^{19}\text{F}$  NMR analysis: for the reduced product,  $\delta = -137.05$  ( $\text{CF}_2\text{H}$ ); for the cyclized  $\text{C}_5$ , 5-exo-product,  $\delta = -134.05$  (2F from the ring); for the cyclized  $\text{C}_6$ , 6-endo-product,  $\delta = -118.19$  (4F from the ring).

Table 5-18. Competition Data for the Reaction of 1,1,2,3,3,4,4-Heptafluoro-6-bromo-1-hexene **42** with  $\text{Bu}_3\text{SnH}^a$ 

[Precursor], M	$[\text{Bu}_3\text{SnH}]$ , M	[Reduced]/ $[\text{C}_5]^b$	Yield
0.031	0.320	1.43	97
0.031	0.355	1.63	98
0.031	0.391	1.80	95
0.031	0.426	1.92	99
0.031	0.462	2.15	96
0.031	0.497	2.28	98

<sup>a</sup> The samples were photolyzed under ambient light for 12 hr.<sup>b</sup> Obtained by  $^{19}\text{F}$  NMR analysis: for the reduced product,  $\delta = -188.13$  ( $\text{CF}_2 = \text{CF}-$ ), for the cyclized  $\text{C}_5$ , 5-exo-product,  $\delta = -182.24$  ( $t\text{-C-F}$ ).Table 5-19. Competition Data for the Reaction of 6-bromo-perfluoro-1-hexene **43** with  $\text{Et}_3\text{SiH}^a$ 

[Precursor] (M)	$[\text{Et}_3\text{SiH}]$ (M)	[Reduced]/ $[\text{C}_5]^b$	Yield
0.106	1.060	1.705	95
0.106	1.273	2.081	96
0.106	1.486	2.332	94
0.106	1.700	2.790	93
0.106	1.913	3.096	97
0.106	2.126	3.283	92

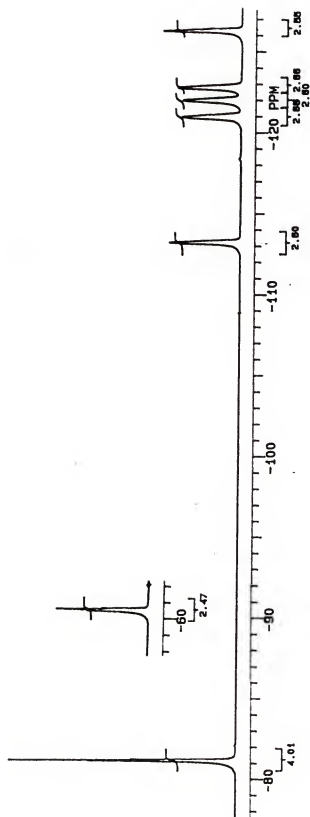
<sup>a</sup> The samples were photolyzed with Rayonet lamps for 4 hr.<sup>b</sup> Obtained by  $^{19}\text{F}$  NMR analysis: for the reduced product,  $\delta = -136.97$  ( $\text{CF}_2\text{H}$ ); for the cyclized  $\text{C}_5$ , 5-exo-product,  $\delta = -135.48$  ( $\text{CF}_2\text{H}$ ).Table 5-19. Competition Data for the Reaction of (1,1,2,2,3,3-Hexafluoro-3-bromo)propyl trifluorovinyl ether **44** with  $\text{Bu}_3\text{GeH}^a$ 

[Precursor] (M)	$[\text{Bu}_3\text{GeH}]$ (M)	[Reduced]/ $[\text{C}_5]^b$	Yield
0.052	0.412	2.710	98
0.052	0.515	3.065	98
0.052	0.618	3.569	96
0.052	0.687	3.884	97
0.052	0.743	4.103	97
0.052	0.824	4.493	99

<sup>a</sup> The samples were photolyzed with Rayonet lamps for 10 min.<sup>b</sup> Obtained by  $^{19}\text{F}$  NMR analysis: for the reduced product,  $\delta = -137.26$  ( $\text{CF}_2\text{H}$ ); for the cyclized  $\text{C}_5$ , 5-exo-product,  $\delta = -139.26$  (1F from  $\text{CF}_2\text{H}$ ).

## APPENDIX SELECTED $^{19}\text{F}$ NMR SPECTRA

The  $^{19}\text{F}$  NMR spectra of radical precursors as well as their derives are graphically illustrated in this appendix. The spectra ( $^1\text{H}$  and  $^{13}\text{C}$ ) are presented numerically in their respective areas in Chapter 5.

Figure A-1. Radical Precursor C<sub>7</sub>F<sub>13</sub>I



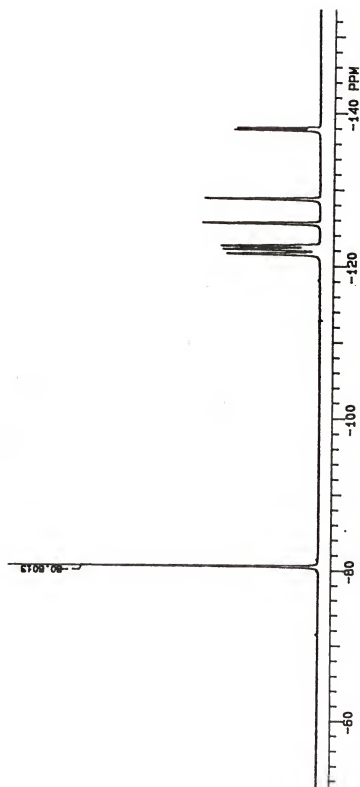


Figure A-2. Reduced Product  $\text{C}_7\text{F}_{13}\text{H}$  (30)

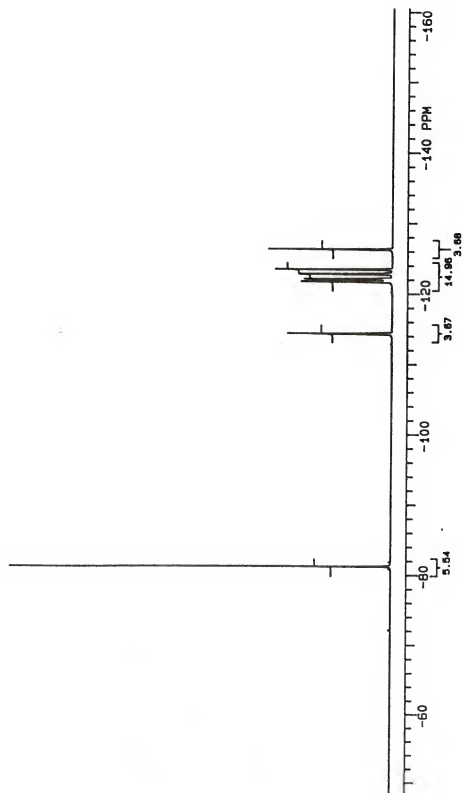


Figure A-3. Addition Product  $\text{C}_7\text{F}_{15}\text{-C}_8\text{H}_{13}$  (31)

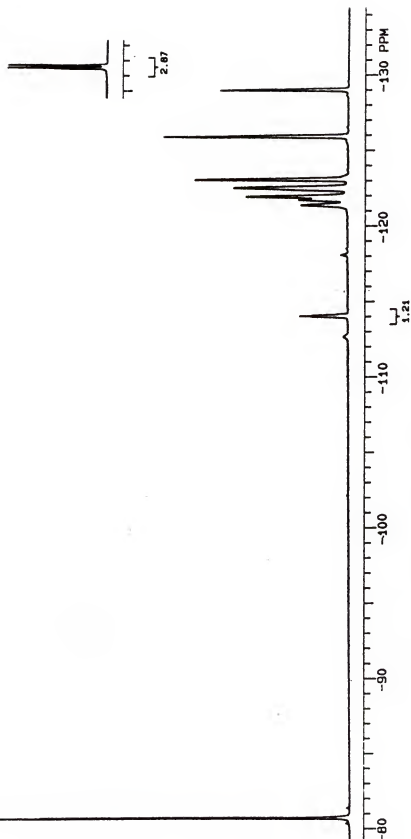


Figure A-4. A Typical  $^{19}\text{F}$  NMR Spectrum of the Reaction Mixtures from Radical  $\text{C}_7\text{F}_{15}$ .

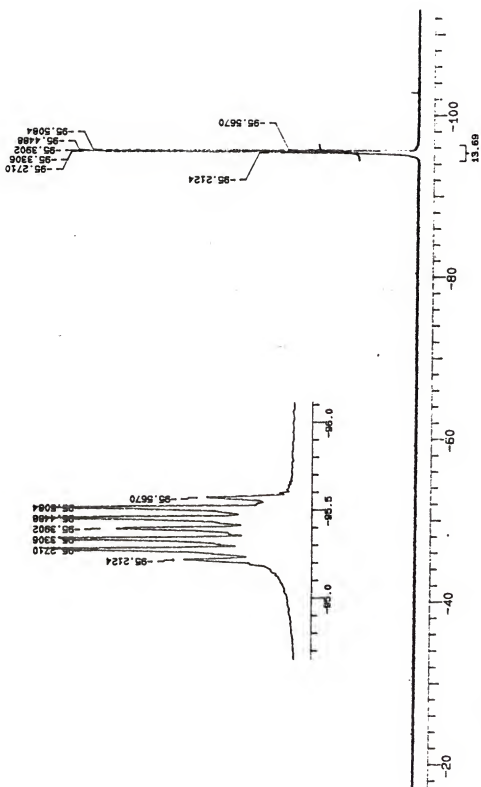
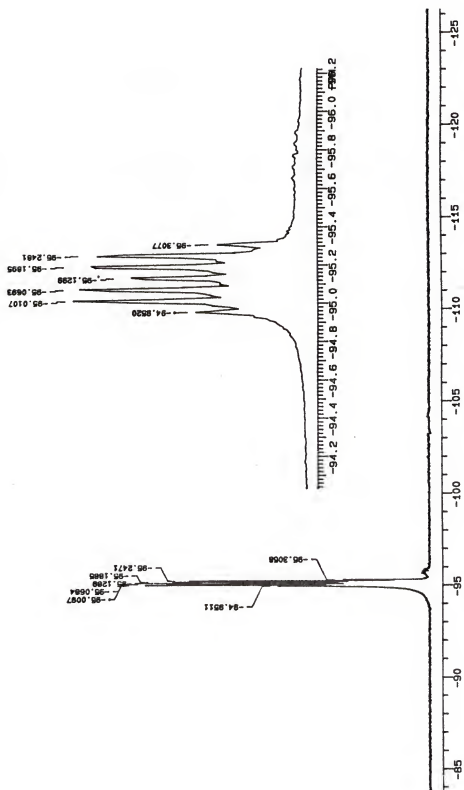


Figure A-5. Radical Precursor 35



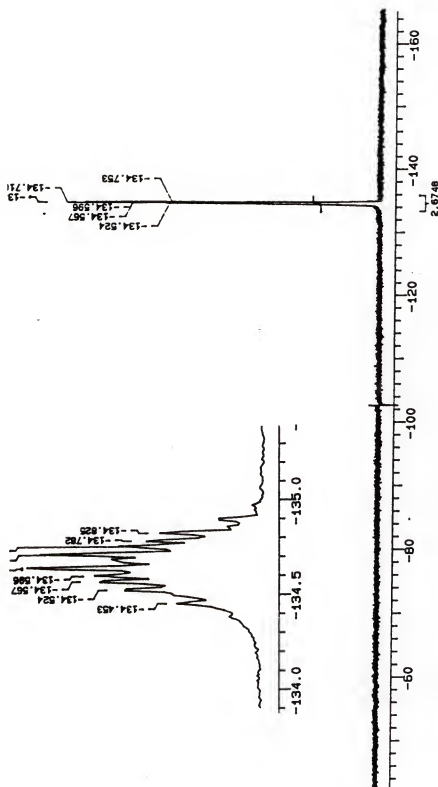
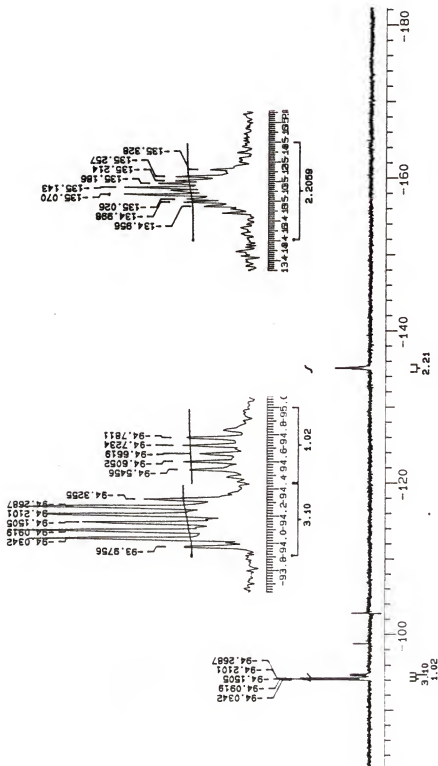


Figure A-5-2. 5-exo Cyclized Product 35-2

Figure A-5-3. One of the  $^{19}\text{F}$  NMR Spectra of the Reaction Mixture from Radical 35

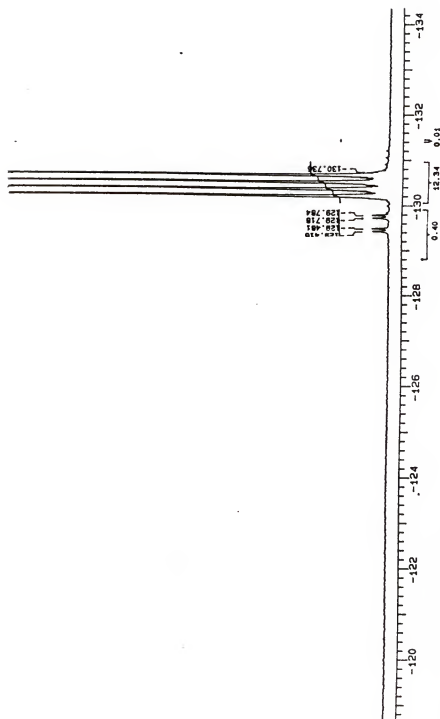


Figure A-6. Radical Precursor 36



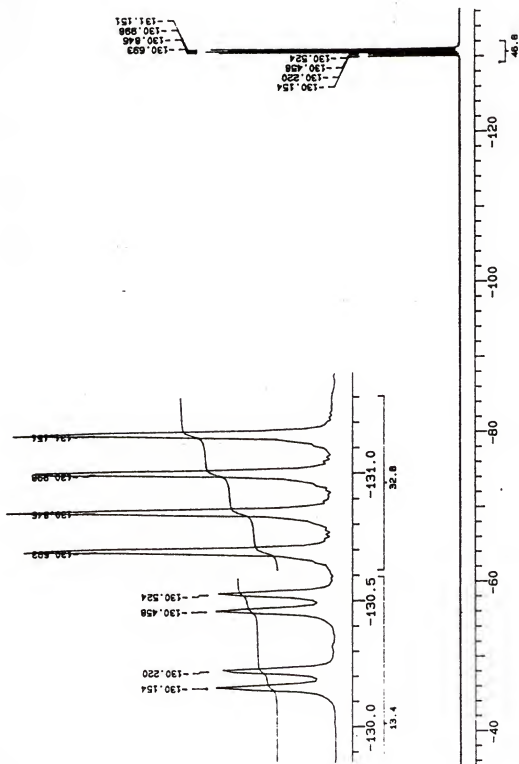


Figure A-6-1. Reduced Product 36-1

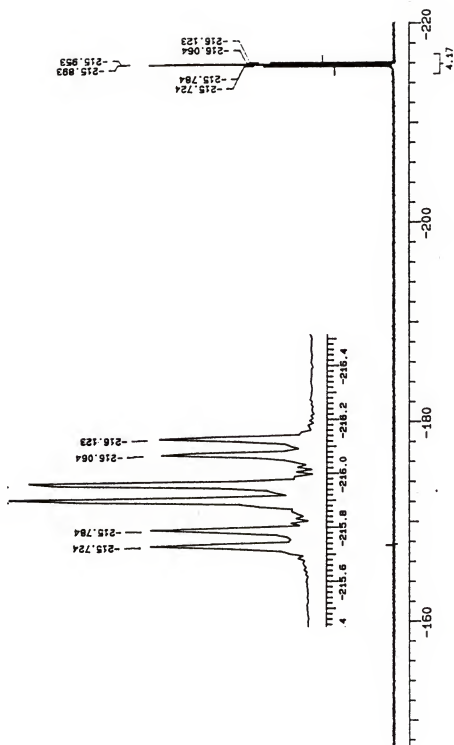
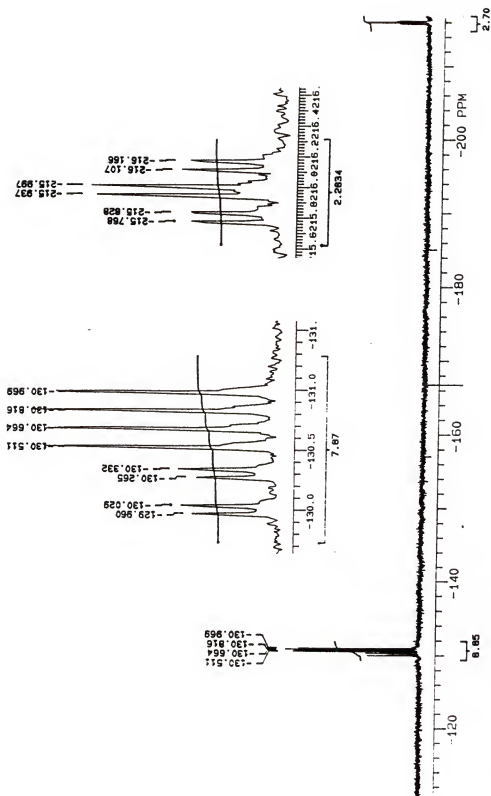


Figure A-6-2. 5-exo Cyclized Product 36-2



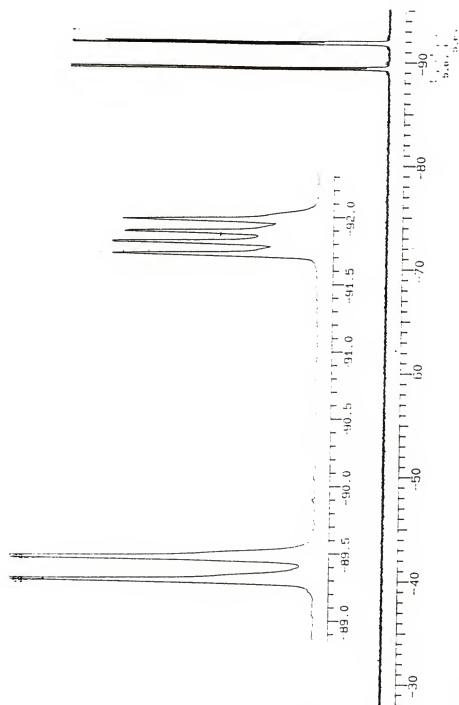


Figure A-7. Radical Precursor 37

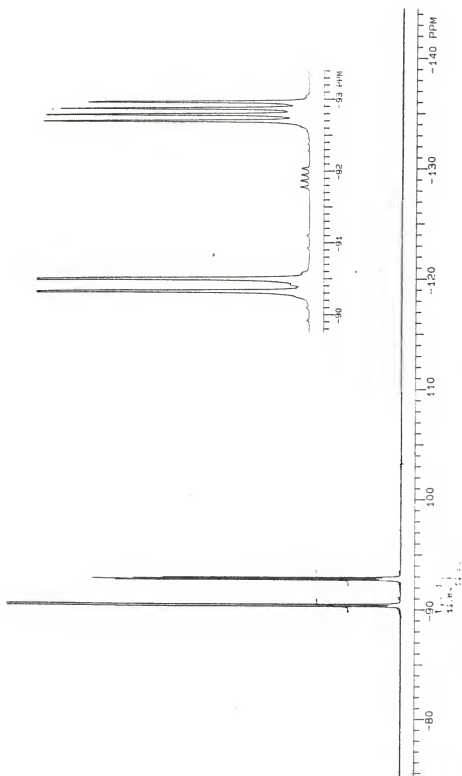


Figure A-7-1. Reduced Product 37-1

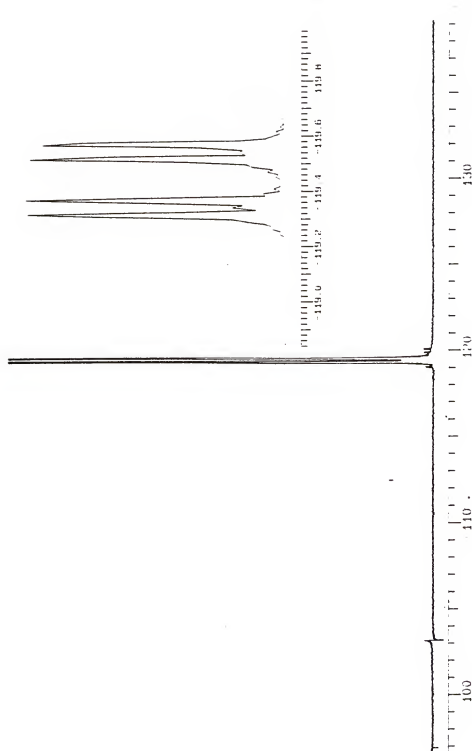
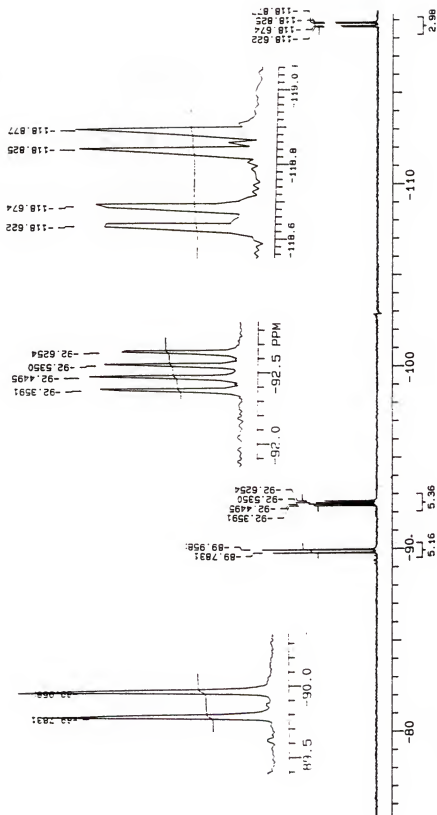


Figure A-7-2. 5-exo Cyclized Product 37-2

Figure A-7-3. One of the  $^{19}\text{F}$  NMR Spectra of the Reaction Mixtures from Radical 37

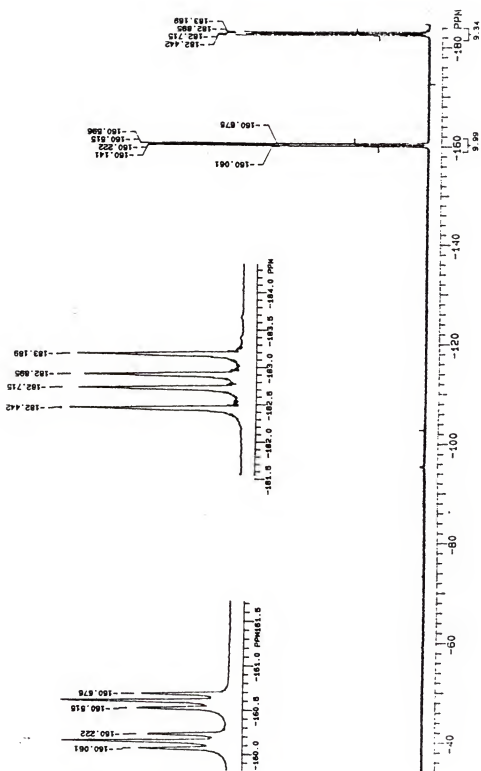


Figure A-8. Radical Precursor 38



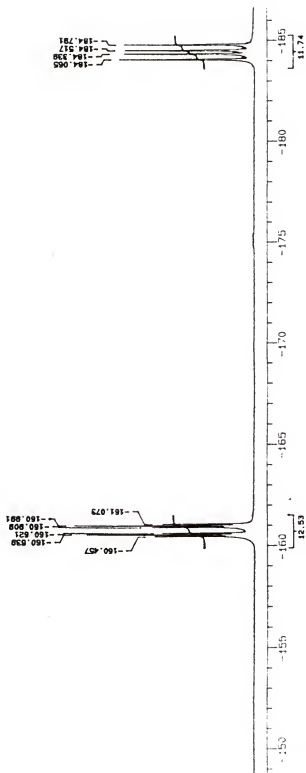


Figure A-8-1. Reduced Product 38-1

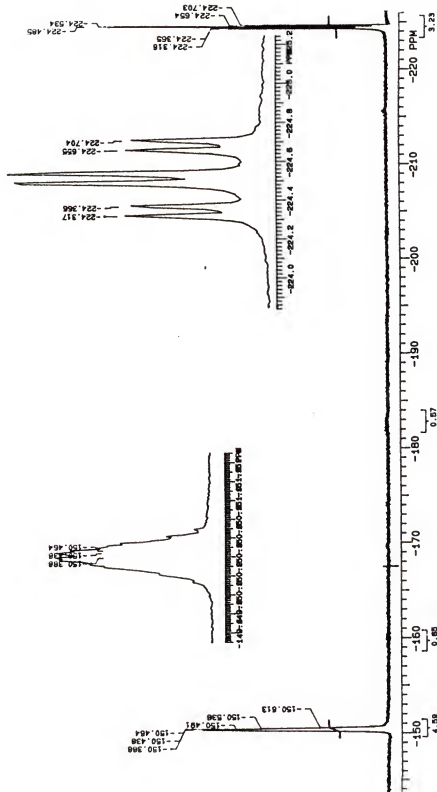
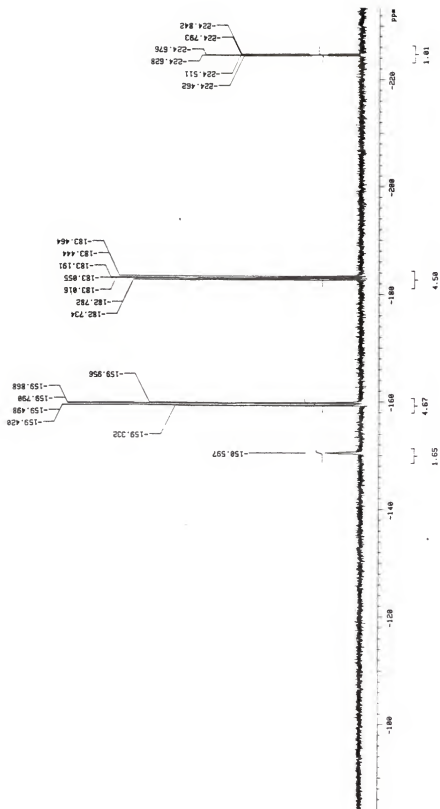


Figure A-8-2. 5-exo Cyclized Product 38-2

Figure A-8-3. One of the  $^{19}\text{F}$  NMR Spectra of the Reaction Mixtures from Radical 38

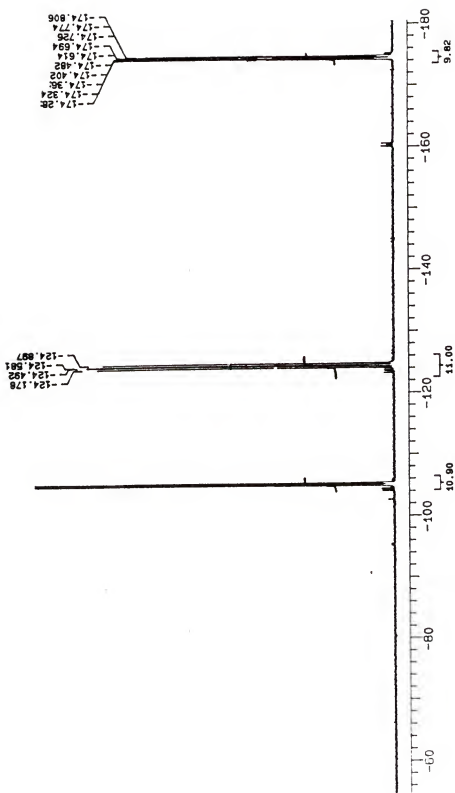


Figure A-9. Radical Precursor 39

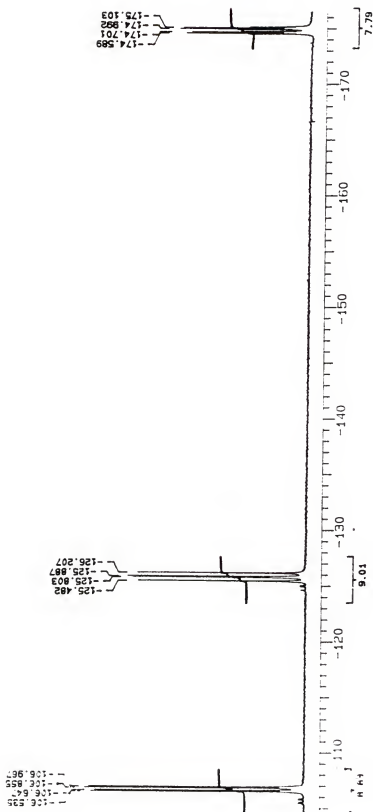


Figure A-9-1. Reduced Product 39-1

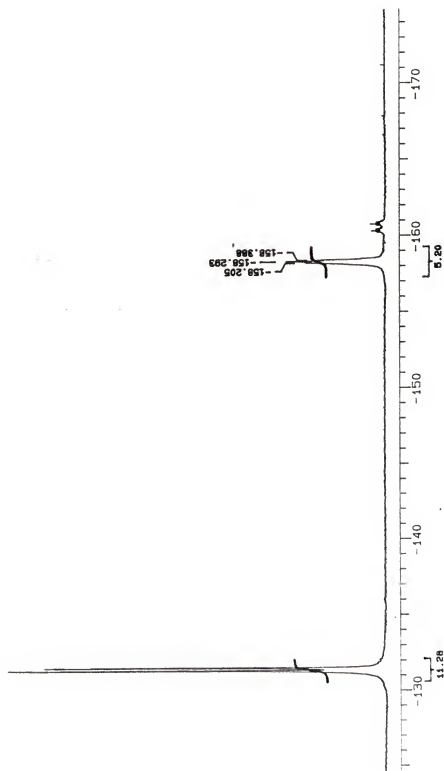


Figure A-9-2. 5-exo Cyclized Product 39-2

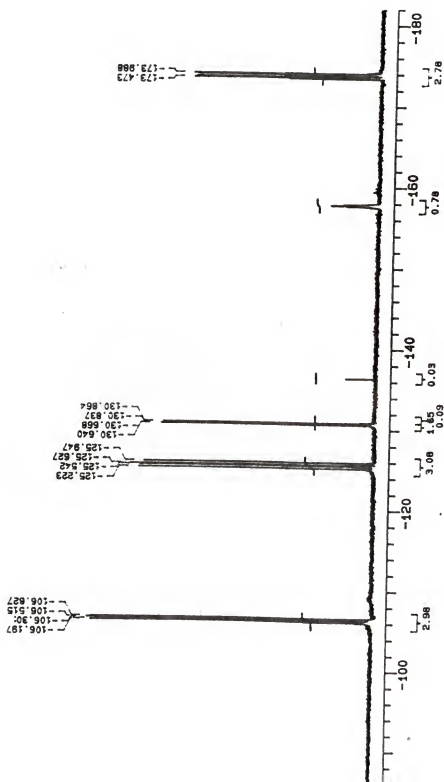


Figure A-9-3. One of the  $^{19}\text{F}$  NMR Spectra of the Reaction Mixtures from Radical 39

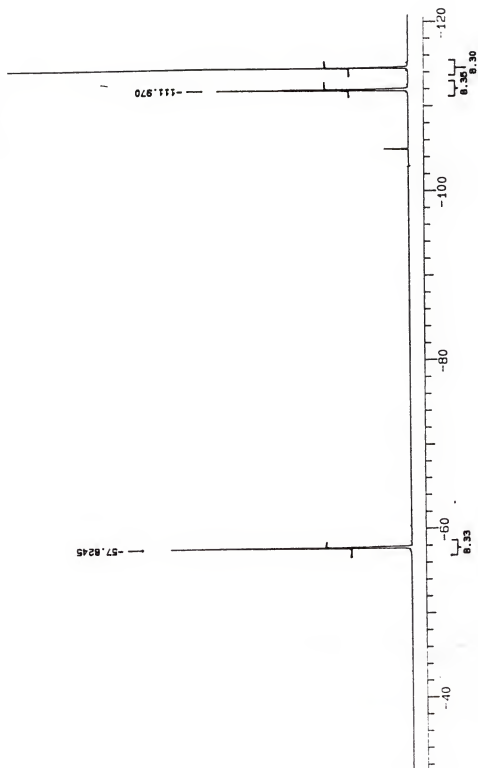


Figure A-10. Radical Precursor 40



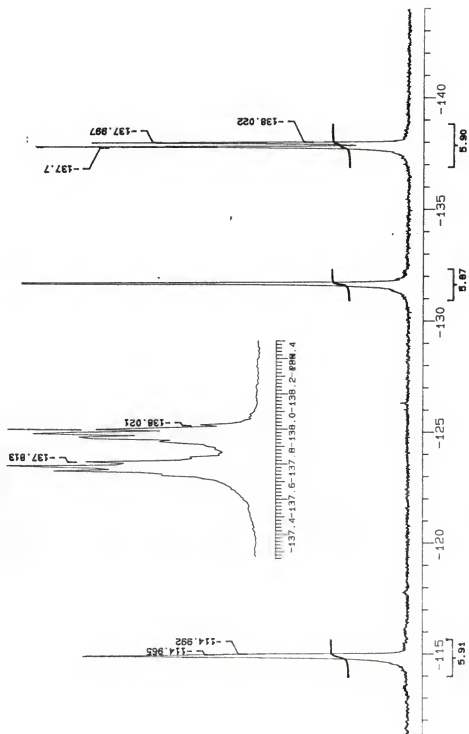


Figure A-10-1. Reduced Product 40-1

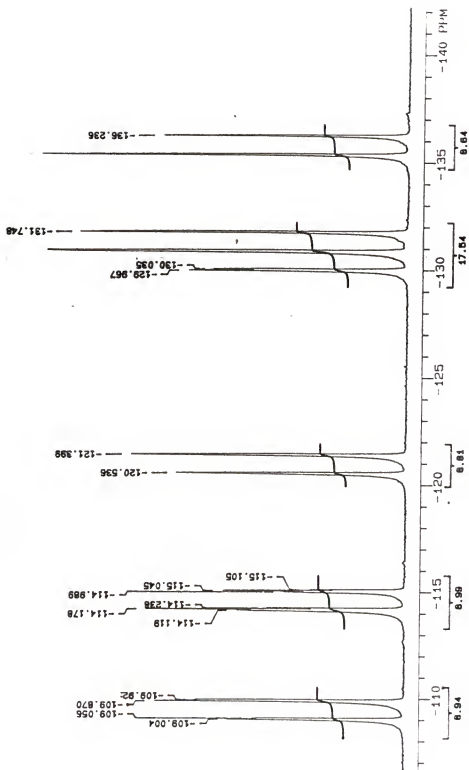


Figure A-10-2. 5-exo Cyclized Product 40-2

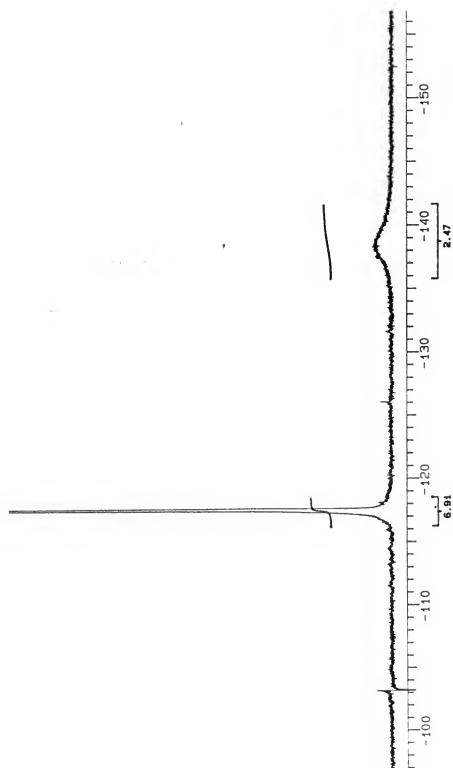


Figure A-10-3. 6-endo Cyclized Product 40-3

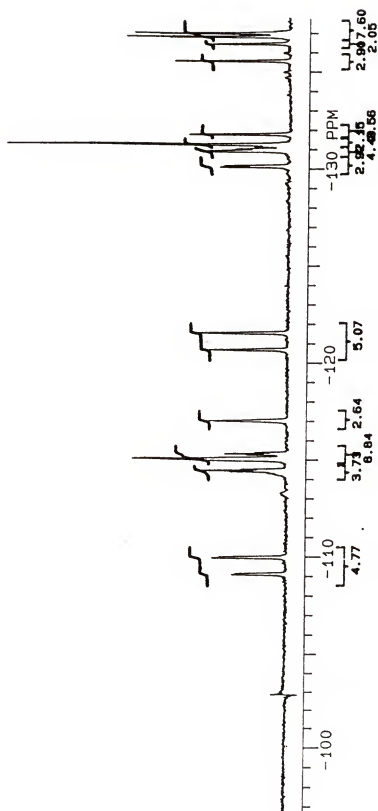


Figure A-10-4. One of the  $^{19}\text{F}$  NMR Spectra of the Reaction Mixtures from Radical 40

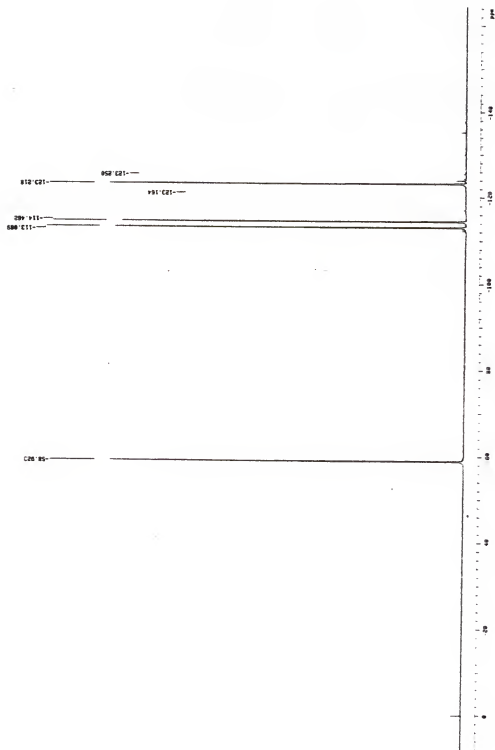


Figure A-11. Radical Precursor 41

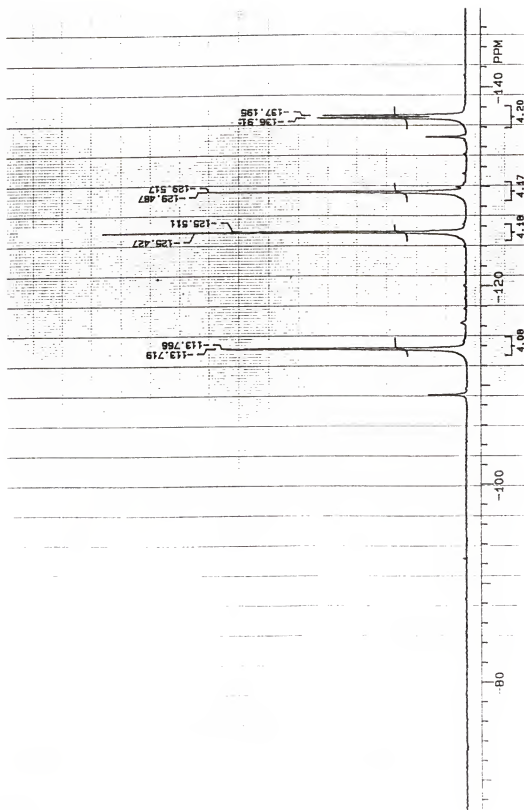


Figure A-11-1. Reduced Product 41-1

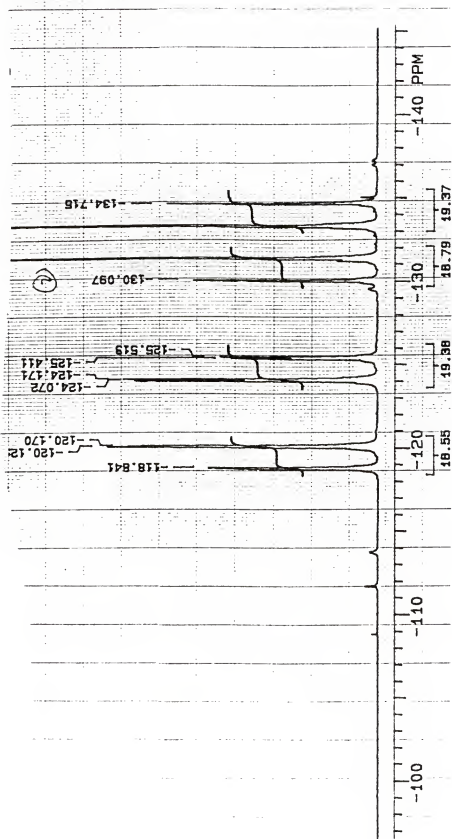


Figure A-11-2. 5-exo Cyclized Product 41-2

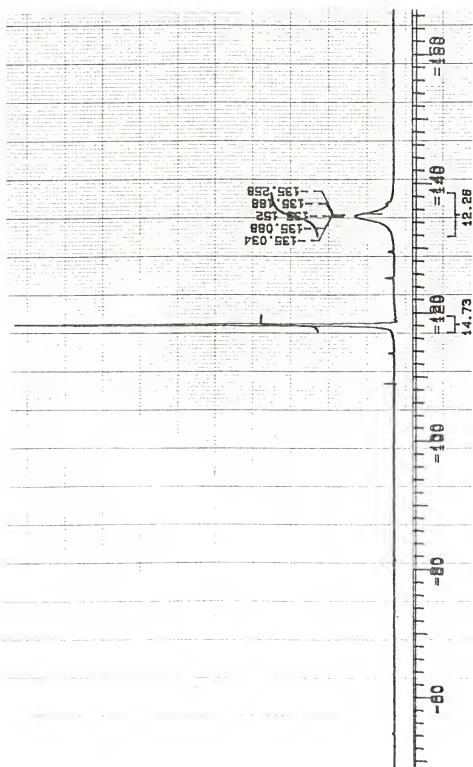


Figure A-11-3. 6-endo Cyclized Product 41-3



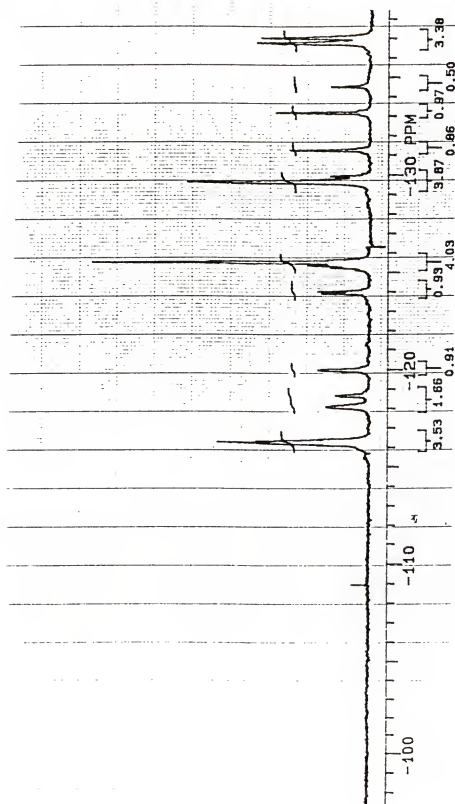


Figure A-11-4. One of the  $^{19}\text{F}$  NMR Spectra of the Reaction Mixtures from Radical 41

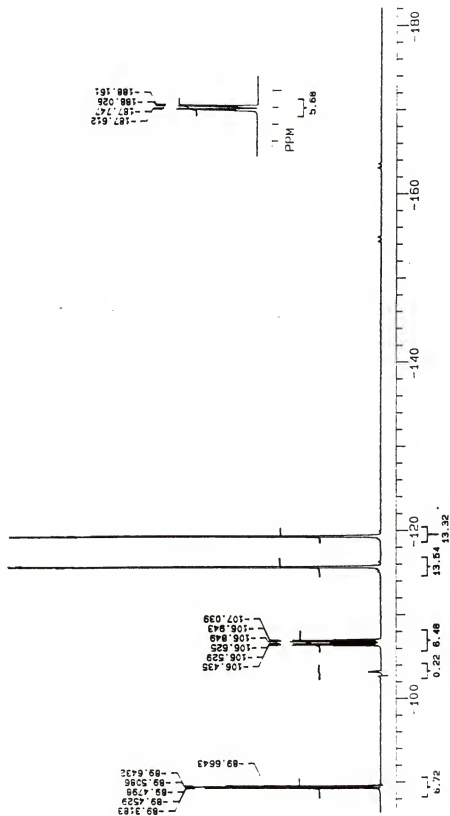


Figure A-12. Radical Precursor 42

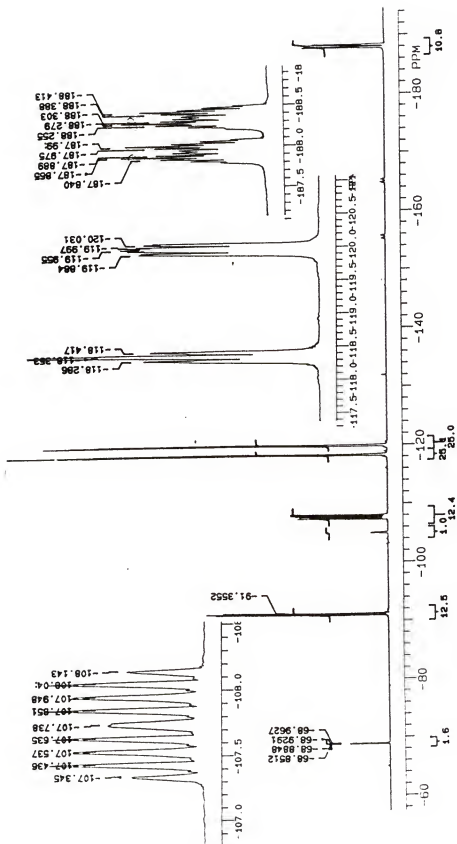


Figure A-12-1, Reduced Product 42-1

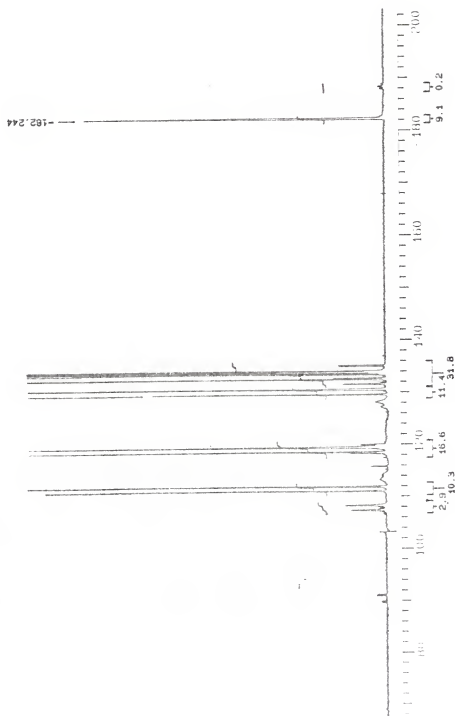


Figure A-12-2. 5-exo Cyclized Product 42-2

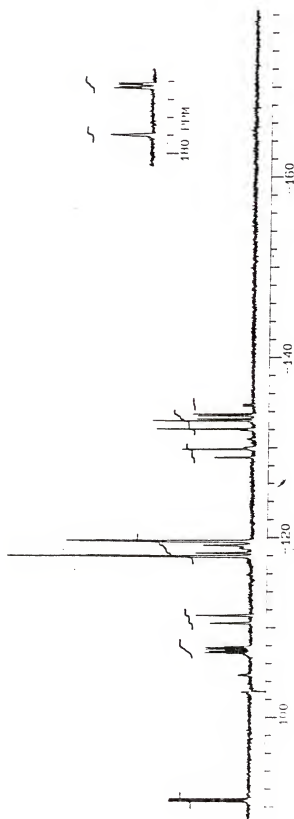


Figure A-12-3. One of the  $^{19}\text{F}$  NMR Spectra of the Reaction Mixtures from Radical 42

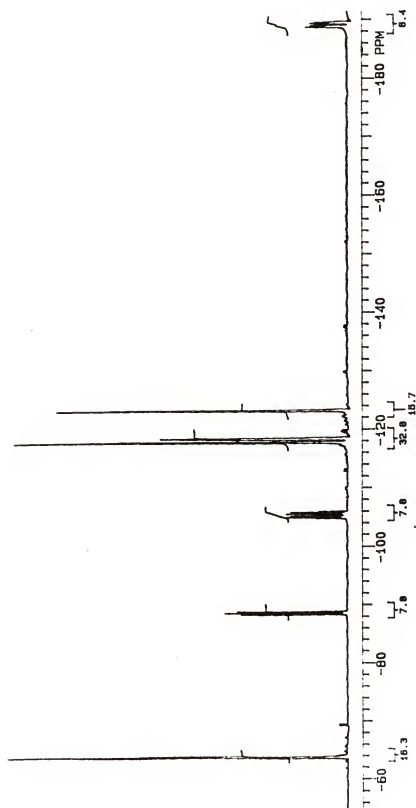


Figure A-13. Radical Precursor 43

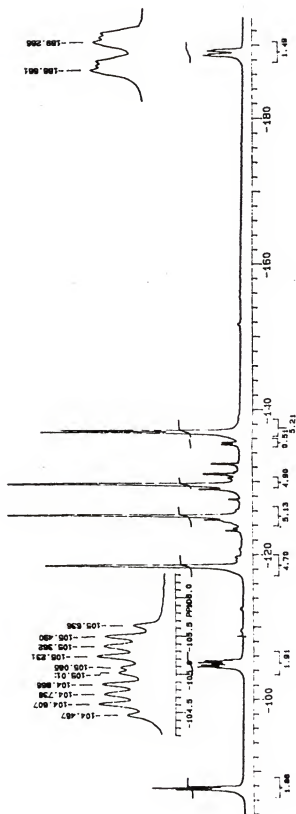


Figure A-13-1. Reduced Product 43-1

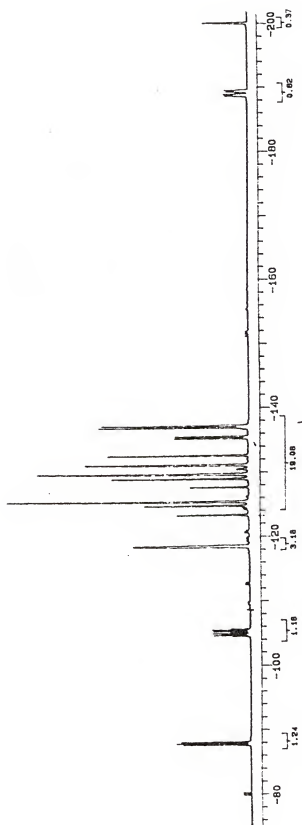


Figure A-13-2. the Mixture of 5-exo Cyclized Product 43-2 and Reduced Product 43-1



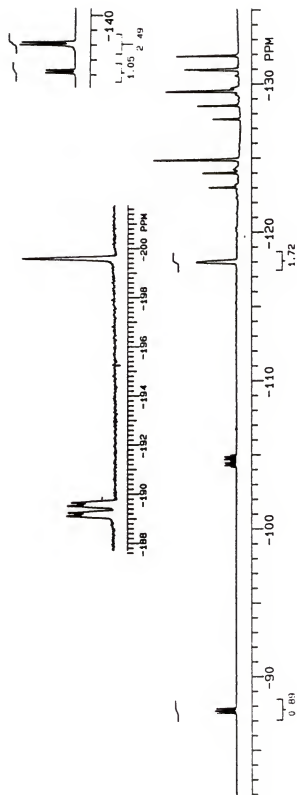


Figure A-13-3. One of the  $^{19}\text{F}$  NMR Spectra of the Reaction Mixtures from Radical 43

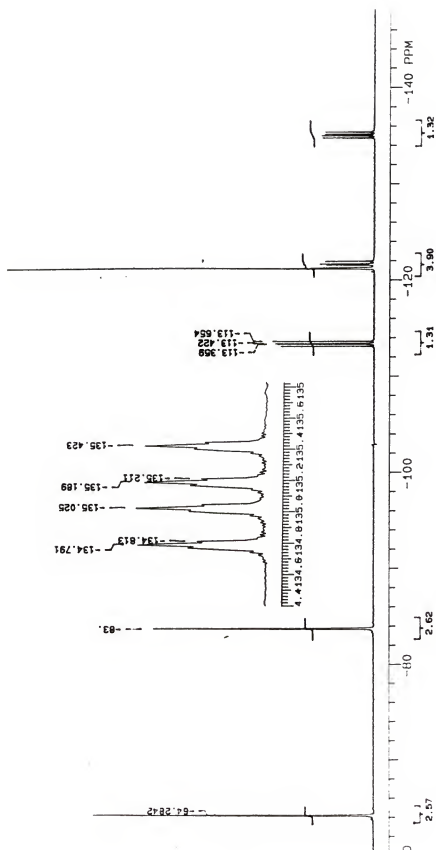


Figure A-14. Radical Precursor 44

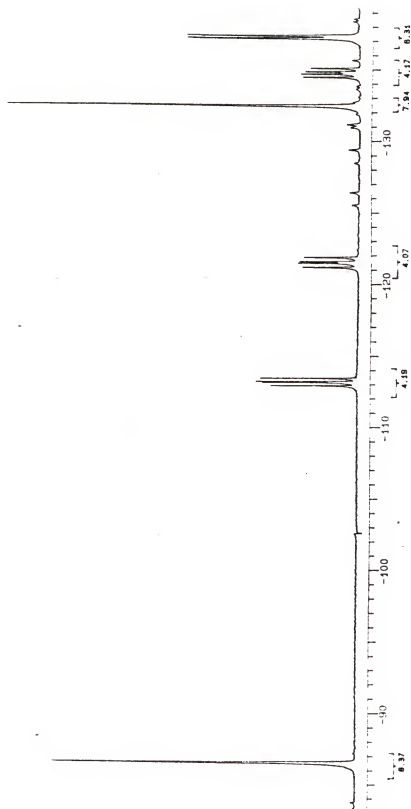


Figure A-14-1. Reduced Product 44-1

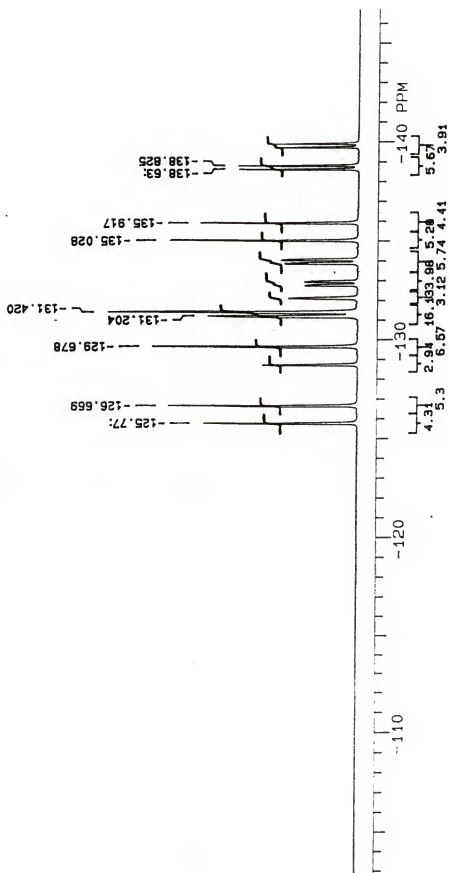


Figure A-14-2. 5-exo Cyclized Product 44-2

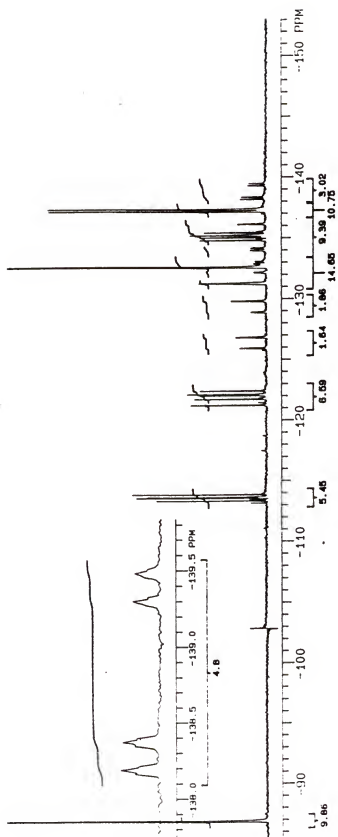


Figure A-14-3. One of the  $^{19}\text{F}$  NMR Spectra of the Reaction Mixtures from Radical 44

## REFERENCES

1. Curran, D. P.; Fevig, T. L. *Chem. Rev.* **1991**, 91, 1237.
2. Dowd, P.; Zhang, W. *Chem. Rev.* **1993**, 93, 2091.
3. Gomberg, M. *J. Am. Chem. Soc.* **1900**, 22, 757.
4. Beckwith, A. L. *J. Chem. Soc. Rev.* **1993**, 143.
5. (a) *The Chemist's Companion*, Editor: Gordon, A. J.; Ford, R. A. John Wiley and Sons, New York, NY **1972**. (b) Pauling, L. *The Nature of the Chemical Bond*, Cornell University Press, Ithaca, NY **1960**.
6. (a) Chatgililoglu, C.; Ingold, K. U.; Scaiano, J. C. *J. Am. Chem. Soc.* **1981**, 103, 7739. (b) Ingold, K. U.; Carlsson, D. J. *J. Am. Chem. Soc.* **1968**, 90, 7047.
7. (a) Kuivila, H. G. *Synthesis*, **1970**, 499. (b) Neumann, W. P. *Synthesis*, **1987**, 665. (c) Giese, B.; Witzel, T. *Angew. Chem. Int. Edn. Engl.* **1984**, 23, 69.
8. Tedder, J. M.; Walton, J. C. *Acc. Chem. Res.* **1976**, 9, 183.
9. (a) Rüchardt, C. *Angew. Chem. Intt. Edn. Engl.* **1970**, 9, 830. (b) Beckwith A. L. J.; Ingold, K. U. in '*Rearrangements in Ground and Excited State*', ed. P. de. Mayo, Academic Press, New York **1980**, Vol. 1, 161.
10. Tedder, J. M.; *Tetrahedron*, **1982**, 38, (31), 313.
11. (a) Chatgililoglu, C.; Dickhaut, J.; Giese, B. *J. Org. Chem.* **1991**, 56, 6399. (b) Chatgililoglu, C. *Acc. Chem. Res.* **1992**, 25, 188. (c) Chatgililoglu, C.; Guerrini, A.; Lucarini, M. *J. Org. Chem.* **1992**, 57, 3405. (d) Ballestri, M.; Chatgilialu, C.; Guerra, M. *J. Chem. Soc. Perkin Trans 2*, **1993**, 421. (e) Chatgililoglu, C.; Ferrer, C.; Lucarrini, M. *J. Org. Chem.* **1983**, 58, 249.
12. Luszyk, J.; Maillard, B.; Lindsay, D. A.; Ingold, K. U. *J. Am. Chem. Soc.* **1983**, 105, 3578.
13. Benson, S. W. *Thermochemical Kinetics*, Wiley, New York, **1973**.
14. Tedder, J. M.; Walton, J. C. *Tetrahedron*, **1980**, 36, (6), 701.
15. Beranek, I.; Fischer, H. in '*Free Radicals in Synthesis and Biology* ', Minisci, F.; ed.; Kluwer, Bostou, **1989**, 303.
16. (a) Burkey, T. J.; Majewski, M.; Griller, D. *J. Am. Chem. Soc.* **1986**, 108, 2218. (b) Griller, D.; Wagner, D. M.; *Pure and Appl. Chem.* **1989**, 61, (4), 717.

17. Evans, M. G.; Polanyi, M.; *Trans. Farad. Soc.* **1938**, 34, 11.
18. Momillen, D. F.; Golden, D. M. *Ann. Rev. Phys. Chem.* **1982**, 33, 493.
19. (a) Chatgililoglu, C.; Ingold, K. U.; Luszyk, J.; Nazran, A. S.; Scaiano, J. C. *Organometallics* **1983**, 2, 1332. (b) Chatgililoglu, C.; Scaiano, J. C. Ingold, K. U. *Organometallics* **1982**, 1, 466. (c) Jackson, R. A.; Ingold, K. U.; Griller, D.; Nazran, A. S. *J. Am. Chem. Soc.* **1985**, 107, 208.
20. (a) Chatgililoglu, C.; Rossiui, S. *Bull. Soc. Chim. Fr.* **1988**, 2, 298. (b) Goldberg, I. H.; *Acc. Chem. Res.* **1991**, 24, 191.
21. Beckwith, A. L. *J. Tetrahedron* **1981**, 37, 3073.
22. Fleming, I. *Frontier Orbitals and Organic Chemical Reactions*, Wiley, London, **1976**.
23. (a) Hoyland, J. R. *Theoret. Chim. Acta.* **1971**, 22, 229. (b) Fujimoto, H.; Yamabe, S.; Minato, T.; Fukui, K. *J. Am. Chem. Soc.* **1972**, 94, 9205. (c) Houk, K. N.; Paddon-Row, N.; Spellmeyer, D. C.; Rondam, N. G.; Nagase, S. *J. Org. Chem.* **1986**, 51, 2874. (d) Gonzalez, C.; Schlegel, H. B.; *J. Phys. Chem.* **1989**, 83, 2435.
24. Hammond, G. S. *J. Am. Chem. Soc.* **1955**, 77, 334.
25. Tedder, J. M. *Angew. Chem. Int. Ed. Engl.* **1982**, 21, 401
26. Giese, B. *Angew. Chem. Int. Ed. Engl.* **1983**, 22, 753.
27. Beckwith, A. L. J.; Schiesser, C. H. *Tetrahedron* **1985**, 41, 3925
28. (a) Houk, K. N.; Spellmeyer, D. C. *J. Org. Chem.* **1987**, 52, 955. (b) Zipse, H.; Jianing, He; Houk, K. N.; Giese, B. *J. Am. Chem. Soc.* **1991**, 113, 4324.
29. (a) Lamb, R. C.; Ayer, P. W.; Tomey, M. K. *J. Am. Chem. Soc.* **1963**, 85, 3483. (b) Brace, N. O. *J. Org. Chem.* **1967**, 32, 2711. (c) Cooley, J. H.; Walling, C.; Ponaras, A. A.; Racah, E. J. *J. Am. Chem. Soc.* **1966**, 88, 5361. (d) Corey, E. J.; Shimoji, K.; Shih, C. *J. Am. Chem. Soc.* **1984**, 106, 6425.
30. (a) Ingold, K. U.; Griller, D.; *Acc. Chem. Res.* **1980**, 13, 317. (b) Beckwith, A. L. J.; Easton, C. J.; Serelis, A. K. *J. Chem. Soc. Chem. Commun.* **1980**, 482. (c) Beckwith, A. L. J.; Easton, C. J.; Serelis, A. K. *J. Chem. Soc. Chem. Commun.* **1980**, 482.
31. Ingold, K. U.; Maillard, B.; Waton, J. C. *J. Chem. Soc. Perkin 2* **1981**, 6, 970.
32. (a) Beckwith, A. L. J.; Easton, C.; Lawrence, T.; Serelis, A. K. *Aust. J. Chem.* **1983**, 36, (3), 545. (b) Beckwith, A. L. J.; Blair, I. A.; Phillipou, G. *Tetrahedron lett.* **1974**, 26, 2251. (c) Beckwith, A. L. J.; Glover, S. A. *Aust. J. Chem.* **1987**, 40, (1), 157. (d) Beckwith, A. L. J.; Cliff, M. D.; Schiesser, C. H. *Tetrahedron* **1992**, 48, 4641.
33. (a) Luszyk, J.; Maillard, B.; Deycard, S.; Lindsay, D. A.; Ingold, K. U. *J. Org. Chem.* **1987**, 52, 3509. (b) Walling, C. J.; Cioffari, A. *J. Am. Chem.* **1972**, 94, 6059.

34. Babu, T. V. *Acc. Chem. Res.* **1991**, 24, 139.
35. (a) Julia, M.; Maumy, M. *Bull. Soc. Chim. Fr.* **1966**, 434. (b) Julia, M.; Maumy, M. *Bull. Soc. Chim. Fr.* **1967**, 2641. (c) Walling, C.; Cioffari, A. *J. Am. Chem. Soc.* **1972**, 94, 6064.
36. Park, Seung-Un; Chung, Sung-Kee; Newcomb, M. *J. Am. Chem. Soc.* **1986**, 108, (2), 240.
37. Allinger, N. L.; Zalkow, V. J. *Org. Chem.* **1960**, 25, 701.
38. Canadell, E. *J. Chem. Soc. Perkin Trans 2* **1985**, 1331.
39. Houk, K. N.; Munchausen, L. L. *J. Am. Chem. Soc.* **1976**, 98, 937.
40. Paso, J. D. *J. Org. Chem.* **1992**, 57, 1139.
41. Tanner, D. D.; Zhang, L. *J. Am. Chem. Soc.* **1994**, 116, 6683.
42. Avila, D. V.; Ingold, K. U.; Luszyk, J.; Dolbier, W. R., Jr.; Pan, H. Q. Muir, M.; *J. Am. Chem. Soc.* **1994**, 116, 99.
43. Newcomb, M. *Tetrahedron* **1993**, 49, (6), 1151.
44. Griller, D.; Ingold K. U.; *Acc. Chem. Res.* **1980**, 13, 317.
45. Smart, B. E. in *The Chemistry of Functional Groups, Supplement D*, John Wiley and Sons, New York, NY, **1983**, Chapter 14, 603.
46. Smart, B. E. in *Molecular Structure and Energetics*, VCH Publisher Inc. Deerfield Beach, FL, **1986**, Vol. 3, Chapter 4, 141.
47. (a) Random, L.; Hehre, W. J.; Pople, J. A. *J. Am. Chem. Soc.* **1971**, 93, 289. (b) Random, L.; Hehre, W. J.; Pople, J. A. *J. Am. Chem. Soc.* **1972**, 94, 2371.
48. Holtz, D. *Progr. Phys. Org. Chem.* **1971**, 8, 1.
49. (a) Bent, H. A. *Chem. Rev.* **1961**, 61, 275. (b) Wiberg, K. B.; Rablen, P. R. *J. Am. Chem. Soc.* **1993**, 115, 614.
50. Mellish, C. E.; Linnett, J. W. *Trans Far, Soc.* **1954**, 50, 657.
51. Epiotis, N. D.; Cherry, W. *J. Chem. Soc. Chem. Commun.* **1973**, 278.
52. Epiotis, N. D. *J. Am. Chem. Soc.* **1973**, 95, 3087.
53. Brundle, C. R.; Robin, M. B.; Kuebler, N. A.; Basch, H. *J. Am. Chem. Soc.* **1972**, 94, 1451.
54. Sell, A. J.; Mintz, D. M.; Kuppermann, A. *Chem. Phys. Lett.* **1978**, 601.
55. Chiu, N. S.; Burrow, P. D. *Chem. Phys. Lett.* **1979**, 121.
56. Dolbier, W. R., Jr.; Piedrahita, C. A.; Al-Sader, B. H. *Tetrahedron Lett.* **1979**, 2957.



57. Dolbier, W. R., Jr.; Medinger, K. S. *Tetrahedron* **1982**, 38, 2415.
58. *Fluorine: The First Hundred Years (1886-1986)*, Editor: Banks, R. E.; Sharp, D. W. A.; Tatlow, J. C.; Elsevier Sequoia. New York, NY. **1986**.
59. Streitwieser Jr., A.; Mares, F. J. *Am. Chem. Soc.* **1968**, 90, 2444.
60. Blint, R. J.; McMahon, T. B.; Beauchamp, J. L. *J. Am. Chem. Soc.* **1974**, 96, 1269.
61. Williamson, A. D.; Lebreton, P. R.; Beauchamp, J. L. *J. Am. Chem. Soc.* **1976**, 98, 2705.
62. Jiang, X. K.; Li, X. Y.; Wang, K. Y. *J. Chem. Soc. Chem. Commun.* **1986**, 745.
63. Pasto, D. J.; Krasnansky, R.; Zercher, C. J. *Org. Chem.* **1987**, 52, 3062.
64. (a) Fessenden, R. W.; Schuler, R. H. *J. Chem. Phys.* **1965**, 43, 2704. (b) Beveridge, D. L.; Dobosh, P. A.; Pople, J. A. *J. Chem. Phys.* **1968**, 48, 4802.
65. Mile, B. *Angew. Chem. Internat. Edit.* **1968**, 7, 507.
66. Tedder, J. M.; Walton, J. C. *Acs. Sympo. Ser.* **1978**, 7, 4.
67. Andreades, S. *J. Am. Chem. Soc.* **1964**, 86, 2003.
68. Lioyd, R. V.; Rogers, T. *J. Am. Chem. Soc.* **1973**, 95, 1512.
69. Krusic, P. J.; Bingham, R. C. *J. Am. Chem. Soc.* **1976**, 98, 230.
70. (a) Morikawa, T. Uejima, M.; Kobayashi, Y. *Chem. Lett.* **1989**, 623. (b) Morikawa, T. Uejima, M.; Kobayashi, Y. *Tetrahedron Lett.* **1989**, 2407. (c) Morikawa, T. Uejima, M.; Kobayashi, Y. *Chem. Pharm. Bull.* **1991**, 39, 2462.
71. Alia, D. V.; Ingold, K. U.; Luszytk, J.; Dolbier, Jr. W. R.; Pan, H-Q; Mair, M. J. *Am. Chem. Soc.* **1994**, 99, 116.
72. Rong, X. X.; Pan, He-Q; Dolbier, Jr. W. R. *J. Am. Chem. Soc.* **1994**, 116, 4521.
73. Dolbier, Jr. W. R.; Rong, X. X. *Tetrahedron Lett.* **1994**, 35, (34), 6225.
74. Tedder, J. M.; Walton, J. C. *Acs. Sympo. Ser.* **1978**, 66, 107.
75. (a) Luszytk, J.; Maillard, B.; Ingold, K. U. *J. Org. Chem.* **1986**, 51, 2457. (b) Ingold, K. U.; Luszytk, J.; Scaiano, J. C. *J. Am. Chem. Soc.* **1984**, 106, 343.
76. Hansch, C.; Leo, A.; Taff, R. W. *Chem. Rev.* **1991**, 91, 165.
77. Feldman, K. S.; Romanelli, A. L.; Ruckle, R. E., Jr.; Jean, G. J. *Org. Chem.* **1992**, 57, 100.
78. Barton, D. H. R.; Chrich, D.; Motherwell, W. B. *Tetrahedron* **1985**, 41, 3901.

79. (a) Franz, J. A.; Bushaw, B. A.; Alnajjar, M. S. *J. Am. Chem. Soc.* **1989**, 111, 268. (b) Newcomb, M.; Manek, M. B. *J. Am. Chem. Soc.* **1990**, 112, 9662.
80. Avila, D. V. unpublished results.
81. (a) Griller, D.; Kanabus-Kaminska, J. M.; Maccoll, A. *Theochem.* **1988**, 163, 125. (b) McMillen, D. F.; Golden, D. M. *Ann. Rev. Phys. Chem.* **1982**, (33), 493.
82. Pearson, R. G. *J. Org. Chem.* **1989**, 54, 1423.
83. Stein, S. E.; Rukkers, J. M.; Brown, R. L. *NIST. Standard Reference Database 25 NIST Structures and Properties Database and Estimation Program*; National Institute of Standards and Technology, Gaithersburg, MD, **1991**.
84. Kim, S. S.; Kim, S. Y.; Ryou, S. S.; Lee, C. S.; Yoo, K. H. *J. Org. Chem.* **1993**, 58, 192.
85. Das, P. K.; Encinas, M. V.; Steenken, S.; Scaiano, J. C. *J. Am. Chem. Soc.* **1981**, 103, 4162.
86. (a) Scheldon, R. A.; Kochi, J. K. *J. Am. Chem. Soc.* **1970**, 92, 4395. (b) Ashby, E. C.; Bowers, J.; Depriest, R. *Tetrahedron Lett.* **1980**, 21, 3541. (c) Ashby, E. C.; Depriest, R. N.; Goel, A. B.; Wenderoth, B.; Pham, T. N. *J. Org. Chem.* **1984**, 49, 3545. (d) Ashby, E. C.; Coleman, D. *J. Org. Chem. Soc.* **1987**, 52, 4554. (e) Beckwith, A. L. J.; Hay, P. B. *J. Am. Chem. Soc.* **1989**, 111, 2674.
87. Bunn, C. W.; Howells, E. R. *Nature* **1954**, 174, 549.
88. Dolbier, Jr. W. R.; Rong, X. X.; He, Y. H. *Tetrahedron Lett.* **1993**, 34, 5185.
89. Stang, P. J.; White, M. R. *J. Am. Chem. Soc.* **1981**, 103, 5429.
90. Takeyama, Y.; Ichinose, Y.; Oshima, K.; Utimoto. *Tetrahedron Lett.* **1989**, 30, 3159.
91. Wong, G. B.; Kurtz, D. M., Jr.; Holm, R. H.; Mortenson, L. E.; Upchurch, R. G. *J. Am. Chem. Soc.* **1979**, 101, 3078.
92. Chi, D. Y.; Kiesewetter, D. O.; Katzenellenbogen, J. A.; Kilbourn, M. R.; Welch, M. J. *J. Fluorine Chem.* **1986**, 31, 99.
93. Brown, H. C.; Rao, C. G.; Kuikarni, S. U. *Synthesis* **1979**, 704.
94. Cox, D. G.; Gurusamy, N.; Burton, D. J. *J. Am. Chem. Soc.* **1985**, 107, 2811.
95. Nace, D. G.; Burton, D. J. *Synth. Commun.* **1973**, 3, 197.
96. Detty, M. R. *Tetrahedron Lett.* **1979**, 43, 4189.
97. Corey, E. J.; Venkateswarlu, A. *J. Am. Chem. Soc.* **1972**, 94, 6190.
98. Bailey, W. F.; Punzalan, E. R. *J. Org. Chem.* **1990**, 55, 5404.
99. Normant, Jean-F. *J. Organometallic Chem.* **1990**, 400, 19.

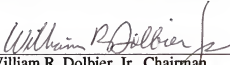
100. Dubuffet, T.; Sauvêtre, R.; Normant, Jean-F. *J. Organometallic Chem.* **1988**, 341, 11.
101. Gillet, J. P.; Sauvêtre, R.; Normant, J. F. *Synthesis* **1986**, 355.
102. Krespan, C. G. *J. Org. Chem.* **1958**, 23, 2016.
103. Babler, J. H.; Spina, K. P. *Synth. Commun.* **1984**, 14, (14), 1313.

## BIOGRAPHICAL SKETCH

Xiao Xin Rong was born in January, 1956, in Beijing, P. R. China. He received his B.S. degree in analytical chemistry from Shanghai University of Technology in August, 1982. He then worked as a research chemist in the Central Research Institute of Building & Construction Ministry of Metallurgic Industry. In October, 1987, Xiao X. Rong was invited by Professor and Chairman of Chemistry William R. Dolbier, Jr. to study and work under Dr. Roy King in mass-spectrum lab at the University of Florida as a visiting scholar.

In January, 1990, Xiao X. Rong initiated graduated studies in the Department of Chemistry at the University of Florida under the supervision of Professor William R. Dolbier, Jr. Upon completion of his doctoral studies, Xiao X. Rong looks forward to new challenges in his life.

I certify that I have read this study and that in my opinion it conforms to acceptable standards of scholarly presentation and is fully adequate, in scope and quality, as a dissertation for the degree of Doctor of Philosophy.

  
William R. Dolbier, Jr., Chairman  
Professor of Chemistry

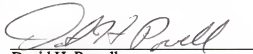
I certify that I have read this study and that in my opinion it conforms to acceptable standards of scholarly presentation and is fully adequate, in scope and quality, as a dissertation for the degree of Doctor of Philosophy.

  
William M. Jones  
Distinguished Service Professor of  
Chemistry


I certify that I have read this study and that in my opinion it conforms to acceptable standards of scholarly presentation and is fully adequate, in scope and quality, as a dissertation for the degree of Doctor of Philosophy.

\_\_\_\_\_  
Merle A. Battiste  
Professor of Chemistry

I certify that I have read this study and that in my opinion it conforms to acceptable standards of scholarly presentation and is fully adequate, in scope and quality, as a dissertation for the degree of Doctor of Philosophy.

  
David H. Powell  
Associate Scientist of Chemistry

I certify that I have read this study and that in my opinion it conforms to acceptable standards of scholarly presentation and is fully adequate, in scope and quality, as a dissertation for the degree of Doctor of Philosophy.

  
James F. Klausner  
Assistant Professor of Mechanical  
Engineering

This dissertation was submitted to the Graduate Faculty of the Department of Chemistry in the College of Liberal Arts and Sciences, and to the Graduate School and was accepted as partial fulfillment of the requirements for the degree of Doctor of Philosophy.

August, 1995

---

Dean, Graduate School